


# A STUDY OF POLYELECTROLYTE COMPLEXES WITH DYNAMIC LIGHT SCATTERING

by  
Dolly Theodora Kylpassis

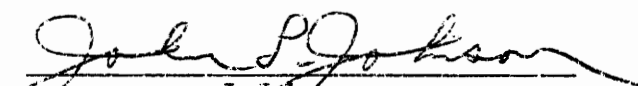
Thesis submitted to the Faculty of the  
Virginia Polytechnic Institute and State University  
in partial fulfillment of the requirements for the degree of

Master of Science  
in  
Chemical Engineering

APPROVED:

  
R. M. Davis, Chairman

  
W. Velander

  
J. Johnson

June 1991  
Blacksburg, Virginia

LD

5655

V855

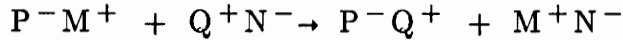
1991

K967

C.2

## ABSTRACT

Polyelectrolyte complexes (PEC) are a novel class of copolymers formed from the reaction between polyanions and polycations (PE's) in polar solvents. Complex formation results from the combination of a polyanion  $P^-M^+$ , and a polycation  $Q^+N^-$ , according to:



where  $M^+$  and  $N^-$ , are the low molecular weight counterions of the polyanion and polycation, respectively. The attraction between  $P^-$  and  $Q^+$  results in self-assembling structures with a rich and diverse phase behavior.

Electrostatic interactions are the main attractive forces, which control PEC structure. Their formation and their final structure are a function of the

ratio of equivalent concentrations, defined as  $Z = \frac{[Q^+N^-]}{[P^-M^+]}$  where  $[Q^+N^-]$  is

the guest polymer- the one in deficient amount, and  $[P^-M^+]$  is the host polymer- the one in excess, the ionic strength  $I$  of the solution, the nature of the solvent, pH, temperature, and structure of the PE's such as geometrical features of the chain and charge density. Thus, PEC's are very environmental sensitive materials. Mixtures of PE's with opposite charges form large nonequilibrium structures and precipitate almost instantly at low ionic strength. As the ionic strength of the solution increases, the range of  $Z$  at which that PEC can stay in solution, broadens.

The PEC system studied in this work was a dilute NaCl solution of sodium polystyrene sulfonate (NaPSS) and poly-L-lysine hydrobromide (PLL). Dynamic light scattering was used to measure translational diffusion coefficient. For  $Z < Z_c$ , where  $Z_{crit}$  is the ration above which interhost complexes are formed, equilibrium structures are formed whose size is constant, with varying polymer ratio  $Z$ .  $Z_{crit}$  increases with the ionic strength. At an ionic strength of  $I=1M$ , interhost complexes donot form below  $Z=1.53$ . At this ionic strength

intramolecular complexation was observed. For  $Z > Z_{crit}$  large nonequilibrium structures are formed, whose size is difficult to reproduce. High temperatures ( $T \simeq 47^\circ\text{C}$ ) break down those nonequilibrium structures to equilibrium or less nonequilibrium ones. High pH also break down those complexes, due to lower PLL charge density, and thus smaller binding ability. PLL conformation from  $\alpha$ -helix to coil or  $\beta$ -sheet structures, plays a very important role. The molecular weight ratio of guest/host plays an important role also. The aggregation point,  $Z_{crit}$ , shifts at lower values when guest/host ratio exceeds a certain value.

Hydrophobic interactions, which favor PLL  $\beta$ -sheet structure, are possibly responsible for the aggregation. A possible mechanism is that the PLL serves as a bridge, between the host PSS molecules, either by forming intermolecular hydrogen bonds or by simply "connecting" two host molecules.

## ACKNOWLEDGMENTS

I would like to express my sincere thanks and gratitude to Dr. Rick M. Davis for his constant guidance and suggestions throughout the fulfillment of this degree and the writing of this thesis. I also wish to thank Dr.J.Johnson and Dr.W.Velander for their valuable suggestions.

I would also like to thank my friends and roommates Nickos Kontoyannis and George Tsoflias for their help, their friendship and their patience and also my best friend JoEllen Kelly for many helpful discussions and all the good times we spent together.

Finally this thesis would not have been possible without the support and encouragement of my father Yannis Kylpassis, my mother Angeliki Kylpassis my brother Nickos Kylpassis and Christopher Karanassos.

# TABLE OF CONTENTS

**1.0 INTRODUCTION..... 1**

1.1 INTRODUCTION..... 1

1.2 PE’S AND PEC’S APPLICATIONS ..... 3

    1.2.1 Industrial Applications

    1.2.2 PEC’s in Biological Systems

1.3 OBJECTIVES..... 9

**2.0 PHYSICAL CHEMISTRY OF PEs & PECs..... 13**

2.1 INTRODUCTION..... 13

2.2 POLYELECTROLYTES..... 14

    2.2.1 Properties and behavior

    2.2.2 Chemical Structure

    2.2.3 Physical Chemistry of PE’s

        2.2.3.1 The Kuhn length

        2.2.3.2 Excluded volume

        2.2.3.3 Radius of gyration

    2.2.4 Characterization Techniques for PE’s solutions

        2.2.4.1 Concentration regimes

        2.2.4.2 Dynamic light Scattering

        2.2.4.3 Viscosity

2.3 POLYELECTROLYTE COMPLEXES ..... 25

    2.3.1 Physical Chemistry of PEC’s

    2.3.2 The Coacervate Phase

    2.3.3 PEC’s formation and structure

<b>3.0 EXPERIMENTAL .....</b>	<b>41</b>
3.1 MATERIALS .....	41
3.2 EQUIPMENTS .....	43
3.3 SODIUM POLYSTYRENE SULFONATE .....	44
3.3.1 General information	
3.3.2 Solution Preparation	
3.3.3 NaPSS concentration measurements	
3.4 POLY-L-LYSINE HYDROBROMIDE.....	48
3.4.1 General information	
3.4.2 Solution Preparation	
3.5 PEC MIXING PROCEDURE .....	51
3.5.1 NaPSS Density data	
3.5.2 Effective Ionic Strength	
3.5.3 PLL/NaPSS Mixing Calculations	
3.5.4 Mixing order	
 <b>4.0 DYNAMIC LIGHT SCATTERING.....</b>	 <b>58</b>
4.1 INTRODUCTION.....	58
4.2 THEORY OF DYNAMIC LIGHT SCATTERING .....	60
4.3 STRUCTURE FACTOR AND SCATTERING ANGLE .....	63
4.4 PARTICLE INTERACTIONS .....	64
4.5 DLS EXPERIMENTAL PROCEDURE.....	65
4.5.1 Sample Preparation	
4.5.1.1 Glassware Treatment	
4.5.1.2 Filtration	
4.5.2 Dynamic Light Scattering Procedure	
4.5.2.1 Equipment Description	
4.5.2.2 Latex Calibration test	
4.5.2.3 Dark count rate test	
4.5.2.4 ISINETHETA Test	
4.6 DETERMINATION OF THE DIFFUSION COEFFICIENT .....	71

4.7 ERROR ANALYSIS..... 75

4.8 DYNAMIC LIGHT SCATTERING CONDITIONS..... 77

**5.0 RESULTS AND DISCUSSION..... 80**

5.1 TECHNIQUE VERIFICATION ..... 81

5.2 PURE POLYMER DATE..... 92

    5.2.1 Sodium Polystyrene Sulfonate

    5.2.2 Pure Poly-L-Lysine data

5.3 POLYELECTROLYTE COMPLEXES DATA .....105

    5.3.1 Ionic Strength Effects

    5.3.2 Temperature Effects

    5.3.3 The effect of pH on PEC's binding

    5.3.4 The effect of Molecular Weight on PEC's binding

**6.0 CONCLUSIONS AND FUTURE WORK .....132**

6.1 CONCLUSIONS.....132

6.2 FUTURE WORK.....134

**APPENDIX .....135**

**BIBLIOGRAPHY .....144**

**VITA.....147**

## LIST OF ILLUSTRATIONS

Figure 1.1 Polyelectrolyte's activity as flocculant .....	11
Figure 1.2 Polyelectrolyte complexes activity as flocculants..	12
Figure 2.1 (A) Polyacrylic acid partially neutralized .....	34
Figure 2.1 (B) Copolymer of acrylic acid and vinyl alcohol ...	35
Figure 2.2 Conductance behavior of a reaction mixture .....	36
Figure 2.3 The effect of salt on complex concentration .....	37
Figure 2.4 Dependence of $R_g$ of an NPEC on $Z$ .....	38
Figure 2.5 Kabanov's picture for PEC's structure .....	39
Figure 2.6 Structures of NPEC .....	40
Figure 3.1 Polystyrene Sulfonate monomer structure .....	56
Figure 3.2 PLL Monomer structure .....	57
Figure 4.1 An example of the ACF for two particles of different radius .....	78
Figure 4.2 Block diagram of BI-2030 .....	79
Figure 5.1.1 Determination of $R_h$ .....	89
Figure 5.1.2 Determination of the dilute regime .....	90
Figure 5.1.3 Determination of PEC dilute regime .....	91
Figure 5.2.1.1 Effect of Ionic Strength on $R_H$ , of PEC's.....	99
Figure 5.2.1.2 Expansion factor vs Ionic Strength .....	100
Figure 5.2.2.1 The polypeptide $\alpha$ -helix bond .....	101
Figure 5.2.2.2 Temperature and Ionic Strength effects on Pure PLL .....	103
Figure 5.2.2.3 pH effects on Pure PLL .....	104
Figure 5.3.1.1 Ionic Strength effects on PEC's $R_H$ .....	114
Figure 5.3.1.2 PLL bridges through beta-structures H-bonds....	115
Figure 5.3.1.3 Kabanov's model of PEC aggregation .....	116
Figure 5.3.1.4 PLL Bridges model.....	117
Figure 5.3.2.1 Kinetics of PEC's size reduction with T.....	126

Figure 5.3.2.2 Kinetics of PEC’s size reduction with T.....127

Figure 5.3.3.1 pH effects on PEC’s binding.....128

Figure 5.3.4.1 Effect of Molecular weight on PEC binding .....129

Figure 5.3.4.2 Effect of Molecular weight on PEC binding .....130

Figure 5.3.4.3 Effect of Molecular weight on PEC binding .....131

Figure App. 1.1 Reproducibility test.....140

Figure App. 1.2 Reproducibility test.....141

Figure App. 1.3 Reproducibility test.....142

# LIST OF TABLES

Table 3.1.1 Structural parameters for polyelectrolytes .....	41
Table 3.1.2 Table of materials .....	42
Table 3.2.1 Table of equipments .....	43
Table 3.3.1 NaPSS concentration measurements .....	47
Table 3.4.1 PLL concentration measurements .....	50
Table 5.1.1 Determination of $R_H$ .....	83
Table 5.1.2 Test of filtration technique .....	88
Table 5.2.2.2 PLL's thermal history dependence .....	102
Table 5.3.2.2 Polymer ratio vs Hydrodynamic radius .....	118
Table 5.3.2.3 Polymer ratio vs Hydrodynamic radius .....	119
Table 5.3.2.4 Polymer ratio vs Hydrodynamic radius .....	120
Table 5.3.2.5 Polymer ratio vs Hydrodynamic radius .....	121
Table 5.3.2.6 Polymer ratio vs Hydrodynamic radius .....	122
Table 5.3.2.7 Polymer ratio vs Hydrodynamic radius .....	123
Table 5.3.2.8 Polymer ratio vs Hydrodynamic radius .....	124
Tables App.1-App.9 Reproducibility tests .....	135-139

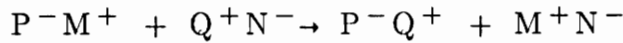
# 1.0 INTRODUCTION

## 1.1 Introduction

Polyelectrolytes (PE's) are ion-containing polymers, which are soluble in water. The conformations of these polymers and, hence, their solution properties, are profoundly affected by the fixed charges, which can be located on the polymer backbone, or on side groups.

The extremely large expansion factors that can result from the mutual repulsion of fixed charges on the polymers, can give rise to highly viscous solutions, which find use in a large number of rheology control applications. The fixed charges also can result in effective colloidal stabilization when the polymer adsorb onto colloidal particles in suspensions.

Polyelectrolyte complexes are a novel class of copolymers formed from the reaction between polyanions and polycations in polar solvents [15]. Complex formation results from the combination of a polyanion  $P^-M^+$ , and a polycation  $Q^+N^-$ , according to:



where  $M^+$  and  $N^-$ , are the low molecular weight counterions of the polyanion and polycation, respectively. The attraction between  $P^-$  and  $Q^+$  results in self-assembling structures with a rich and diverse phase behavior, ranging from colloidal dispersions of droplets in a dilute polymer solution [15], to gels and semicrystalline fibers [15]. A large number of PEC's can be made by combining different polycations and polyanions.

Electrostatic interactions are the main attractive forces, which control PEC structure. Their formation and their final structure are functions of: (i) ionic strength,  $I$ , (ii) nature of solvent, (iii) pH, (iv) temperature, (v) structural features of the polyanion and polycation such as charge density, chain stiffness, and accessibility of the fixed charges, (vi) the ratio of equivalent concentration  $Z$

defined by  $Z = \frac{\text{guest equivalents}}{\text{host equivalents}}$ , where the host polyelectrolyte is the species

present in excess and the guest species is present in relatively small amounts. Thus, PEC's are very sensitive to their solution environment. Mixtures of oppositely charged polyelectrolytes with highly dissociated fixed charges form large nonequilibrium structures and precipitate almost instantly at low ionic strength due to strong electrostatic attractive forces. As the ionic strength of the solution increases, the range of  $Z$  at which the PEC can stay in solution broadens. The behavior and physical chemistry of PEC's are described in detail in Chapter 2.

PEC's have a variety of applications since it is possible to control the water content, polycation/polyanion ratio, and solubility of PEC's. PEC's are used for: (i) selectively permeable membranes for dialysis and ultrafiltration [3], (ii) microencapsulation agents [3,15], (iii) biomedical implants [3], (iv) separation of protein mixtures [3,15], (v) flocculation agents for colloidal suspensions [3,15].

Beside their industrial applications, PE's and PEC's have also proven useful in the study of biopolymer such as nucleoproteins and nucleoprotamines, and complexes formed by them. PEC's also serve as models for the adsorption of polyions on the surfaces of oppositely charged solid particles in suspensions [21].

## 1.2 PE's and PEC's applications

### 1.2.1 Industrial applications

a. *Flocculants in paper making.* An important problem in papermaking industry is the improvement of the retention of fiber particles, inorganic fillers and other small particulate matter within a paper sheet, during the sheet consolidation process [22]. Both PE's and PEC's flocculate or agglomerate these colloidal particles onto fibers so they are not removed in the process of drainage. Figure 1.1 illustrates the adsorption and flocculation process for a cationic PE. The electrostatic field around a polycation attracts and adsorbs onto negatively charged fibers. This causes the hydrophobicity of the chain to increase and the chain contracts, forming a loop where it keeps and "protects" the important particles. A large number of these partly hydrophobic structures aggregate due to Van der Waals forces and thus form large flocculated particles. PE's with very high molecular weight, such as cationic polyacrylamides, are particularly effective flocculants due to binding flocculation [22].

Nonstoichiometric PEC's, ( $Z \neq 1$ ) which have a net charge, are even more effective flocculants than PE's since NPEC's have both hydrophilic and hydrophobic regions so they can adsorb onto both hydrophilic and hydrophobic particles. (Fig. 1.2).

PE's and PEC's also improve liquid-water removal or drainage. Fine or filler particle tend to be retained in the sheet by a filtration mechanism where they tend to plug the pores in the structure, decrease the permeability and decrease thus the drainage rate. PE's act as flocculants, redistributing the fines and the fillers so they don't plug the pores, thus improving the drainage rates [22].

PE's usually used in papermaking are: polyacrylamides, polyamines, polyamides, cationic starch [22].

b. *In municipal waste water treatment:* During the late 1950's water soluble PE's and PEC's started replacing the inorganic flocculants used to agglomerate suspended solids, phosphate compounds, nitrogen compounds and pathogenic compounds in municipal water. PE's have higher removal efficiency due to their higher molecular weight and their ability to flocculate solids. PE's have lower costs and reduced material-handling problems [23].

c. *Flocculation of chrome-plating wastes:* In the metal finishing industry, PEC's and PE's have partially replaced the commonly used method of reduction-precipitation using ferrous sulfate and lime [24] .

d. *Petroleum recovery:* PE's used in this case are: polyamines, vinyl polymers, modified celluloses, polysaccharides. They serve in: 1)water-loss control, 2)viscosity control, 3)flocculation, 4)suspensions, 5)turbulent friction reduction, 6)mobility control. Again here PE's act as "size controllers" due to their ability of flocculating, or expanding depending on their environment. Thus they control the friction coefficient of a particle, and as a result the viscosity, a property extremely useful in drilling techniques [25].

Generally the technique involves an inexpensive fluid (PE solution) that exhibits different viscosities in varying environments in a petroleum reservoir and increasing recovery.

e. *Selectively permeable membranes for dialysis and ultrafiltration:* Anion polystyrene sulfonate PSS and cationic PVTACl (poly(vinylbenzyltrimethylammoniumchloride)), comprise a well-known PEC system developed by Amicon Corp. [3]. "The permeability and permselectivity of solutes through membranes made from these complexes are controlled by moisture sorption and water content" [3]. Generally water sorption is easy to control since it is a function of chemical structure of polymer components, charge density, ratio Z, pH, salt concentration and procedure employed in complex preparation.

Permeability and permselectivity of ionic solutes through a PEC gel

membrane, depend on its water content, the site binding properties of the ions, charge density and excess of net charges.

f. ***Microencapsulation agents:*** Polyelectrolyte complexes of gelatin and gum arabic, are used as microencapsulation agents, i.e. carbonless copy paper [3].

g. ***Biomedical implants :*** PEC's, especially those with a slight excess of sulfonate charges, have antithrombogenic properties [3].

h. ***Separation of protein mixtures:*** It is possible to separate a mixture of proteins by adding a polyanion, and adjusting the pH of the solution between the isoelectric points of the two proteins. Precipitation occurs, which is maximum at the point of electroneutrality. Adjusting the pH, so that it is equal or close to the isoelectric point of each protein, precipitation is reversed, so it is possible to obtain each protein in solution, separately [3]. A mixture of proteins bovine serum albumin (BSA) and oxyhemoglobin, can be separated by adding the polyanion polymethacrylate, at a pH between the isoelectric points of the two proteins.

### 1.2.2 PEC's in Biological systems

This is probably the most important area in PEC's and PE's applications, due to the great importance of charged, water-soluble polymers in biochemical processes. For example Regelson [26] writes : " We are dealing with polymers that can be likened to blood proteins which redistribute themselves via blood or lymphatic circulation, or, through cellular transport, with the cooperation of phagocytic cells or adsorbing cell surfaces. Solubility is a function of molecular weight and charge, interacting with the natural proteins or lipoproteins of the tissue fluid or cell surface".

The similarity of synthetic PE's to proteins, glycoproteins, polynucleotides make them able to control a variety of biologic-responses "related to "host defense reactions which include resistance to viral, bacterial,

protozoal and fungular infections. In some way PE's mimic the action of infecting organisms and thus modify their action on the host." Other processes that PE's can control are enzyme activity, the regulation of cell division, intravascular coagulation, nuclear informational transfer [26].

Some examples in older literature mention the heparoids, whose action immitate that of heparin, a native acid mucopolysacharide. Synthetic PE's of this type are polysulfonates, pyran copolymers and related polycarboxylic, maleic anhydride copolymers. They function as anticoagulants and lipolytic agents. The anticoagulant effect of heparin or heparinoids and "its possible relation to calcium binding is also related to inhibition of tumor growth" [26].

**Immunostimulants:** Kabanov et al. have done extensive research on the biologic activity of the PE's and PEC's [19,27,28,29,48,49,50]. In particular the immunostimulant activity of various PE's was described [27]. Pasteur's method of vaccination from 1881, is the principle method in immunology practise. Attenuated or killed microbes (antigens) are introduced in an organism to cause the organism produce the antibodies (special proteins) which bind to antigens and to the foreign proteins and polysacharides of the pathogen and block them. "The immune response strength is characterized by the number of antibodies or antibody forming cells produced by the organism in response to the antigen" [27]. There are some serious drawbacks to this method. The most serious one is that "the strength of the organism protective reaction to the introduced antigens is genetically programmed by special immune response genes(Ir-genes). Thus, the efficiency of the immune response is a function of these genes. To overcome this restriction, several studies [27,28,29] have been carried out on the activation of the immune system with the help of different PE's. These immunostimulant PE's act by complexing with the antigens, which lead to cooperative sorption on the surface of the immune cells.

B-lymphocytes and T-lymphocytes are the most important components of mammalian immune systems. B-lymphocytes are the "antibodies factory" and their operation begin as soon as they receive the signal by the T-lymphocytes

which recognise antigens. PE immunostimulants attached to the individual antigens activate B-lymphocytes without the help of T-lymphocytes and result into the production of highly specific antibodies. Furthermore, the antigens attached on the PE with strong chemical or adsorption bonds, can "survive" in the "unfriendly" environment of the cell for several hours until they manage to "switch on " the immune system.

In summary, PE's immunostimulants open the way to artificial vaccines which will secure and increase the specific immune response, its T-independence, and the absence of Ir-gene control of its strength.

PE's immunostimulants are: polyacrylic acid (PAA), copolymers of acrylic acid and vinylpyrrolidone, poly-4-vinylpyridine (PVP) etc.[27] .

***Tool for efficient cell transformation:*** Nucleic acid penetration into the cell increases with increasing hydrophobicity ("artificial hydrophobization")[28]. In case of DNA (polyanion), hydrophobicity can be introduced by cooperative binding of its charges with polycations which produces hydrophobic sites, resulting in a polyelectrolyte complex structure. This structure does not prohibit the recognition of DNA by the enzymes but does increase the efficiency of the DNA transfer through a cell membrane. This transformation efficiency can be regulated by increasing polycation concentration or its length. Kabanov reports an experiment of transformation of *B.subtilis* cell by pBC16 plasmid. Incorporation of the plasmid DNA into a PEC with PVP leads to a considerably increase of transformation efficiency [28]. "The polycation complexed with DNA represents a "building block" which can be easily conjugated with any target recognizing molecule." The DNA molecule is addressed to the target cell. Wo et al. as in Kabanov[28] "realized *in vivo* transformation of liver cells by the plasmid incorporated into PEC with poly-L-lysine coupled with liver-specific hormone."

A second advantage of this incorporation of DNA molecules into PEC's is that they are protected from cleavage by nucleases present in living organisms

[28], so this way DNA is "saved" from elimination on its travel to the target cell.

In summary, PEC structures can be regarded as "mimic of artificial virus with the "core" formed by nucleic acid and the cover containing receptor recognizing molecules which can interact with the cell membrane" [27].

### 1.3 Objectives

The PEC system studied in this work was NaPSS (sodium polystyrene sulfonate) and poly-L-lysine hydrobromide (PLL) dissolved at very dilute concentration in water with added NaCl. These polymers were chosen because there is a great deal known about their pure solution behavior, and they were available in molecular weight ranges that permitted a detailed study of the effect of host/guest molecular weight on PEC formation.

There were several questions that were addressed in this work. These were:

(1) Do low molecular weight "guest" polyelectrolytes bind with high molecular weight "host" polyelectrolytes at all values of  $Z$ , or only above critical values of  $Z$  where large-scale aggregation is observed?

(2) How is the critical  $Z$  value,  $Z_c$ , related to ionic strength, guest or host polyelectrolyte linear charge density, temperature, and host/guest molecular weight?

(3) How do the initial conformations of either the host or guest PE affect binding?

(4) Do the PEC's formed at  $Z > Z_c$  initially have equilibrium structures and, if not, can temperature changes lead to PEC's with equilibrium structures?

Therefore, our objectives were to:

(1) Measure  $Z_c$  and host PE size for  $Z < Z_c$  as a function of ionic strength, pH, temperature and molecular weight of host and guests PE's.

(2) Vary ionic strength, pH, and temperature of the initial host and guest PE solutions to vary their conformations.

(3) Once PEC aggregates form for  $Z > Z_c$ , cycle the temperature to break up the aggregates and allow them to reform structures that are possibly closer to equilibrium.

(4) Evaluate existing theories for PEC's formation with the experimental results, in an effort to further refine fundamental understanding of PEC formation and structure.

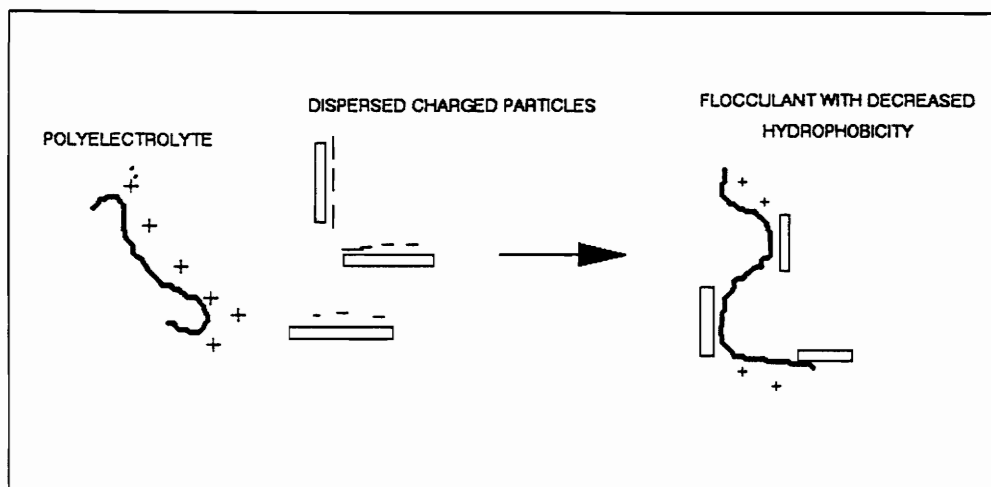


FIGURE 1.1 POLYELECTROLYTE'S ACTIVITY AS FLOCCULANT

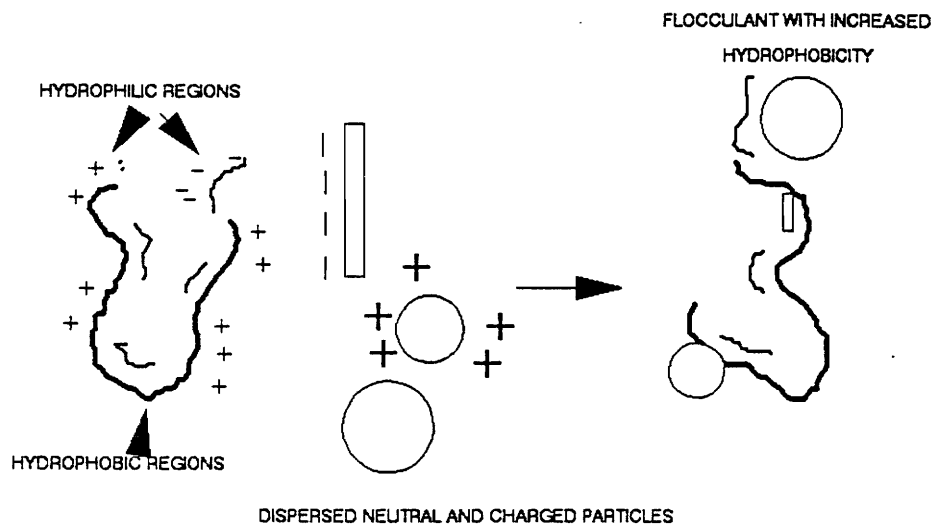


FIGURE 1.2 POLYELECTROLYTE COMPLEXES' ACTIVITY AS FLOCCULANTS

## **2.0 PHYSICAL CHEMISTRY OF PEs & PECs**

### **2.1 Introduction**

Ample data in the literature demonstrate the effect of polymer molecular structure and solution condition on the conformation and, hence, properties of polyelectrolytes and polyelectrolyte complexes. This chapter concerns the physical chemistry of polyelectrolyte solutions in section 2.2 and of polyelectrolyte complexes in section 2.3. In the latter section, particular emphasis is placed on the mechanism of formation, and the structure of polyelectrolyte complexes.

## 2.2 Polyelectrolytes

Polyelectrolytes are water-soluble macromolecules having many ionizable groups. In solution they dissociate into polyvalent macroions (polyions) and a large number of small ions of opposite charge (counterions). The high charge of the macroion produces a strong electric field. The strong electric interactions between the polyvalent macroion and counterions account for the characteristic properties of polyelectrolytes [5], including large expansion factors, second virial coefficients which depend on ionic strength and pH, and low counterion activity coefficients [45,46]. By comparison, water-soluble nonion polymers, tend to have relatively low expansion factors and second virial coefficients.

### 2.2.1 Properties and behavior

Dilute solution properties of polyelectrolytes can be described in terms of electrostatic repulsions between the charges on the chain. According to Debye-Huckel theory [37], the ion atmosphere surrounding each charge, has a potential at a distance  $r$  proportional to  $\frac{e^{-\kappa r}}{r}$ , where  $\kappa$  is the Debye length. In order to bring two same charges closer, the electrostatic free energy is positive, and the smaller the  $\kappa$ , thus the smaller the ionic strength, the more positive the free energy is going to be. The chain, thus, exhibits its extend conformation which is thermodynamically favored. At high ionic strengths, the potential surrounding each charge is lower, so the electrostatic free energy of bringing two same charges closer is smaller. The chain assumes the coil conformation which is of higher entropy and thermodynamically favored.

Dilute polymer solutions properties are often described in terms of the excluded volume  $z$  and chain stiffness  $L_k$  effects [7]. The large expansion factors for polyelectrolytes are due to a combination of chain stiffness effects,

characterized by the Kuhn length  $L_k$ , and excluded volume effects, characterized by the excluded volume parameter  $z$ . The Kuhn length is the contour distance along the backbone over which the backbone is rodlike. Repulsion between fixed backbone charges leads to greater stiffness and higher values of  $L_k$ . The magnitude of the electrostatic repulsion is governed by the electrostatic potential around the backbone which, in turn, is controlled by the polymer charge density and the solution ionic strength. Very strong repulsion, i.e., at high charge density and low ionic strength, can cause polyelectrolytes initially in a random coil state to become rodlike.

Excluded volume effects refer to the volume around a given polymer segment from which other segments are excluded. Electrostatic repulsion governed by charge density and solution ionic strength determines this segmental excluded volume. As the segmental excluded volume increases with either decreasing ionic strength or increasing charge density, the polyelectrolyte chain expands.

Thus both  $L_k$  and  $z$  are strongly affected by polymer charge density and ionic strength. Charge density is a structural feature, i.e., charges/monomer, but it is also affected by solution parameters such as pH, which can easily change the PE conformation by modifying the number of charges on the chain, and by temperature [3,9,38-44].

### 2.2.2 Chemical structure

Figure 2.1 gives a picture of the chemical structures of some different PE's [5].

Polyacrylic acid (Fig. 2.1a) is a commonly used PE whose degree of dissociation in pure water is very low. On the addition of alkali, however, the carboxyl groups are dissociated and the macroions gain an increasing number of negative charges producing counterions [5].

In Figure 2.1b a copolymer of polyvinyl alcohol and polyacrylic acid is shown. Polyacrylic acid can be charged with the addition of alkali. In this case the final charge of the macroion is regulated by the ratio of the two monomers, i.e. the original molecular structure [5].

Finally, Deoxyribonucleic acid neutralized (DNA) is one of the very important anionic biopolymer [5].

### 2.2.3 Physical chemistry of PE's

Many efforts have been made to predict solution properties such as viscosity  $\eta$ , osmotic pressure  $\pi$ , and radius of gyration  $R_g$ , in terms of molecular parameters such as molecular weight and charge density, and solution parameters such as ionic strength, pH, and polymer concentration. Highly and semidilute concentrations regimes studies have received special attention by many authors [10,11,12,13], since these are the interesting "working" regimes for large scale industrial applications.

The wormlike chain model theory proposed by Odijk and Houwaart [14] has been quite successful in describing the thermodynamic properties of dilute PE solutions including radius of gyration  $R_g$ , and second virial coefficient  $A_2$ . This model was initially developed for the line charge limit, i.e., for zero backbone diameter [7], and later was modified to include the effect of finite backbone diameter [7,10, 45,46].

The relevant electrostatic interactions include the repulsive interactions between the fixed charges on the chain involving both pairs close to one another and distantly connected on the same chain, as well as pairs on different polymer chains [1]. These interactions are governed by the electrostatic potential  $\psi$ , which is described by the scaled form of the Poisson-Boltzmann equation written in cylindrical coordinates with the origin fixed at the center of the polymer

backbone [45,46]:

$$\nabla^2\psi = \sinh\psi \quad (2.1)$$

where  $\psi$  is the dimensionless potential related to the unscaled potential  $\psi^*$ , by:

$$\psi = \frac{\psi^*e}{kT} \quad (2.2)$$

and the dimensional radial distance from the polymer  $r$ , is related to the unscaled distance  $r^*$  by:

$$r = \frac{r^*}{\kappa^{-1}} \quad (2.3)$$

where  $\kappa$  is the Debye length describing the effective range of electrostatic interactions in solution and is defined by:

$$\kappa^{-1} = (8\pi L_b I)^{-1/2} \quad (2.4)$$

and  $L_b$  is the Bjerrum length defined by:

$$L_b = \frac{e^2}{4\pi\epsilon kT} \quad (2.5)$$

where  $e$  is the electric charge and  $\epsilon$  is the dielectric constant [44,45].

Numerous solutions exist for equation (2.1) in various limits. The most generally useful solution involves matching an analytic solution for (2.1), valid near the polymer backbone, with solution for the linearized version of (2.1), where  $\sinh\psi \simeq \psi$ , which is valid far away from the chain. This approach has been discussed by a series of recent papers [45,46].

### 2.2.3.1 The Kuhn length

The Kuhn length  $L_k$  is related to the contour length,  $L$ , by:

$$L = N_k L_k \quad (2.6)$$

where  $N_k$  is the number of Kuhn segments in the chain. In a nonionic polymer in solution the backbone contour fluctuates due to Brownian motion and steric hindrances resist the bending [10]. In PE's solutions electrostatic repulsions also resist this bending. Thus, the total Kuhn length for PE's is:

$$L_k = L_o + L_e \quad (2.7)$$

where  $L_o$  accounts for the steric contributions and  $L_e$  accounts for the electrostatic repulsions. The electrostatic interactions term,  $L_e$  is described by the following expression: [4, 45,46 ]

$$L_e = \frac{G(a\kappa^{-1}, \frac{L_b}{L_c})}{2\kappa^2 L_b} \quad (2.8)$$

The ratio  $L_b/L_c$ , with  $L_c$  representing the average spacing along the backbone, defines a dimensionless backbone charge density.

The line charge theory by Odjiik and Houwart [14] assumes low electrostatic potentials around the polymer backbone. This crude assumption results in the value  $G=1$  for  $L_b/L_c > 1$  and an effective charge density [4,45,46]:

$$\left[\frac{L_b}{L_c}\right]_{eff} = \frac{L_b}{L_c} \quad \text{for } \frac{L_b}{L_c} < 1 \quad (2.9.a)$$

$$\left[\frac{L_b}{L_c}\right]_{eff} = 1 \quad \text{for } \frac{L_b}{L_c} > 1 \quad (2.9.b)$$

For PE's with stoichiometric charge density  $L_b/L_c > 1$ , the electrostatic potentials around the backbone is so high that the line charge theory is in substantial error and so a numerical solution of equation (2.1) is needed to calculate  $(L_b/L_c)_{eff}$  [10,45,46].

The effective ionic strength of the solution due to added salt and dissociated counterions is given by:

$$I = I_s + \frac{L_{mon}}{2L_b M_{mon}} \left[ \frac{L_b}{L_c} \right]_{eff} C_p \quad (2.10)$$

where  $I_s$  is the ionic strength due to added salt,  $M_{mon}$  is the monomer molecular weight and  $C_p$  is the PE concentration.

### 2.2.3.2 Excluded volume

The excluded volume parameter  $z$  is dimensionless and is proportional to the volume from which a polymer segment of  $L_k$  excludes other segments [10, 45,46].

For very long wormlike chains :

$$z_{\infty} = \lim_{N_k \rightarrow \infty} (z) = \left( \frac{3}{2\pi L_k^2} \right)^{3/2} \beta N_k^{1/2} \quad (2.11)$$

where  $\beta$  represents the volume from which one segment exclude all others, and is related to the mean potential energy  $V$  with which a given segment interacts with its neighboring segments. This is usually dominated by electrostatic repulsion [10,45,46] and can be calculated by averaging segment-segment interactions over all possible orientations and separations with a given molecule as:

$$\beta = \int \langle 1 - e^{-V/kT} \rangle d^3r \quad (2.12)$$

Complete description of the model can be found in papers by Davis and Russel [10,45].

With the means of the above nonlinear electrostatic model, the radius of gyration  $R_g$  can be calculated.

### 2.2.3.3 Radius of gyration

The size and the conformation of a polyelectrolyte is a function of the electrostatic interactions. The electrostatic wormlike chain theory accounts for these ionic interactions, in dilute solution of monodisperse polyelectrolytes in terms of chain stiffening and excluded volume effects [45].

At low ionic strengths, a polyelectrolyte can have an extended end-to-end distance due to strong excluded volume and chain stiffening effects. The total

chain expansion factor,  $\alpha_T$ , is given by:

$$\alpha_T = \alpha_z \frac{R_g^0}{(R_g^0)_\theta} \quad (2.13)$$

where  $\alpha_z$  is the expansion factor due to excluded volume effects,  $R_g^0 = R_g^0(L_k)$  is the radius of gyration due to chain stiffening, and  $(R_g^0)_\theta$  is the unperturbed  $R_g$  at theta conditions [45]. Theta conditions are the solution parameters, i.e. temperature, nature of solvent, concentration, at which polymer chain has each unperturbed dimensions. Above theta conditions, polymer chain is in its "swollen" dimensions, it is soluble in the particular solvent, and the solvent is a good solvent. On the contrary a polymer chain below theta conditions is in its collapsed dimensions, it is not soluble in the particular solvent and the solvent is

a "bad solvent".

According to the wormlike chain model, the radius of gyration, in terms of the Kuhn segments, characterizing the backbone segments, and assuming no excluded volume effects is: [45]

$$R_{g0}^2 = L^2 \left[ \frac{1}{6N_k} - \frac{1}{4N_k^2} + \frac{1}{4N_k^3} - \frac{1-e^{-2N_k}}{8N_k^4} \right] \quad (2.14)$$

where  $N_k$  is the number of Kuhn segments.

In the limit of  $N_k \rightarrow \infty$ , equation (2.14), reduces to the radius of gyration for a Gaussian coil and, for  $N_k \rightarrow 0$ , reduces to the rod limit [45].

Modifications accounting for the excluded volume effect, involve the excluded volume parameter  $z$ , defined by equation (2.11). The chain expansion factor for the radius of gyration,  $R_{g0}$ , due to excluded volume effects is given by the Yamakawa-Tanaka equation [45] :

$$\alpha = \{ 0.541 + 0.459(1 + 6.04z)^{0.46} \}^{1/2} \quad (2.15)$$

"The radius of gyration is then a product of the chain expansion factor due to excluded volume effects,  $\alpha(z)$ , and the radius of gyration due solely to chain stiffening,  $R_{g0}$ " [45] :

$$R_g = \alpha(z) R_{g0} \quad (2.16)$$

For a random coil polymer, radius of gyration,  $R_g$ , is related to the hydrodynamic radius,  $R_H$ , by [55] :

$$R_H = 0.665R_g \quad (2.17)$$

## 2.2.4 Characterization Techniques for PE's solutions.

Techniques often used to characterize polyelectrolyte solutions, are i) static light scattering, which provides thermodynamic equilibria measurements, radius of gyration, second virial coefficient ii) dynamic light scattering (DLS) which provides information on dynamic properties like hydrodynamic radius iii) viscometry measurements, which provides information on the hydrodynamic radius of the polymer, (iv) conductance measurements [20], and (v) fluorescent dye binding experiments. In our work we used DLS to characterize the polyelectrolyte and polyelectrolyte complexes solutions. Before describing this technique, the dilute and semi-dilute concentration regimes will be described.

### 2.2.4.1 Concentration Regimes

In dilute solutions the polymer molecules are separated by solvent molecules. As the polymer concentration increases the individual chains begin to overlap considerably. The overlap concentration which also marks the transition to the semi-dilute regime is defined by :[7,11,12,13]

$$C^* = \frac{DP}{4/3\pi R_g^3} \quad (2.18)$$

where DP is the degree of polymerization. Above  $C^*$  intermolecular entanglements produce cooperative modes analogous to those of permanent network and the characteristic dimensions is the correlation length  $\xi$  which represents the average distance between the successive entanglements along a chain. The correlation length is independent of the molar mass of the chain and concentration dependent according to a  $C^{-0.75}$  power law [11,12,13].

#### 2.2.4.2 Dynamic Light Scattering

Dynamic light scattering measures the translational diffusion coefficient,  $D_T$ , of the polymer molecules in solution. According to deGennes DLS performed at low concentrations should give information about the translational diffusion coefficient of the individual coils [11]. The diffusion coefficient is related to the hydrodynamic radius,  $R_H$ , of the polymer coil through the Einstein-Stokes equation:

$$D_T = \frac{kT}{6\pi\eta R_H} \quad (2.19)$$

where  $k$  is the Boltzman factor and  $\eta$  is the viscosity of the solution.

In the semidilute regime where intermolecular interactions are significant and the coils interpenetrate, DLS probes cooperative diffusion modes of strongly entangled chains for which the correlation length  $\xi$  is the essential length scale so that:

$$D_T = \frac{kT}{6\pi\eta\xi} \quad (2.20)$$

The above relation holds when the chain is extremely long ( $l \gg \xi$ ).

Mandel [11,12,13] proved experimentally that for  $C \ll C^*$  (dilute regime) diffusion coefficient changes only slightly with  $C$ . When  $C \gg C^*$  a decrease of diffusion coefficient with  $C$  is observed, nearly independent of the molecular weight.

The critical concentration  $C^*$  is a function of the radius of gyration which in turn is a function of ionic strength. At very low concentrations diffusion coefficient does not practically change with concentration, but its value decreases with decreasing ionic strength [53]:

$$D_T = D_{T_0} \left\{ 1 + \left( \frac{K_{eff}^2}{2C_s} + A_2 \right) C_p \right\} \quad (2.21)$$

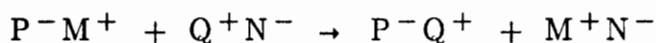
where  $D_T$  is the translational diffusion coefficient at polymer concentration  $C_p$ ,  $D_{T_0}$  is the translational diffusion coefficient at infinite dilution,  $K_{eff}$  is the effective charge of the macroion,  $C_s$  is the salt concentration and,  $A_2$  is the second virial coefficient which is characteristic of the excluded volume, thus ionic strength dependent. In the semidilute regime diffusion coefficient increases with increasing PE concentration.

#### 2.2.4.3 Viscosity

The intrinsic viscosity is a direct measure of the hydrodynamic volume of the isolated polymer molecule and thus viscometry can provide direct information of variations in experimental conditions. Polyelectrolyte molecules with flexible chains generally have more expanded conformations than those of nonionic polymers (particularly at high charge densities of the chain and low ionic strength of the solvent) because of the electrostatic repulsions between the fixed charges. Thus, the viscosity of PE's is frequently more sensitive to shear rate than that of nonionic polymers [1,2].

## 2.3 Polyelectrolyte Complexes

Polyelectrolyte complexes are intermolecular complexes formed from the reaction between two oppositely charged polyelectrolytes, in polar solvents.



where  $P^{-}M^{+}$ ,  $Q^{+}N^{-}$  are the polyelectrolytes [3,4,15].

Electrostatic interactions constitute the main attractive forces in polyelectrolyte complexes (PEC's) formation. The range of these forces is characterized by the Debye length,  $\kappa^{-1}$ . As ionic strength increases either by adding salt or by counterions released by the charged polymers, the Debye length decreases eventually to a point where attractive electrostatic forces become so weak that thermal forces with energy  $kT$  can break up the PEC. These forces are a function of polymer chain charge density,  $Z$  and, counterion valence. The polymer chain charge density, in turn, is a strong function of pH.

Other attractive forces playing a significant role in determining the PEC ultimately structure are:

- i) Hydrophobic forces which become essentially important as charge density decreases.
- ii) Hydrogen bonds
- iii) Van der Waals forces which are a function of structure and composition of the polymer chain [3,15].

### 2.3.1 Physical chemistry of PEC's

Polyelectrolyte complexes consist of a Host Polyelectrolyte (HPE) which is the polyelectrolyte in excess in a PEC solution and a Guest Polyelectrolyte (GPE) which is the polyelectrolyte present in relatively low amounts. The ratio

of the GPE equivalent concentration and HPE equivalent concentration,  $Z$ , is given by:

$$Z = \frac{[GPE]}{[HPE]}$$

If  $Z=1$  the PEC is stoichiometric (SPEC) and has a net zero charge. Thus, those SPEC's made of charged polymers with hydrophobic backbone are insoluble in polar solvents. If  $Z \neq 1$ , the PEC is nonstoichiometric (NPEC) and has a net charge [3,19].

PEC's solubility generally increases as  $Z$  approaches unity. Figure 2.2 [3] shows a conductometric titration of sodium polystyrene sulfonate and poly(vinylbenzyltrimethylammonium chloride) (PVBTAOL) where maximum precipitation occurs at the stoichiometric equivalence point and a minimum in the conductivity vs mixing ratio is observed.

NPEC's are insoluble if the GPE and/or HPE backbones are sufficiently hydrophobic, and soluble if the partially neutralized backbones are hydrophilic. In general, NPEC solubility increases as  $Z$  differs increasingly from unity. NPEC's can be formed when weak PE's bind together, or if there is poor accessibility of the ionic groups due to geometrical constraints, i.e., branching [3].

The structure of the complexes is a function of many factors such as temperature, pH,  $Z$ , solvent, and polymer chain structure. Tsuchida et al. [16] report that PEC's of pendent type (charges on the side chain) have an equimolar composition at any mixing ratio of two component polymers. They are insoluble in water "because of the increase in the hydrophobic property after the neutralization of the hydrophilic parts". However PEC's of integral-pendent type can form a water-soluble complex in addition to a complex with equimolar composition.

PEC's are solubilized greatly in the presence of salts. Solubilization increases with increasing  $I$  but it is also a function of the foreign salt valency.

The magnitude of the solubilization increases as the valency of the anionic component of the foreign salt increases. Electrostatic shielding effect of foreign salts of high valencies is substantial against the macrocation-macroanion attraction [17].

The critical condition defining the onset of PEC formation depend on the host and guest polymer structures, i.e. charge density, rigidity and conformation of the macromolecular chains as well as on the chemical environment, i.e. ionic strength, pH, temperature, concentration of the polymers, and nature of the solvent. The solution parameters are particularly important since they can affect the conformation of the chain. Blackwell et.al. [6,7,8,9], report: "a conformational change is induced in the presence of the polysaccharides". Blackwell et.al. studied PEC's comprised of PLL-C6 (poly-l-lysine, chondroitin 6-sulfate) [9]. Using circular dichroism, they determined that chondroitin (a polysaccharide) induced a conformation change in the polypeptide PLL. This conformation change was temperature dependent. At low temperatures ( $T \leq 10^\circ\text{C}$ ), PLL is mostly in the  $\alpha$ -helix conformation. The  $\alpha$ -helix conformation "melts" at a specific temperature ( $T=47^\circ\text{C}$ ) [9], above which PLL is totally transformed from  $\alpha$ -helix to a random coil conformation. At  $10^\circ \leq T \leq 47^\circ\text{C}$ , both conformations can be found [9,38,44]. The  $\alpha$ -helical directing effect for the PLL in PLL/C6 complex is also dissrupted upon increasing the ionic strength ( $I > 0.4\text{M}$ ) or decreasing the pH [9,38-44]. Detailed discussion of the pure PLL conformations is following in Chapter 5.

There are different events that can follow the formation of the PEC 's :

1. The PEC can stay in solution. This can lead to turbid solution if the PEC's are sufficiently large, i.e. above 100-200 nm.
2. Phase separation, so the solution is slightly turbid. In this case the coacervate phase has the highest concentration of PEC's and the dilute phase has a low concentration of PEC.
3. Precipitation, that usually follows the phase-separation step and it is a time dependent process.

Our DLS experiments described in detail in Chapter 4 and 5, were designed to probe the formation and structure of PEC's in solution, i.e. in step 1. Most prior experimental work on PEC's have focussed on steps 2 and 3.

### 2.3.2 The Coacervate phase

In ternary systems containing two dissimilar polymer components and a single solvent in which each polymer is soluble, phase separation often occurs such that each phase is enriched with only one of the polymer components [3,18]. PEC's, though, are different in that their polymer-polymer interactions are energetically favored. Phase separation still may occur but there is now a concentrated and a dilute phase both, containing both polymers. The concentrated, or coacervated phase, usually contains the two polymers in some fixed ratio regardless their initial mixing ratio [18].

The formation of the complex is described by the degree of the coacervation,  $\rho$ , which is the fraction of polymer in concentrated coacervate phase, the ratio of polymers concentrations in the concentrated and dilute phase  $\epsilon$ , and the intensity of coacervation  $\theta = \epsilon\rho$ . The degree of coacervation is at maximum when the polyions are present in electrically equivalent quantities. Increased charge density on the two macromolecules enhances the intensity of coacervation. The charge density of PE is a function of pH [3,18].

Both the degree of the coacervation and the intensity are complex functions of salt concentration. Figure 2.3 [18] presents the effect of the salt on the phase diagram for complex coacervation.  $[NM]$  denotes salt concentration and  $C_M$  is the initial mixture concentration. The area under the curve represents the two phases area (coacervate and dilute). The line of "equivalence" denotes the phase relationship for "symmetrical" mixtures (point of equivalence for the charges). At concentration  $C_M$ , the addition of low

molecular weight salt will raise  $[NM]$  to  $[NM]_T$  – at this point coacervation is suppressed. The difference  $[NM]_T - [NM]_E$  is the salt tolerance of the system. The intensity of the coacervation is directly related to the charge densities of the polyions. As they increase,  $\theta$  and salt tolerance increases.

Other factors affecting coacervation are the molecular weight heterogeneity of the two PE's and temperature. The higher molecular weight PE tends to segregate into the coacervate phase [3].

### 2.3.3 PEC's formation and Structure

Mechanisms for PEC formation and structure have been reported in a number of studies [3,19]. They were reviewed recently by Schmidt and Fish [3]. While the details of PEC formation are still not well understood, it is generally believed that PEC formation begins with initial pairing of opposite, fixed charges on HPE and GPE segments, which align themselves by bond rotations to form stable ionic cross links in a manner analogous to teeth aligning in a zipper [3]. This is followed by local realignment to adjust for short range errors during the ion pairing. The driving force of the complex formation is largely entropic owing to the release of microions. Cooperative effects facilitate the ion pairing since the formation of one cross-link promotes interactions of adjacent charges because of their forced proximity [3].

Hydrophobic interactions between polymer backbones or substituents also contribute to the complex forming process by determining solubility properties and the degree of swelling [13]. To date, no predictive model for PEC formation takes hydrophobicity and charge effects into account satisfactorily.

Some of the most detailed experiments on PEC formation and discussions of PEC formation mechanisms were presented by Kabanov [19]. This work showed that soluble products (NPEC) are formed only if the degree of

polymerization of HPE is greater of the degree of polymerization of the GPE. The solubility is also affected by a small molecular weight electrolyte whose amount and nature depends on the nature of the PE. When properly prepared NPEC's have equilibrium structures which allow them to be analyzed with a broad range of experimental techniques developed for studying equilibrium polyelectrolyte solutions. Kabanov, et al. used static light scattering to characterize the changes in NPEC structure with changing ionic strength,  $I$ , polymer ratio,  $Z$ , and molecular weight, for a PEC system consisting of PDMAEMA · HCl-PP. The molecular weight of the NPEC increased with  $Z$ , for  $Z < Z_{crit}$  and corresponds to the molecular weight of the HPE. The radius of gyration,  $R_g$  decreased as  $Z$  increased for  $Z < Z_{crit}$ , and it was in the range of HPE size (Fig. 2.4)[19].

Two extremes cases for PEC structure are described in the literature. One is the "scrambled egg" where charge neutralization is a random process in a network of oppositely charged polymers. The second is the "ladder type" where two chains are complexed to one another and the ionic cross links are ordered in a regular fashion. This arrangement is likely to produce a more crystalline complex [15]. The structures of most PEC's fall between those two and they depend on the structure of the individual PE's chains, the presence of salt, the nature of the solvent and the temperature. Both structures are depicted in Fig.2.6.

The "scrambled egg" structure forms NPEC's and is favored whenever the fixed charges on one or both polymers are inaccessible to the other, because of (i) branching, (ii) when the one of the polymer has a rigid backbone and the other a flexible one, (iii) when one or both polymers have integral charged groups rather than pendent ones.

Ladder structures tend to give stoichiometric polyelectrolyte complexes, SPEC's. They are formed when the charge spacings on both chains are equal or sometimes when scrambled structures rearrange, over time, to form ordered semicrystalline ladder structures. Extended chain conformations at low salt

concentrations favor ladder type structures of the complex whereas random ion pairing prevails at high salt concentrations, since chains are more coiled at high ionic strength [3].

Rapid formation of PEC's usually yield amorphous products. This occurs especially in concentrated solutions where random ion pairing between charged groups of different polymer chains result in the formation of "scrambled egg" type structures. In dilute solutions the initially formed amorphous structures, frequently rearrange themselves into more ordered structures with time [3,16,47]. Tsuchida observed [47], a fibrous and network-structured complexes, obtained by the combination of the solution of poly(methacrylic acid) and the solution of poly(N,N,N',N'-tetramethyl-N-p-xylylene-N-alkylene diammonium dichloride) (poly[(dimethylimino)ethylene(dimethylimino)methylen-1,4-phenylenemethylene dichloride]). The formation of these structures is explained by the increased hydrophobicity, after complexing, which leads in a regularly growing along the direction of their main chain and finally to an expand to network structures by loosing their aggregating directions [47]. Kabanov, et.al. has shown that high ionic strengths favor rearrangement of PEC structures due to weakened electrostatic forces [19].

NPEC's are considered to have a conformation of double-strand ladder but they are not necessarily extended rods. On the contrary, because of their increased hydrophobicity they must show a tendency to fold up at the sides, forming drop-shaped clusters so that the requirement of minimum free energy is met (Fig 2.5) [19]. In water the hydrophobic double stranded sections segregate due to nonpolar interactions and the hydrophilics sections are responsible for the NPEC's solubility. In dilute solutions this segregation tends to be intramolecular in structure whereas intermolecular aggregation is favored in concentrated solutions. Double strand sections show an increased rigidity and a high hydrophobicity. That is why NPEC's overloaded with GPE ( $Z > Z_{crit}$ ) lose their solubility in water. Kabanov concludes by considering the NPEC as a block-copolymer with rigid hydrophobic parts and flexible hydrophilic [19].

Excluded volume is a key parameter in PEC's as well as PE's. The second virial coefficient,  $A_2$ , is a measure of intermolecular excluded volume. For a pure polyelectrolyte in solution, a simplified theory for  $A_2$  gives:

$$A_2 = \frac{10^3 z^2}{4M^2 I} \quad (2.22)$$

where  $z$  is the effective charge of the polyanion,  $M$  is the molecular weight,  $I$  is the ionic strength of the solution [19]. For a dilute solution where each solute molecule has an excluded volume  $u$ , the second virial coefficient,  $A_2$ , is [35]:

$$A_2 = 1/2 \frac{N_A u}{M^2} \quad (2.23)$$

where  $N_A$  is the Avogadro number,  $M$  is the molecular weight of the polyelectrolyte. By analogy with equation (2.22), the main contributions to the excluded volume and hence  $A_2$  of an NPEC is made by electrostatic repulsions of similarly charged units of the single strand hydrophilic group. From the above equation we also see that high ionic strength will cause a lower excluded volume due to ionic screening of the unneutralized fixed charges on the NPEC.

Summarizing Kabanov et.al.'s work: (1) Low molecular weight salts cause dissociation of intermolecular ionic bonds and this is accompanied by a rearrangement of HPE and GPE segments and the appearance of compact conformation of NPEC particles. This increase in compactness causes a decrease in the entropy of mixing in the polymer-solvent system which is compensated by an increase to the internal combinatorial entropy of the NPEC due to different conformations that the molecules can have because of the increasing number of loop-shaded defects. (2) When the fraction of ionic bonds in the chain become sufficiently small, the increase in the combinatorial entropy cannot compensate for the degree at the entropy of mixing so interchange by GPE short chains between different NPEC particles occurs. Some of the NPEC chains become depleted in GPE and become considerably more extended.

In recent work done by Chatterjee et al.[20], another theoretical and experimental approach is reported. Measurement were made of reduced viscosity  $\eta/C_p$ , pH and conductance versus  $Z$  of an aqueous solution of PEI (Polyethylenimine) by adding PMA (Polymethacrylic acid). As the PMA was added, the reduced viscosity fell initially. This was interpreted as follows: PEI is a weak base, however is observed in an extended conformation in aqueous solution (probably because of repulsive forces between alike forces). Upon adding PMA, the PEC forms, resulting in a partial neutralization of the charges so there is a shrinkage due to increased hydrophobicity. This causes a drop in reduced viscosity. For  $Z > 1/4$  an abrupt change in reduced viscosity was observed due to the formation of ladder like structures between the complementary binding sites of the component PEC's. As a result, the rigidity of the macromolecular chains likely increased, resulting in the abrupt rise in the reduced viscosity. The reduced viscosity also have risen due to the formation of relatively large intermolecular PEC aggregates.

The conductance decreased with increasing  $Z$  up to  $Z = 1/4$  due to acid base reaction. However, increasing  $Z$  for  $Z > 1/4$  resulted in increasing conductance. A continuous drop in pH with increasing  $Z$  was observed, during all stages of complex formation due to the addition of the strong acid, PMA.

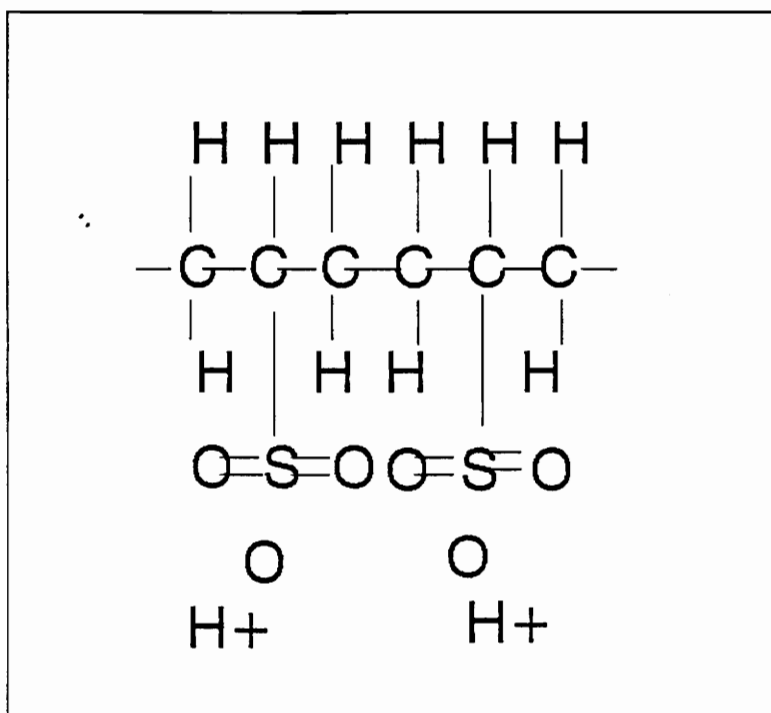


FIGURE 2.1 (A) POLYACRYLIC ACID PARTIALLY NEUTRALIZED

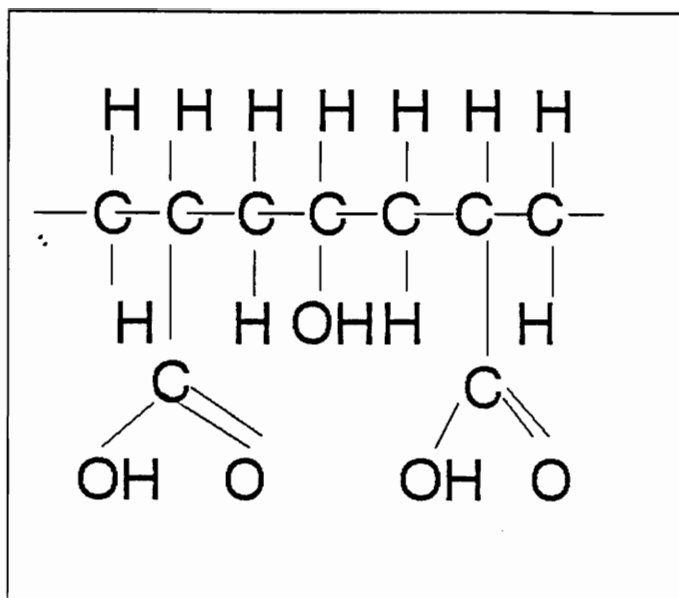


FIGURE 2.1 (B) COPOLYMER OF ACRYLIC ACID AND VINYL ALCOHOL

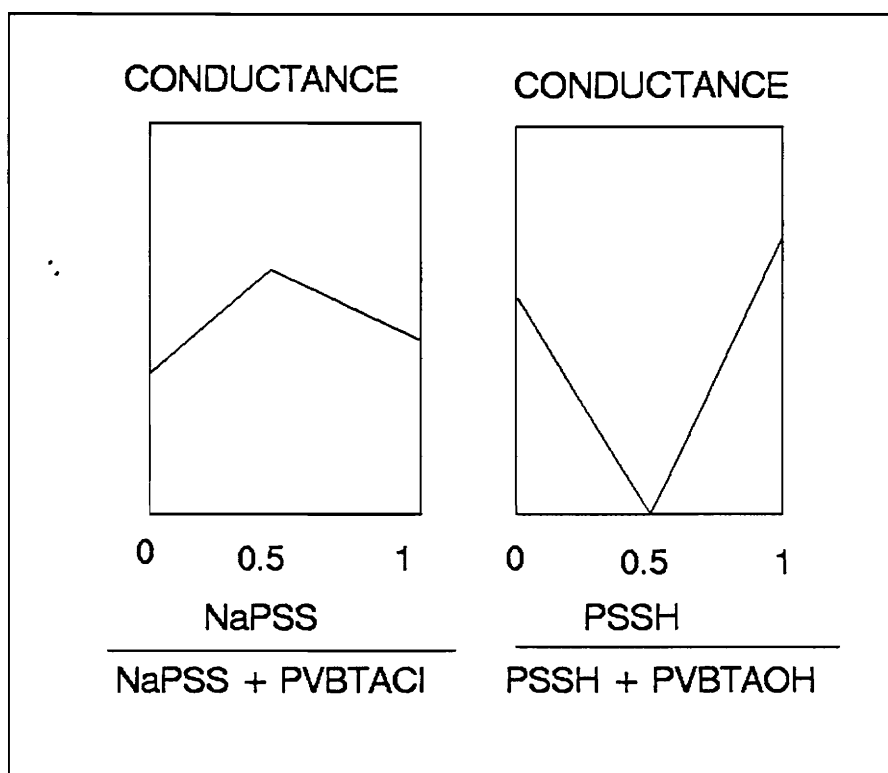


FIGURE 2.2 CONDUCTOMETRIC TITRATION OF SODIUM POLYSTYRENE SULFONATE AND PVBTACL.

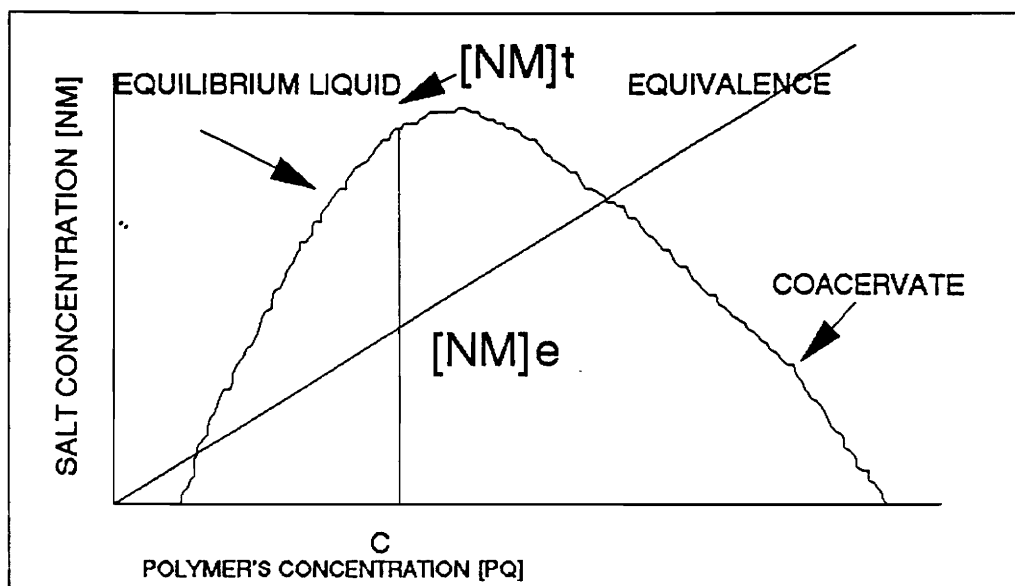


FIGURE 2.3 THE EFFECT OF SALT ON COMPLEX CONCENTRATION

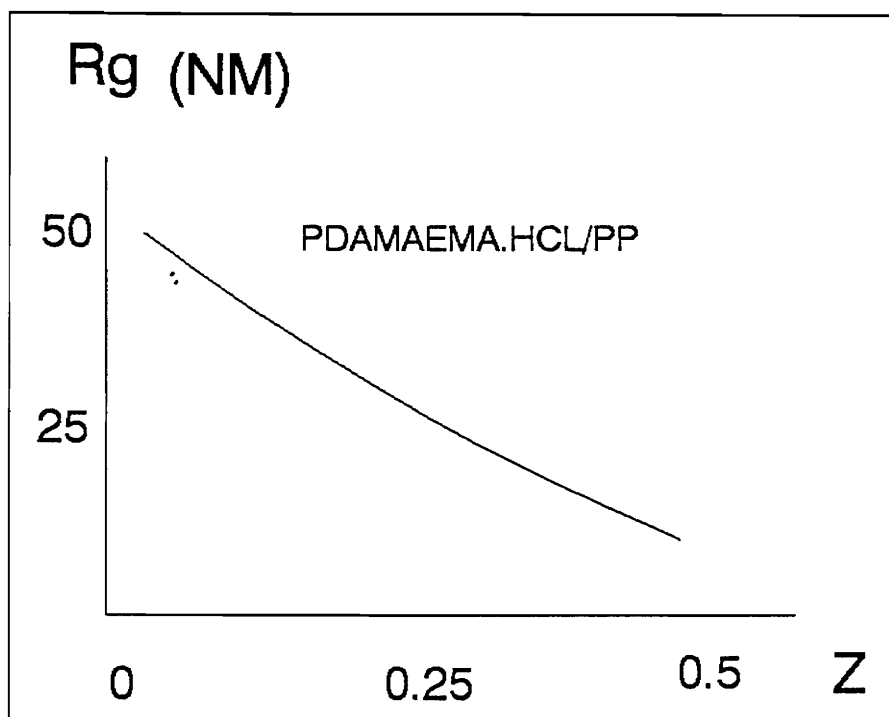


FIGURE 2.4 DEPENDENCE OF  $R_g$  OF AN NPEC ON  $Z$ .  
 CONDITIONS: pH=4, I=0.1M NaCl, T=20°C.

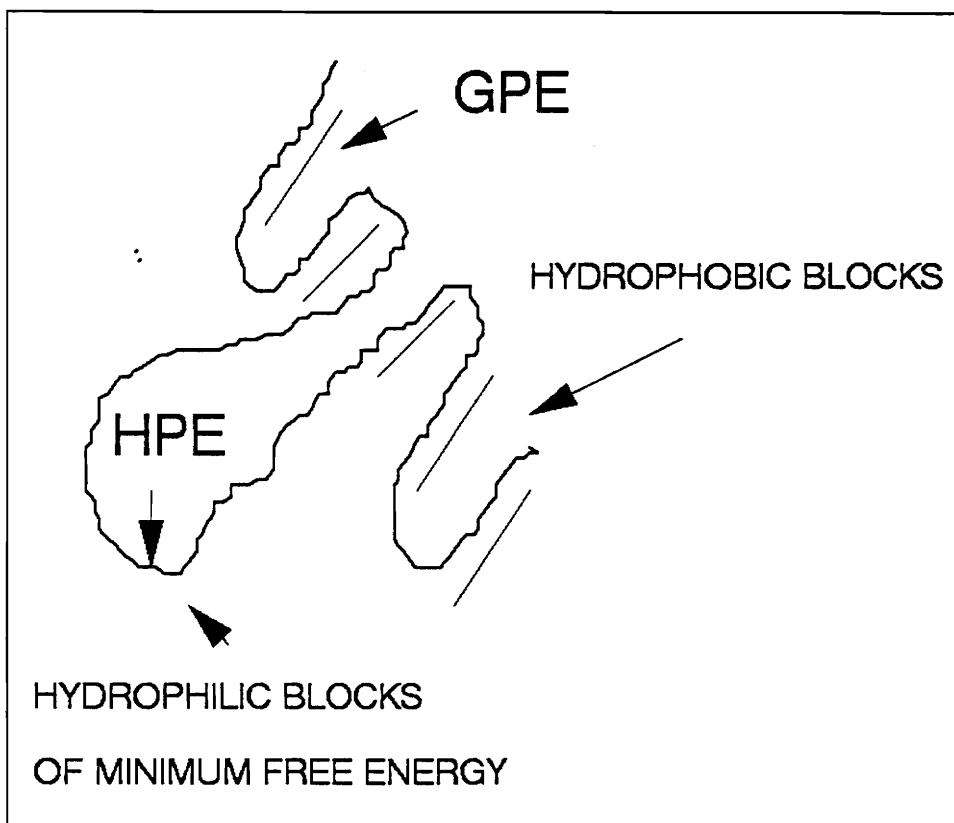


FIGURE 2.5 KABANOV'S PICTURE FOR PEC'S STRUCTURE

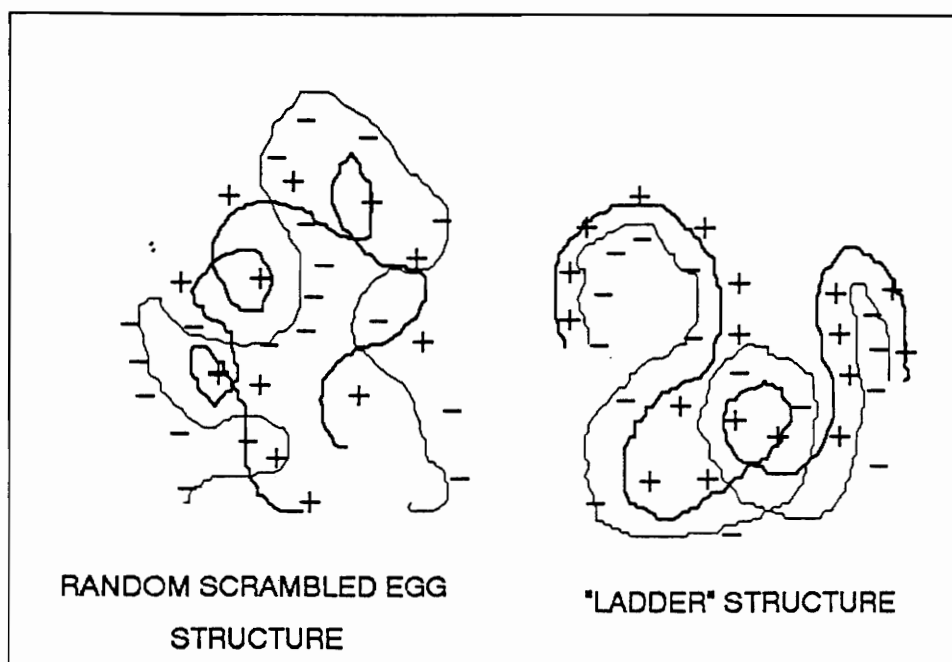


FIGURE 2.6 STRUCTURES OF NPEC

## 3.0 EXPERIMENTAL

### 3.1 Materials

The materials that have been used in this work are presented in Tables 3.1.1 and 3.1.2.

**Table 3.1.1 Structural Parameters for polyelectrolytes**

Polymer type	$M_{mon}$	$L_{mon}$	MW	$M_w/M_n$	Lot#
NaPSS <sup>1</sup>	206.2	0.252nm	$1.2 \times 10^6$	2.2	17
NaPSS	206.2	0.252nm	$2 \times 10^5$	1.56	26D
PLL <sup>2</sup>	189.02	0.252nm	10,200	1.3	128F-5033
PLL	189.02	0.252nm	50,000	1.31	69F55111

- (1) Sodium Polystyrene sulfonate from Pressure Chemical Co., Pittsburg,PA.
- (2) poly-L-lysine from Sigma Chemical Company.

**Table 3.1.2 Table of materials**

<b>Material</b>	<b>Purchased from</b>	<b>Specifications</b>	<b>Lot#</b>
NaCl	Fisher	Crystal,ACS	S271-500
HNO <sub>3</sub>	Fisher	12M	
CH <sub>3</sub> OH	Fisher	Certified ACS	893770
Toluene	Fisher	99.9%, Reag.ACS	D24620
SiCl(CH <sub>3</sub> ) <sub>3</sub>	Petrarch		100,292
HCl	Fisher	Reagent ACS	892974
Water		Deionized,17.6mohm	
Decalene	Fisher	Reagent grade,ClassII	893711

### 3.2 Equipments

The equipment used in this work is described in Table 3.2.1.

**Table 3.2.1 Table of equipments**

Equipment	Model#	Details	Manufacturer
DLS <sup>1</sup>		BI2030AT correlator 136 channels 2 Watt Argon Laser	BROOKHAVEN
UV spectrophotometer	2400		GILLFORD
Wrist Action Shaker	75		BURELL
pH METER	SA720		ORION
Acrodisc filters		Hydrophilic, 0.2 $\mu$ m	FISHER
Syringes		Individually wrapped, sterile (5cc,10cc)	BDF

(1) Dynamic light scattering

### 3.3 Sodium Polystyrene Sulfonate(NaPSS)

#### 3.3.1 General information

SodiumPoly(styrene sulfonate) is the salt of Poly(styrenesulfonic acid) which is a very strong polyacid [1]. Its monomer structure is shown in Figure 3.1. NaPSS with a narrow molecular weight distribution is obtained by sulfonating polystyrene, which itself has a narrow distribution since it is prepared by a living polymerization method [1]. NaPSS with weight average/number average, ( $\frac{M_w}{M_n}$ ), values of 1.1 can be obtained this way.

Since the NaPSS was prepared by sulfonation of polystyrene, it is quite important to check the extent of this conversion, especially with commercial samples. This check can be done by carrying out elemental analysis for the sulfur content, by colloid titrations to estimate the content of polymeric acid groups [1], and by proton NMR. A sample of the NaPSS was analyzed in aqueous solution by proton NMR at Virginia Tech, and was found to be 100% sulfonated.

Another aspect that should be taken under consideration is the water content of the dry sample. It is very difficult, not to say impossible, to remove all the water from a dry sample since it is so hygroscopic. Even freeze-dried samples still contain about 2% water. Thus, NaPSS solutions concentrations cannot be accurately determined by conventional dry weight analysis.

The polymer content of a solution can be determined by UV absorption at 261.5 nm. The value of the extinction coefficient depends upon the degree of sulfonation, the degree of the tacticity and the ionic strength of the solution [1]. All the concentration measurements were performed with salt-free stock NaPSS solutions, using the extinction coefficient of 1834 cm<sup>2</sup>/gr reported by Mandel and Koene [11].

### 3.3.2 Solution Preparation

Due to  $\text{Na}_2\text{SO}_4$  impurities in Pressure Chemical's Lot#17, this polymer was dialyzed prior to use in experiments. However Lot#26D had already been dialyzed by Pressure Chemical and was used as received. Dry, powdered NaPSS was mixed with deionized water using a magnetic stirring bar in a beaker for almost 24 hours. Typically 2 grams were dissolved in approximately 200 mls of water. The solution were next dialyzed using molecular porous membranes (SPECTRA/POR2) were used to remove microions or simple electrolytes. The dialysis tubing was washed with deionized water before using, and after pouring the solution into it, it was sealed at both ends with SPECTRA/POR2 clamps. The membranes are manufactured from natural cellulose and have a molecular weight cutoff 12,000-14,000. Dialysis depends on the differential transport of solutes of different sizes across a porous barrier separating two liquids. The driving force is the concentration gradient. The NaPSS solutions were dialyzed against deionized water. During the first 12 hours the water was changed every three hours in order to keep the concentration gradient high enough. After that, the water was changed three times a day. The whole process lasted about 3 days.

The pH of the PSS solutions was measured and found to be typically in the range of [3.1 – 3.8] indicating that excess  $\text{Na}_2\text{SO}_4$  had been removed and that some  $\text{Na}^+$  counterions had been exchanged for  $\text{H}^+$  ions. Titration with NaOH was then performed to raise the pH to 7, giving a salt-free NaPSS stock solution. The equivalence point of pH=7 was sometimes overshoot, resulting in pH values of 10 and necessitating the addition of HCl, to reduce the pH to about 7. However, this does not lead to any significant error in the final ionic strength in the experiments, since the lowest ionic strength value studied was  $I=0.01\text{M}$ . Given a pH overshoot of 10, the added HCl necessary to reduce the pH to 7 led to excess NaCl in the stock solution of excess  $\text{NaCl} = 10^{\text{pH}_0 - 14}$ , where  $\text{pH}_0 = \text{pH overshoot}$ . Thus, for a pH overshoot of 10, the excess NaCl

concentration in the final, neutralized NaPSS stock solution was  $10^{-4}\text{M}$ , which is negligible. The final pH for the different solutions we used were in the range of 6.2 to 7.5.

### 3.3.3 NaPSS concentration measurements

The NaPSS concentration was measured with a Gillford UV spectrophotometer. Due to the presence of the aromatic phenyl ring, NaPSS can absorb in the UV spectra at 261.5 nm as mentioned above. The value of the extinction coefficient reported by Mandel et al.[11] is  $1834\text{ cm}^2/\text{gr}$ , for salt-free NaPSS solutions.

Salt-free NaPSS solution at four different concentrations were prepared to measure the concentration. Their optical densities were measured by the spectrometer. The absorbance OD of dilute solutions follows Beer's law where:

$$\text{OD} = \epsilon l c$$

where  $\epsilon$  is the extinction coefficient,  $l$  is the cuvette length which is a standard size of 1 cm, and  $c$  is the concentration of the solution in (gr/ml).

In order to calculate the concentration after these measurements, a graph of O.D.'s values vs  $\frac{\epsilon l}{\text{dilution factor}}$  was created. The observed points should fall

on a straight line. The slope of this line, estimated by first order regression analysis performed by SigmaPlot software, was the concentration. The goodness of the fit is given by the regression coefficient calculated also by the software, and in all case were greater than 99.8%. The results for the five different stock solutions are shown in Table 3.3.1.

**Table 3.3.1. NaPSS concentration measurements**

Molecular weight	Stock solution #	Concentration(g/ml)
1,200,000	1	$2.3425 \times 10^{-3} \pm 8.046 \times 10^{-4}$
1,200,000	2	$1.33 \times 10^{-3} \pm 2.832 \times 10^{-5}$
1,200,000	3	$2.33 \times 10^{-3} \pm 6.457 \times 10^{-5}$
1,200,000	4	$6.023 \times 10^{-4} \pm 4.54 \times 10^{-5}$
200,000	5	$3.8245 \times 10^{-3} \pm 1.378 \times 10^{-5}$

The  $\pm$  values represent 50% confidence limit error bars defined as  $\pm 2/3\sigma$ , where  $\sigma$  is the standard deviation of the slope of the line determined from equation [3.1] by linear regression.

### 3.4 Poly-L-lysine hydrobromide

#### 3.4.1 General information

PLL is an important polypeptide used commonly in biochemical research. Its structure is shown in Figure 3.2.. Like many polypeptides, PLL can exist in a variety of conformation in solution. These include random coil,  $\alpha$ -helix, an extended coil conformation, and an intermolecular  $\beta$ -sheet aggregated state [37-44,51,52]. The conformation transitions are affected by ionic strength, pH, and temperature [37-44,51,52].

The pK of PLL is 10.2, at I=0.1M [52]. Thus at pH  $\geq$  10.8, the polymer has less than 50%, charged groups and it undergoes a coil to helix transition. At pH=7, PLL is almost completely charged and exists in an extended coil state [52] at 25°C.

Temperature has the most important effect for PLL in its  $\alpha$ -helix state, i.e., at pH>10.5. Heating to 47°C melts the  $\alpha$ -helix to form a random coil or  $\beta$ -sheet at even higher temperatures [38,51,52]. The  $\beta$ -sheet is favored for pH>10.5 and T>47°C, due to hydrophobic interactions between lysyl side groups on adjacent chains [38-44,51,52].

#### 3.4.2 Solution Preparation

Dry powdered PLL was stored in original containers in freezer at 2°C, until they were used. Stock solutions of PLL were prepared by dissolving powdered PLL in deionized water. No further dialysis was performed since Sigma claims that this is free of low molecular weights impurities. The (%) moisture content of this sample was 3.1 weight %, for the lot#128F-5033, and 9.1% for the lot#69F55111. The concentration was determined as follows:

1. The container's bottle weight was measured before emptying it (closed and sealed),  $B_{bef}$ .

### 3.0 Experimental

2. Empty the bottle container in known volume of deionized water (under the hood),  $V_{water}$ .

3. Measure the empty bottle(closed and sealed),  $B_{aft}$ .

4. Concentration is then easily calculated as :  $C_{PLL} = \frac{B_{bef} - B_{aft}}{V_{water}}$

5. The concentration was corrected for the moisture content, and also titration with NaOH was performed in order to find the amount of HBr in the stock solution. It was found that for the 10,200 molecular weight the HBr content was 28%HBr/PLL monomer, and for the 50,000 was 42%HBR/PLL monomer.

Typical maximum age of PLL stock solution, before stock was discarded, was one month.

The results for six different stock solutions that were used are presented in Table 3.4.1.

**Table 3.4.1 PLL concentration measurements**

<b>Molecular weight</b>	<b>Stock solution #</b>	<b>Concentration (g/ml)</b>
10,200	1	$5.020 \times 10^{-4}$
10,200	2	$3.23 \times 10^{-4}$
10,200	3	$8.64 \times 10^{-4}$
10,200	4	$6.72 \times 10^{-4}$
50,000	5	$2.19 \times 10^{-4}$
50,000	6	$1.34 \times 10^{-4}$

### 3.5 PEC Mixing Procedure

#### 3.5.1 NaPSS Density data

The density for the solutions of NaPSS is given by :

$$\rho = \rho_0 + (1 - \tilde{v}\rho_0)C_p \quad (3.1)$$

where  $\rho_0$  is the density of the solvent, and  $\tilde{v}=0.6$  for NaPSS [54]

For water at 25°C  $\rho_o= 0.99798\text{g/ml}$ .

Thus,  $\rho(\text{g/ml}) = 0.99708 + (1 - 0.6 \times 0.99708)C_p$

Since the polymer concentration we worked with are of the order of  $10^{-4}\text{g/ml}$  or less, it is evident that the solution density can be taken as that of pure water.

#### 3.5.2 Effective Ionic Strength

The  $\text{Na}^+$  counterions which dissociate from the NaPSS contribute to the total effective ionic strength,  $I_{eff}$ . Equation, from Chapter 2 (2.10) gives the effective ionic strength,  $I_{eff}$ , to the polymer solution parameters as:

$$I_{eff} = I_s + \left(\frac{L_b}{L_c}\right)_{eff} \frac{L_{mon}}{L_b} \frac{10^3 C_p}{M_{mon}}$$

where  $I_s$  = molarity of added NaCl,

$L_b$  = Bjerrum length,

$L_c$  = average charge spacing,

$L_{mon}$  = monomer length,

$M_{mon}$  = monomer molecular weight.

For 1-1 salt in water at 25°C  $L_b=0.714\text{nm}$

### 3.0 Experimental

For NaPSS with Degree of sulfonation=1,

$(L_b/L_c)_{eff} \sim 1$  (see sec.2.1)

Monomer length= $L_{mon}=0.252$  nm

Monomer MW =  $M_{mon}=206.2$  g/mole

So for NaPSS:

$$I_{eff}(\text{molar}) = I_{salt} + 0.856 C_p(\text{g/ml})$$

Since  $C_p \sim O(10^{-4})$ , the second term can be neglected and one can assume that  $I_{eff}$  is the one of the salt solution, for  $I_{eff}$  in the range 0.01-1 M.

### 3.5.3 PLL/NaPSS Mixing Calculations

To obtain PEC solutions with a desired ionic strength, it is necessary to mix the stock PSS and PLL solutions with NaCl solutions. To calculate the molarity of NaCl solution needed for dilution,  $I_s^*$ , the following terms are defined:

$V_p$  = Volume of salt-free polymer solution

$V_s$  = Volume of salt solution

$C_p$  = Concentration of salt free polymer solution

$I_s^*$  = Molarity of salt solution to be used in dilutions in order to get the desired final Ionic strength

$I_{eff}$  = Molarity of the final solution

$V_T$  = total volume of PEC solution

For dilute solutions, it is accurate to assume that counterions don't contribute to the final ionic strength, so:

$$I_s^* = \frac{V_T I_{eff}}{V_s} \quad (3.2)$$

The final NaPSS concentration is:

$$C_{pf} = \frac{V_p}{V_s + V_p + V_w} C_p = \frac{V_p}{V_T} C_p \quad (3.3)$$

For example, for  $C_p = 2.33 \times 10^{-3} \text{ g/ml}$ ,  $V_T = 30 \text{ ml}$ ,  $C_{pf} = 5 \times 10^{-5} \text{ g/ml}$ :  
the volume of the salt-free polymer solution that we must use in order to get this dilution is :

$$V_p = 5 \times 10^{-5} (\text{g/ml}) \times 30 / 2.33 \times 10^{-3} (\text{g/ml}) = 0.644 \text{ ml}.$$

The volume of salt-free PLL solution needed is calculated given by the definition of the polymer's equivalent concentration ratio:

$$Z = \frac{[\text{PLL}]}{[\text{NaPSS}]} = \frac{\frac{\text{charge}}{\text{monomer}} \times \frac{\text{monomer}}{\text{MW of monomer}} \times C_{PLLin} \times V_{PLLin}}{\frac{\text{charge}}{\text{monomer}} \times \frac{\text{monomer}}{\text{MW of monomer}} \times C_{NaPSSfin} \times V_{Tot}} \quad (3.4)$$

This equation can be solved for  $V_{PLLin}$  as illustrated in the following calculation for an NaPSS/PLL mixture with a  $Z=0.5$ , with final concentration of NaPSS  $C_{fin} = 5 \times 10^{-5} \text{ g/ml}$ , and  $I_{fin} = 0.1 \text{ M}$ . The NaPSS initial concentration is  $2.33 \times 10^{-3} \text{ g/ml}$  and PLL initial concentration is  $6.023 \times 10^{-4} \text{ g/ml}$ .

From the previous section,

$$V_{NaPSSin} = 0.644 \text{ ml}$$

The volume of PLL solution needed is :

$$Z = \frac{1(\text{ch/mon}) \times 1/\text{MW}_{PLL}(\text{mon} \times \text{mole/gr}) \times 6.023 \times 10^{-4} (\text{g/ml}) \times V_{PLLin}}{1(\text{ch/mon}) \times 1 \text{ mon}/\text{MW}_{NaPSS} \times 5 \times 10^{-5} (\text{g/ml}) \times 30 (\text{ml})}$$

$$Z = \frac{1 \times \frac{1}{189.02} \times 6.023 \times 10^{-4} (\text{g/ml}) \times V_{PLL}}{1 \times \frac{1}{206.2} \times 5 \times 10^{-5} (\text{g/ml}) \times 30 (\text{ml})} \text{ so } V_{PLL} = 1.142 \text{ ml}$$

The remaining volume, 30ml- (0.644 + 1.142) = 28.214ml, is compromised of added NaCl solution with volume  $V_S$  and ionic strength  $I_s^*$  and additional water. The typical values of  $I_s^*$  used in this work were 2 and 5M.

### 3.5.4 PEC Mixing Order

The order of mixing was chosen to minimize the possibility of forming nonequilibrium PEC structures. The optimum mixing order was found to be the following:

NaPSS stock solution + Water + 5M NaCl stock + PLL stock solution.

Several points are worth noting:

1. It is important to add the stock PLL solution at the end. If it were added right after the NaPSS stock solution, the complexes might form very quickly, leading to highly irreproducible results.
2. The NaCl stock solution should be added after the water, especially at high ionic strengths. Otherwise, the NaPSS-NaCl mixture reaches the "theta conditions" ( $I \sim 4\text{M}$ ) and some of the chain may even precipitate.

After PEC's are mixed in 50 mls Erlenmeyer flasks, they are corked and placed on the wrist-action shaker for at least 24 hours (the  $I=1\text{M}$ 's must stay even longer, such as 2 days). Before they are tested in the DLS, they were kept still for at least one hour in the hood, in order to reach a steady state. After this, they were filtered with 0.2  $\mu\text{m}$  Acrodisc hydrophilic filters, purchased from Fisher Scientific, and individually wrapped syringues of 10  $\text{cm}^3$ , purchased from BDF. Each syringue carries two filters in series and each sample was filtered at

least 3 times before being placed in the DLS cells. More details on the procedures used in DLS experiment are presented in the next chapter.

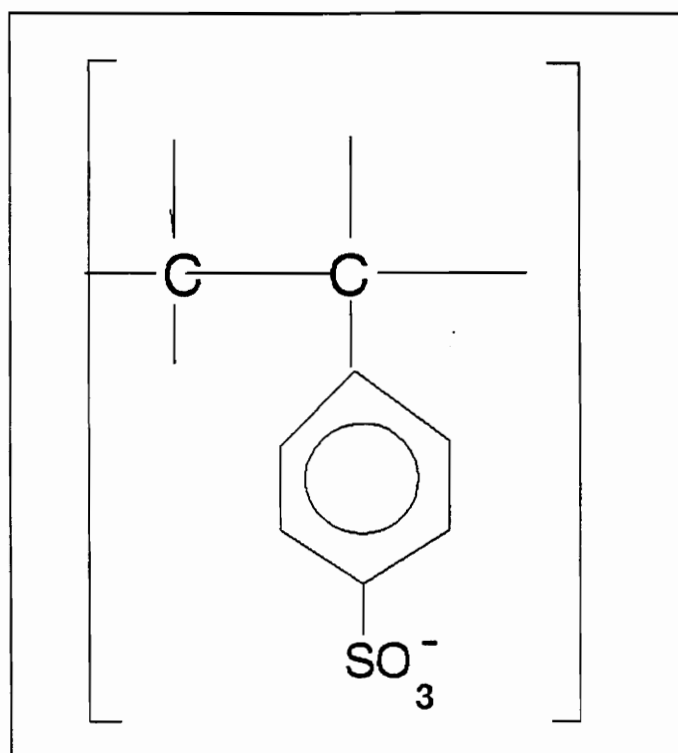


FIGURE 3.1 POLYSTYRENE SULFONATE MONOMER STRUCTURE

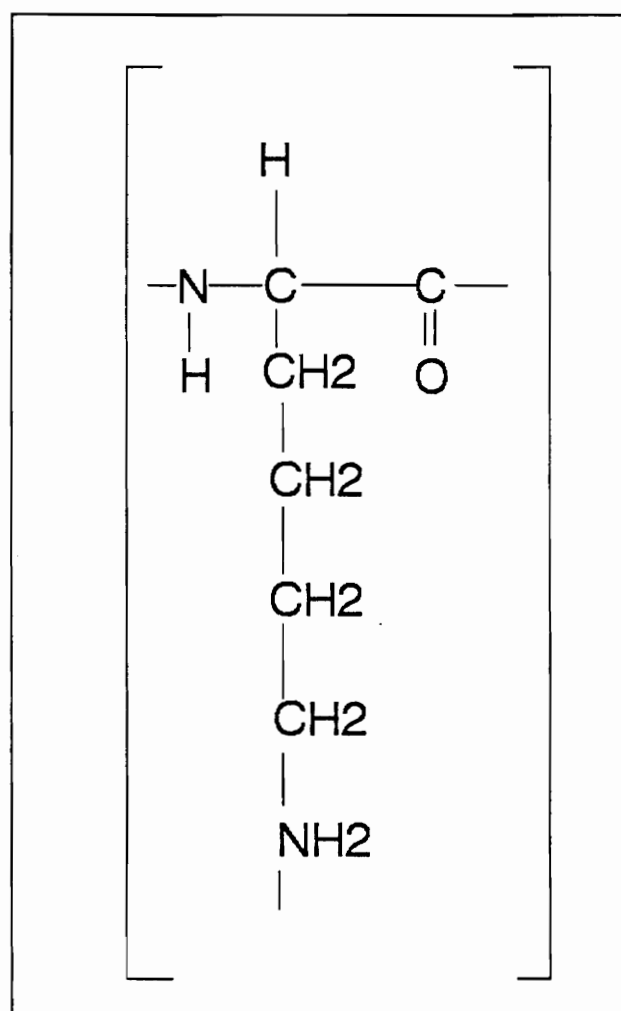


FIGURE 3.2 POLY-L-LYSINE MONOMER STRUCTURE

## 4.0 DYNAMIC LIGHT SCATTERING

### 4.1 Introduction

Light scattering is an established technique for characterizing polymer structure and polymer-solvent and polymer-polymer interactions. Light scattered from solutions of synthetic and natural macromolecules contains information on the dynamic and static polymer properties such as translational diffusion coefficient, rotational diffusion coefficient, size, shape, molecular weight, second virial coefficient, and polydispersity [32, 33, 35,36].

Polymer molecules in solution exhibit a variety of relaxation times due to bond rotations and interactions with solvent molecules and with other polymer molecules. Many of the relaxation times are very fast (on the order of  $10^{-6}$ sec). Before the development of fast photomultiplier tubes (PMT), lasers and fast correlators, only static time averaged scattering intensities could be measured which provided information on equilibrium properties such as  $R_g$ ,  $A_2$ , and shape [32, 33,35]. With modern PMT's, lasers and correlators, it is possible to measure the time dependent scattered intensity which, for polymer solutions, provides information on diffusion processes.

The translational diffusion coefficient  $D$ , of a polymer molecule in dilute solution is related to the hydrodynamic volume,  $R_H$  by the Stokes-Einstein equation:

$$D = \frac{kT}{6\pi\eta R_H} \quad (4.1)$$

where  $\eta$  is the viscosity of the solution. Thus, dynamic light scattering can be

used to determine the size of uncomplexed host PE's, the onset of PEC aggregation, and the size of PEC aggregates. We have measured the translational diffusion coefficient of polyelectrolytes as a function of ionic strength  $I$ , polycation/polyanion equivalent ratio  $Z$ , temperature  $T$ , and pH.

## 4.2 Theory of Dynamic Light Scattering

In dynamic light scattering, DLS, the scattering intensity is measured as a function of time over very small time intervals [32]. The comparison between two neighbouring time intervals and two time intervals separated by a longer delay time is realized by multiplying the number of photons arriving at the detector in those two cases.

$$\langle A_0 A_n \rangle = \langle i(0) i(t) \rangle = G_2(t) \quad (4.2)$$

where  $A_0$  is the number of photons at time  $t=0$ ,  $A_n$  is the number of photons at time  $t=t$ , and  $G_2(t)$  is the correlation function of the scattering intensity, and the bracket signs mean average quantities. For sufficiently short time intervals, the correlation function  $G_2(t)$  has a relatively large value which can be interpreted, for dilute suspensions, as the diffusion of a particle over a relatively short distance from its starting point at time  $t=0$ . For sufficiently long time intervals, there is no correlation between the particle's position at  $t=0$  and  $t=t^*$ , indicating that the particle has diffused so far and has undergone many Brownian collisions with solvent molecules and other particles. At these long times,  $G_2(t)$  has relatively low values and is no longer a function of the time interval. In between the short and long time limits, the autocorrelation function  $G_2(t)$ , decays from its initially high value, to its final, limiting low value. The function  $G_2(t)$  decays faster as the translational diffusion coefficient, increases.  $G_2(t)$  is related to the autocorrelation function (ACF),  $g_1(t)$  by:

$$G_2(t) = \langle i(0) i(t) \rangle = A + B |g_1(t)|^2 \quad (4.3)$$

where  $A$  and  $B$  are instrument constants.

For uniform hard spherical particles or small particles of arbitrary shape, the ACF is a single exponential [32, 33, 35, 36].

$$g_1(t) = \exp(-Dq^2t) \quad (4.4)$$

where  $D$  is the translational diffusion coefficient, and  $q$  is the scattering vector defined by:

$$q = \frac{4\pi n}{\lambda} \sin\left(\frac{\theta}{2}\right) \quad (4.5)$$

where  $n$  is the refractive index of the solvent,  $\lambda$  is the wavelength,  $\theta$  is the scattering angle.

If two variables (or signals) are highly correlated, then a change in the one can be used to predict with confidence, a change in the other. Autocorrelation then, it is simply the correlation between the values of one variable at different times or, mathematically, the average of the product of a variable at time  $t=0$ , and the variable at a later time  $t$ .

Figure 4.1. is a rough illustration of the ACF. Two particles with sizes  $R_1 > R_2$  are in position A at time  $t=0$ . After time  $t+\Delta t$ , they are going to be in positions 1 and 2 respectively. At this position much of the correlation of 2 has been lost, since it is smaller and diffuses faster. However, the first particle's position is still highly correlated to the initial position since it is larger and diffuses more slowly.

The total time over which a measurement is made is the **duration time**. The larger the duration time, the more accurate the measurement due to increased photon counts. The independent axis of the graph is divided in 136 channels, in the DLS instrument used in this work, where the ACF will decay. The x-axis represent the time lag, or a relaxation time of the intensity fluctuations. In this correlator, photon count rates are multiplied and added in parallel in the 136 channels to generate the ACF,  $g_1(t)$ . Each channel represents an increment of the **sample time**,  $\tau$ , which is the time at channel 136. In general the sample time has to be such as to ensure the full decay of the ACF to within

0.1% of the measured final long-time baseline. Obviously a good guess of the particle size, will allow a proper initial choice of the sample time. A small sample time for a large particle, would not be effective due to the small changes of position within that time increment. The ACF then will tend to be constant and linear. Furthermore for small particles a large sample time, would result in a very rapid decay of the ACF due to the rapid change of the scattering site position during the sample time. A constant ACF is unusable because the diffusion coefficient cannot be calculated from it, and a rapidly decaying ACF is not accurately measured because of the inefficient use of the correlator channels. As a rule of thumb, a good choice of sample time makes the ACF decay to the long-time base-line in the last 10 correlator channels.

### 4.3 Structure Factor and Scattering Angle Range

A very important quantity is the structure factor defined by:

$$S(\mathbf{q}, t) = S(\mathbf{q}, 0) \exp (-Dq^2t) \quad (4.6)$$

for a system of noninteracting, isotropic and identical particles, small compared to the wavelength of the light [11].  $D$  stands for the translational diffusion coefficient of the particles, and  $q$  is the length of the scattering vector.

Some useful results then follow [33]:

i)  $qR_H \ll 1$  then  $S(q,t)$  is sensitive to fluctuations whose wavelength ( $q^{-1}$ ) is large compared to the size of the single chain, thus what is probed this way is the diffusive motion of the center of the mass of the single chain (translational diffusion coefficient). The characteristic decay rate is:

$$\Gamma = Dq^2 \quad (4.7)$$

ii) When  $qR_H \gg 1$ , then internal chain distortions become important so we get information for the internal dynamics.

In this work all the experiments were performed in the translational diffusion,  $qR_H \ll 1$ , regime.

## 4.4 Particle interactions

In a system composed of rigid particles and liquid, three types of forces can be involved:

- i) Brownian forces, resulting from collisions with thermally agitated solvent molecules.
- ii) Forces due to interactions between the particles
- iii) Hydrodynamic forces

**Brownian forces:** These are dependent on temperature. Their characteristic fluctuation time is:

$$\tau_B = \frac{M}{\zeta}$$

where  $M$  is the particle mass,  $\zeta$  is the particle friction coefficient  $\zeta=6\pi\eta a$ , where  $\eta$  is the viscosity of the liquid and  $a$  is the particle radius. The characteristic time  $\tau_B$  is much smaller than the shortest DLS delay time  $\tau \simeq 1\text{msec}$ .

**Forces due to interactions between particles :** In this case the "excluded volume effect" is involved, so these forces are important in concentrated solution. Generally there are much weaker than the Brownian forces but with a large characteristic time. All experiments in this work were done at such low polymer concentration that interaction forces between polyelectrolyte molecules and PEC's are negligible.

**Hydrodynamic forces:** As the particles (polymer molecules) diffuse through a solvent, they generate velocity disturbances which affect the motions of other particles. For very dilute systems such as ours, these interactions can be neglected [33].

## 4.5 DLS Experimental Procedure

### 4.5.1 Sample preparation

One of the major problem in DLS experiments is the presence of dust in solutions. Dust particles present a serious and undesirable interference. These particles vary in size from less than 100nm to much larger than 1 micron. Since scattering intensity varies inversely with  $R^4$ , the scattering from dust particles in a polymer solution can easily exceed the scattering intensity of the polymer molecules or associated PEC's, thus making impossible a DLS experiment of diffusion coefficient for the PEC. Therefore, procedures were developed to obtain polymer solution with sufficiently low dust levels. The procedures include glassware treatment, mixing and filtration.

#### 4.5.1.1 Glassware treatment

All the DLS cells were silanated before use. This is a permanent treatment whose objective is to decrease the glass hydrophilicity, so that dust particles in water which tend to be quite hydrophilic, will not adhere to the cell walls. The following treatment was kindly provided to us by **Dr. Paul Russo** from the Chemistry Department at Louisiana State University.

##### 1. Cell Pretreatment

5 min soak in concentrated  $\text{HNO}_3$  (12 M)

Rinse with deionized water

5 min soak in concentrated  $\text{HCl}$ , (Reagent A.C.S., Lot#892974, Fischer)

Rinse with deionized water

Rinse with  $\text{CH}_3\text{OH}$  (Class 1B, Water 0.05%, Certified ACS, Lot#893770, Fischer)

Allow to air dry in a clean area

## **2. Silane solution preparation (do in hood!)**

200 ml toluene,( 99.9%, Reagent, ACS specif., Lot#D24620, Fischer)

5-10 ml  $\text{SiCl}(\text{CH}_3)_3$  (chlorotrimethylsilane), (Lot#100,292, Petrarch Systems Inc.)

## **3. Cell Treatment**

Dry cell with blowgun heater

Put in silane solution while still hot(do in hood)

## **3. Post-treatment**

Rinse with anhydrous  $\text{CH}_3\text{OH}$  (reacts with excess silane)

## **4. Final Preparation**

Rinse with filtered ultimate solvent

Rinse with deionized water

Dry if necessary, in laminar flow hood.

### **4.5.1.2 Filtration**

The cell preparation and the filtration of the solutions were carried out in a laminar-flow hood, model 4HT 30. To filter the samples, individually wrapped, sterile syringes(5cc,10cc) were used (see Chapter 3). For every filtration, two filters in series were used and each sample was filtered at least 3 times before it was placed in the final DLS cell, which are borosilicate (Crown) glass with refractive index  $n=1.46$ . The filter pore size was  $0.2\mu\text{m}$  (see Chapter 3 for details).

## 4.5.2. Dynamic Light Scattering Procedure

### 4.5.2.1. Equipment Description

A Brookhaven DLS instrument with a BI-2030AT correlator with 136 channels, and 6 delay channels was used. This instrument measures scattering intensity at angles ranging from  $15-160^\circ$  using a 2 Watt Lexell Argon Ion Laser. Concentration of less than 0.1% volume are usually required. The size of the colloidal particle can be measured to within  $\pm 10\%$  over a size range of less than 10nm to more than 1000nm. The temperature of the sample cell is controlled with an external bath. The precision of the temperature control bath was  $\pm 0.1^\circ\text{C}$ .

A vertically polarized, laser beam is focused by lens L1 (Fig.4.2 ), onto a sample cell, which is surrounded by a temperature controlled housing [36]. The temperature controlled housing liquid is decalin (decahydronaphthalene) which has a very close index match to glass. The temperature is set and controlled primarily for convenience in determining the viscosity and the refractive index of the liquid in which the particle moves. Sample cells that were used are borosilicate glass and have round cross sections with diameters of approximately 12mm.

Light scattered at a fixed angle with respect to the incident beam is defined by pinholes P1 and P2 and it is focused by lens L2 onto the photomultiplier tube (PMT). The scattered light gives rise to electrical pulses when it strikes the PMT, which are amplified during their travel through the PMT. Another amplifier in conjunction with a discriminator produces uniform electrical pulses, whose variation in time(fluctuations) contain all the information encoded in the scattered light striking the PMT. The frequencies of those fluctuations are related to the speeds and therefore the sizes of the particles. To analyze them, a correlator is used [36].

The laser power was always adjusted to 50mW which was enough to give a good scattering intensity for most samples. A good scattering intensity is

defined as the scattering intensity which gives a count rate at least 100 times larger than the dark count rate (see below at 4.5.2.3). The good scattering intensity, is measured at  $90^\circ$ , because this is where the minimum of the scattering intensity occurs [36,35]. As the angle increases to  $90^\circ$ , the intensity of the laser line image, will decrease as fewer and fewer scatterers are contributing to the image. With a weak scatterer and low laser power, it may be difficult to get a sufficiently high count rate except at low and high angles [36]. At the lowest angle, the count rate should not exceed 1,000,000 count/sec and at  $90^\circ$ , the duration should be long enough to count a minimum of 100,000 pulses for good accuracy.

Whenever the input pulse rate exceeds 15 pulses/sample time increment the **overflow** light starts to blink. This means that the sample contains large dust particles. The number of overflows is recorded and indicated on the screen [36]. Another indication is the fluctuating count rate (photons hitting the PMT/sec). If the overflow light is lit continuously and the overflow indication on the screen is more than 1% of the total photons counted, then the measured correlation function is a distorted version of the true function [36]. There are three ways of solving this problem, and they will be ranked according to their efficiency: (i) the sample can be removed from the DLS and filtered again, (ii) set a function of the software, the **prescale factor**, which statistically discards all the sample times characterized by more than 15 pulses/sample time, and (iii) decrease the duration time decreasing thus the photons number counted and consequently decreasing the probability of counting photons from dust particles scattering. The latter should be avoided because it leads to less accurate ACF measurements. The overflow channel should be less than 0.05% of the "A" channel.

When the intensity is not high enough, it is preferable to set a higher slit size rather than to increase the laser intensity for two reasons: (i) Adjusting the laser intensity is time consuming, because it is necessary to wait at least 30 min every time the power is increased, for the laser to reach steady state. (ii) High

laser power should be avoided so that the sample is not heated by the increased radiation.

After putting the sample in the cell, scattered light from each particle (Fig.4.2.) reaches the photomultiplier tube (PMT) fixed at some angle with respect to the direction of incident light. Since the small particles are moving around randomly due to Brownian motion, the distances that the scattered waves travel to the detector varies as a function of time. Frequencies of the fluctuations around an average value are related to the speeds and therefore the sizes of the particles. This fluctuating signal is analyzed by the correlation function.

#### 4.5.2.2 Latex Calibration Test

Latex test is a quite simple test to check the appropriate function of the DLS. Polystyrene latex spheres, purchased from Duke Scientific corporation, were tested in the DLS at least every two weeks. The specific sample is a monodisperse sample of spheres with radius  $40\text{nm} \pm 1.8\text{nm}$  [36].

An aqueous solution of it was 3-4 drops in 200ml aq.NaOH solution ( $\approx 0.02\text{M}$ ). The sample was filtered 3 times and run at the DLS. The sizes should be in the range given by the product manufacturer. Indeed the sizes we obtained were  $40\text{nm} \pm 2.5\text{nm}$ , which confirms the appropriate function of DLS.

#### 4.5.2.3 Dark count rate test

PMT is tested by adjusting the pinholes in such a position so as light is blocked [36]. An ideal PMT then, should not count any photons. However there are always some photons measured mainly because of thermal energy activating

some of the electrodes on the PMT cathode, which in turn emit photons. This is the **dark count rate**, and it typically increases with temperature. This must be very small for the proper operation of PMT and the accuracy of the results ( $\text{DCR} \leq 200\text{-}350 \frac{\text{counts}}{\text{sec}}$  )

#### 4.5.2.4 ISINTHETA Test

ISINTHETA is a test to check the goniometer 's alignment. This must be checked before any diffusion coefficient measurements are made, using the decalene refractive index fluid bath, without a sample cell, as the scattering medium. The scattering intensity of a Rayleigh scatterer should be independent of angle provided the detector views the same scattering volume [35,36]. However the scattering volume viewed by the detector increases on either side of 90 degrees. Multiplying the intensity by  $\sin\theta$ , corrects for the volume effects and the  $I\sin\theta$  should be constant within a range of 1%. Deviations more than 1% are a measure of all the errors: poor alignment, dust, laser drift, flare, scratches on the DLS cells, photocathode sensitivity, linearity etc(36).

#### 4.6. Determination of the Diffusion Coefficient

ACF is actually the process of the fluctuating signal, produced by the Brownian motion of the small particles.

$$\text{ACF}(t) = A|g_1(t)|^2 + B$$

where  $g_1(t) = \exp(-Dq^2t)$ .

In many cases though, the plot of  $\ln[g_1(t)]$  against time is not a straight line but it shows a tail towards longer delay times [32]. Such behavior arises from molecular weight distribution, in the case of polymer solutions, or particle size distribution in the case of rigid, suspended particles. The function  $\ln[g_1(t)]$  can then be expanded in the infinite series known as the cumulant expansion:

$$\ln[g_1(t)] = -\Gamma_1 t + \frac{\Gamma_2 t^2}{2!} - \frac{\Gamma_3 t^3}{3!} + \dots \quad (4.8)$$

The reduced first cumulant,  $\Gamma_1/q^2$ , is angular and concentration dependent:

$$\frac{\Gamma_1}{q^2} = D(1 + F\langle R_g^2 \rangle q^2 - \dots) = D_{app}(q, C) \quad (4.9)$$

where  $F$  is a constant characteristic of the particle architecture, and  $R_g$  is the radius of gyration at concentration  $C$ . In case of very dilute solutions there is no concentration dependence and  $\Gamma = Dq^2$ .

For a broad distribution of spheres,  $g_1(t)$  must be modified in order to take into account the different relaxation times of the diverse population.

$$g_1(t) = \int_0^\infty G(\Gamma) e^{-\Gamma t} d\Gamma \quad (4.10)$$

where  $G(\Gamma)$  provides size distribution information. This is a Laplace transform

equation [36].

Several schemes for determining size distributions have been proposed [36], and probably the most general and method is the cumulant analysis. The advantage of this scheme is that no assumption is made for the distribution form. In this research the method of cumulants was used by the computer to convert the autocorrelation function to a diffusion coefficient. In this method the ACF is expanded as :

$$\ln[g_1(t)] = -\Gamma_1 \tau + \frac{1}{2!} \Gamma_2 \tau^2 - \frac{1}{3!} \Gamma_3 \tau^3 + \dots$$

The relationship between the cumulants and the moments of the distribution of the decay rates are:

$$\langle \Gamma_1 \rangle = \langle D \rangle \quad (4.11)$$

$$\langle \Gamma_2 \rangle = \langle (\Gamma - \langle \Gamma \rangle)^2 \rangle = (\langle D^2 \rangle - \langle D \rangle^2) \quad (4.12)$$

$$\langle \Gamma_3 \rangle = \langle (\Gamma - \langle \Gamma \rangle)^3 \rangle \quad (4.13)$$

where  $\langle \Gamma_1 \rangle$  is the average decay rate, assuming that ACF contains many decay rates (polydisperse sample). In case of monodisperse sample  $\Gamma = \langle \Gamma \rangle$  and  $\Gamma_2 = \Gamma_3 = 0$ . In this case, first cumulant analysis is sufficient.

The software used in our work, performs a second moment analysis and provides calculations of  $\langle \Gamma_1 \rangle$  as well as the second moment  $\Gamma_2$  (or  $\mu$  as notated in BI). Our sample were always somewhat polydisperse, so all reported PE and PEC sizes were effective values, using the Stokes equation ( $D = \langle D \rangle$ ). The reduced second moment is a convenient indicator of the polydispersity of a size distribution, P.

$$P = \frac{\Gamma_2}{\langle \Gamma_1 \rangle^2} \quad (4.14)$$

This is angular dependent , like the  $D_{eff}$ , and a more well defined value of its value of it is taken with extrapolation to zero angle.

For monodispersed particles  $0 < P < 0.020$   
For narrow distributions  $0.02 < P < 0.08$   
For broader distributions  $P > 0.08$

The intensity of light scattered by a suspension of particles, with diameter  $d$ , is proportional to particle mass  $M$ , particle structure factor  $S(q,d)$  which is size, scattering angle and refractive index dependent.

The average diffusion coefficient is

$$\langle D \rangle = \frac{\sum NM^2 S(q,d) D}{\sum NM^2 S(q,d)} \quad (4.15)$$

sum carried over all the particles, where  $N$  is the number of the particles with molecular weight  $M$ . For particles with sizes much smaller than the wavelength  $S(q,d)=1$ , so the measured diffusion coefficient  $D$  is [36]:

$$\langle D \rangle = \langle D_z \rangle = \frac{\sum NM^2 D}{\sum NM^2} \quad (4.16)$$

which is the z-average. Since  $D \sim 1/d$ :

$$\langle \frac{1}{d_z} \rangle = \frac{\sum NM^2 (1/d)}{\sum NM^2} \quad (4.17)$$

However  $M \sim d^3$  so:

$$\langle \frac{1}{d_z} \rangle = \frac{\sum Nd^5}{\sum Nd^6} \quad (4.18)$$

$$\langle d_z \rangle = \frac{\sum Nd^6}{\sum Nd^5} = d_{eff} \quad (4.19)$$

$d_{eff}$  measured by DLS is larger than the number average diameter:

$$\langle d_N \rangle = \frac{\sum N d}{\sum N} \quad (4.20)$$

It is also larger than the area average :  $\langle d_a \rangle = \frac{\sum N d^3}{\sum N d^2}$  (4.21)

and the weight average :  $\langle d_w \rangle = \frac{\sum N d^4}{\sum N d^3}$  (4.22)

so :  $d_n \leq d_a \leq d_w \leq d_{eff}$  [36].

As discussed above, for dilute solutions,  $\Gamma$  is concentration independent, and only scattering angle dependent. In the limit of small  $q$  (small angle scattering, where  $qR_H \ll 1$ , (see example in Chapter 5),  $\Gamma$  is related to the translational diffusion coefficient for the single chain. For small angles (30-70), the diffusion coefficient represents the slope of a straight line of  $\Gamma$  vs.  $q^2$ . Angles less than  $30^\circ$ , were usually not used, due to the dust problem which can be extremely bad at such small angles. After estimating the slope, the hydrodynamic radius is estimated from Stokes-Einstein law :

$$D = \frac{kT}{6\pi\eta R_H}$$

In the above equation we assumed spherical particles. In case of any other shape of the particles,  $D = kT\chi^{-1}$ , where  $\chi$  is the friction coefficient of this particle in solution [35].

## 4.7 Error analysis

A first order least square analysis was performed for weighting the fit of  $\Gamma_1$  vs  $q^2$ . The following formula was used to estimate the intercept and the slope [34]:

$$\Delta = \sum \frac{1}{\sigma_i^2} \sum \frac{x_i^2}{\sigma_i^2} - \left( \sum \frac{x_i}{\sigma_i^2} \right)^2 \quad (4.23)$$

$$\text{Intercept} = \frac{1}{\Delta} \left( \sum \frac{x_i^2}{\sigma_i^2} \sum \frac{y_i}{\sigma_i^2} - \sum \frac{x_i}{\sigma_i^2} \sum \frac{x_i y_i}{\sigma_i^2} \right) \quad (4.24)$$

$$\text{Slope} = \frac{1}{\Delta} \left( \sum \frac{1}{\sigma_i^2} \sum \frac{x_i y_i}{\sigma_i^2} - \sum \frac{x_i}{\sigma_i^2} \sum \frac{y_i}{\sigma_i^2} \right) \quad (4.25)$$

There are two kinds of error :

1. Precision of an individual measurement which is a function of factors like: misalignment, dark count, and dust.
2. Experimental reproducibility. The factors affecting it are : different samples taken from the same stock solutions, different stock solutions, accuracy of concentration measurements of different stock solutions, mixing procedures.

The first error is easily calculated, because it is given as a relative standard deviation for the  $\langle \Gamma_1 \rangle$  by the software.

Therefore the individual measurements uncertainties were estimated as follows [34]:

$$\sigma_{slope} = \frac{1}{\Delta} \left( \sum \frac{1}{\sigma_i^2} \right) \quad (4.26)$$

$$\sigma_{int} = \frac{1}{\Delta} \sum \frac{x_i^2}{\sigma_i^2} \quad (4.27)$$

The propagated error in hydrodynamic radius was calculated as:[34]

$$\sigma_x^2 \simeq \sigma_u^2 \left( \frac{\partial x}{\partial u} \right)^2 + \sigma_v^2 \left( \frac{\partial x}{\partial v} \right)^2 + \dots \quad (4.28)$$

A short program was written and run by Sigma Plot, version 4.1. (see App.2)  
An example follows at Chapter 5.

The second kind of error, which is the most significant one. In Chapter 5 an example is presented, illustrating all the steps of the procedure, as well as a comparison of the two kinds of error.

#### 4.8. Dynamic Light Scattering conditions

(1) The laser power depends on the concentration of the solution. It was found that 50 mW accommodates the specific range of concentrations we worked with ( $10^{-5} - 10^{-4}$  g/ml). High laser power should generally be avoided because this could cause the sample to overheat.

(2) The incident light wavelength was 514 nm.

(3) The slit size ranged from 200-800 microns.

(4) The temperature in the decalene bath was 25°C, unless otherwise is stated.

Experimental results are summarized and discussed in Chapter 5.

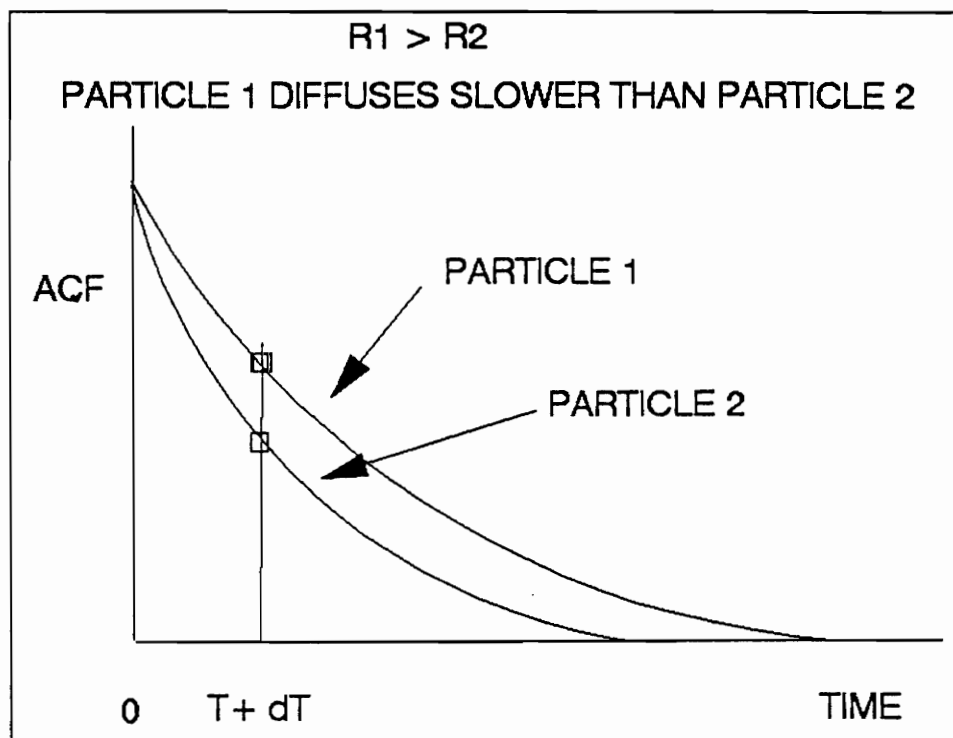


FIGURE 4.1 AN EXAMPLE OF THE ACF FOR TWO PARTICLES OF DIFFERENT RADIUS.

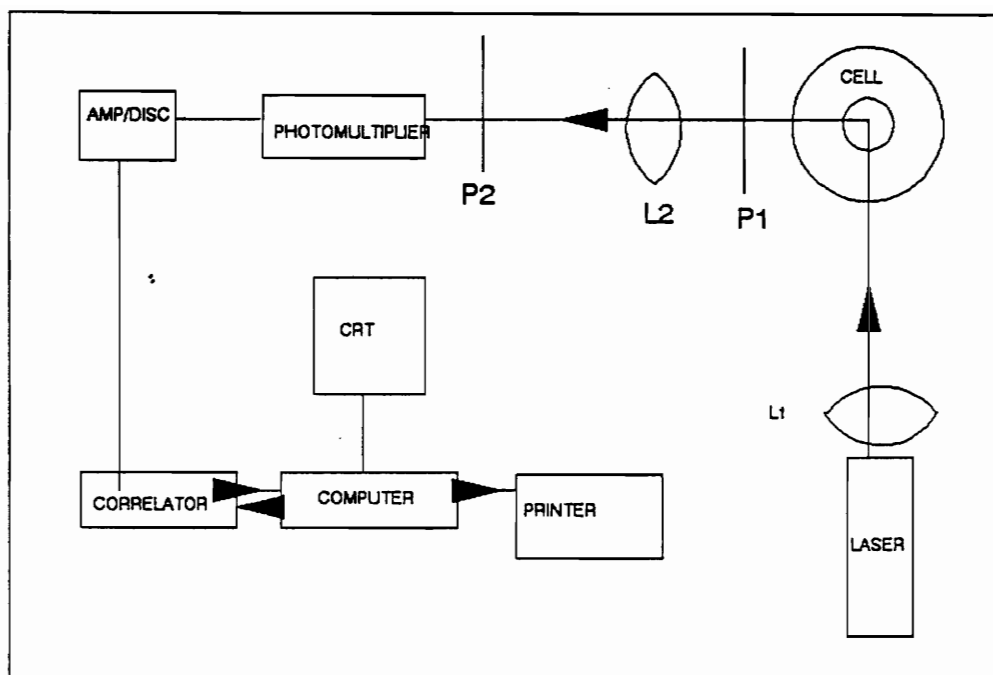


FIGURE 4.2 BLOCK DIAGRAM OF BI-2030

## 5.0 RESULTS & DISCUSSION

Chapter 5 includes the results and discussion of our study of PEC's , and particularly the system of NaPSS/PLL.

Technique verification is the first part, and includes a description of the method used to determine the hydrodynamic radius,  $R_H$ . An illustrative example is also included. The determination of the dilute regime for both pure NaPSS and PEC is also described along with a test for verifying the filtration technique.

The second section concerns pure polymer data, and includes the effect of ionic strength on NaPSS hydrodynamic radius, as well as some pure PLL data on the effect of I, pH, and temperature on the  $\alpha$ -helix to coil transition.

The third section presents the results on the PEC studies. The effect of ionic strength, I, pH, temperature and molecular weight on PEC formation, the onset of aggregation and size of PEC are described. A possible explanation of the mechanism, including the effects of the PLL  $\alpha$ -helix-to-coil transition is presented.

## 5.1. Technique verification

Figure 5.1.1 illustrates how the hydrodynamic radius,  $R_H$ , was determined. As discussed in Chapter 4,  $R_H$  is evaluated from Stokes law using the effective translational diffusion coefficient with  $R_H$  (Chapter 4). The z-average translational diffusion coefficient, which actually is an effective translational diffusion coefficient (see detailed discussion in Chapter 4), is evaluated from the first cumulant  $\Gamma_1 = Dq^2$ . Recalling chapter 4,  $\Gamma_1$  is angular and concentration dependent (4.9). The diffusion coefficient is the slope obtained from extrapolating this line ( $\Gamma$  vs  $q^2$ ) to zero. Figure 5.1.1 is a characteristic plot of  $\Gamma_1$  vs  $q^2$ . A set of different  $\Gamma_1$ 's for angles 30-70° was plotted vs  $q^2$ , with the first order least square scheme described in Chapter 4. In this work,  $\Gamma_1$  was only angular dependent since the solutions were very dilute (Fig. 5.1.1).

The standard deviation of this diffusion coefficient is the same as the s.d. of  $\Gamma_1$ , already evaluated by the BI software and displayed as relative standard deviation (RSD). In this case, the uncertainties are not the same for each data point (different RSD's for different  $\Gamma_1$ 's). It is obvious that the individual measurements uncertainties (Chapter 4), introduced by dust, disalignment, flare and other instrumental factors, are negligible compared to the experimental reproducibilities, introduced by different stock solutions, slight changes in mixing procedure. Especially in the PEC system, which is a highly environmental sensitive system, we were compelled to accept reproducibility errors up to 30% sometimes, without this affecting dramatically the validity of the results.

The following example is the step by step procedure, followed to determine the hydrodynamic radius.(Fig. 5.1.1.)

The sample is a polyelectrolyte complex made with NaPSS=200,000g/mole and PLL=10,200g/mole, polyelectrolyte complex. The conditions were: I=0.1M, pH=7, and T=25°C. The following table 1.1 presents the  $\Gamma_1$  values obtained, for angles from 35-70°, the square of the scattering

vector, and the RSD for each  $\Gamma_1$  value.

**Table 5.1.1. Determination of  $R_H$**

NaPSS:200,000, PLL:10,200

$C_{NaPSSin}: 3.845 \times 10^{-3} \text{ g/ml}$

$C_{NaPSSfin}: 5 \times 10^{-5} \text{ g/ml}$

$C_{PLL}: 3.78 \times 10^{-4} \text{ g/ml}$

pH=7, T=25°C.

$\Gamma(\text{rad/sec})$	RSD(%)	$q^2(\text{nm}^{-2})$
1827	1.48	0.00010
2350	1.15	0.00012
3310	1.7	0.00016
3924	1.98	0.00019
5320	1.92	0.00023
6085	2.92	0.00026
6397	2.75	0.00031
7378	2.57	0.00035

Using the algorithm presented in Chapter 4, performed by the programm presented in Appendix, the slope of the line was calculated.

Slope= Dif.Coef. =  $2.31808 \times 10^7 \text{ nm}^2/\text{sec} = 2.31808 \times 10^{-7} \text{ cm}^2/\text{sec}$ .

The intercept was  $I = -399.24028 \text{ nm}^2/\text{sec} = -399.24028 \times 10^{-14} \text{ cm}^2/\text{sec}$ . This is almost zero, thus verifying that the  $\Gamma$  vs.  $q^2$  is a straight line going through the origin.

The standard deviations of the Intercept and the slope were:

$$\sigma_I = 49 \times 10^{-14} \text{ cm}^2/\text{sec} \quad (5.1)$$

$$\sigma_S = 0.0363056 \times 10^{-7} \text{ cm}^2/\text{sec} \quad (5.2)$$

The 50% probable error, P.E., which indicates the magnitude of the error which

we estimate we have made in our determination of the results, is defined to be the absolute value of the deviation  $|D - D_{mean}|$ , such that the probability for the deviation of any random observation  $|D_i - D_{mean}|$  to be less is equal to 1/2 [34]. The relation between the P.E. and the standard deviation  $\sigma$  is defined as [34]:

$$\text{P.E.} = 0.6745\sigma \quad (5.3)$$

In this case the P.E. of the slope and the intercept values, from (5.1), (5.2), (5.3) is:

$$\text{P.E.}_I = 0.6745 \times 49 \times 10^{-14} = 33.05 \times 10^{-14} \text{ cm}^2/\text{sec} \quad (5.4)$$

$$\text{P.E.}_S = 0.6745 \times 0.0363056 \times 10^{-7} = 0.0245 \times 10^{-7} \text{ cm}^2/\text{sec} \quad (5.5)$$

so  $D = 2.31808 \times 10^{-7} \pm 0.0245 \times 10^{-7} \text{ cm}^2/\text{sec}$  which is almost 1% error, and intercept  $I = -399.24028 \times 10^{-14} \pm 33.05 \times 10^{-14} \text{ cm}^2/\text{sec}$  which is almost 8% error.

The hydrodynamic radius is calculated from Stokes law:

$$R_H = \frac{kT}{6\pi\eta D} = 10.56 \text{ nm} \quad (5.6)$$

The propagated error due to errors at the individual measurement is given by [34]:

$$\sigma_R = \pm \sigma_D \left( \frac{\partial R}{\partial D} \right) \quad (5.7)$$

$$\frac{\partial R}{\partial D} = -aD^{-2} = -RD^{-1}, \text{ where } a = \frac{kT}{6\pi\eta} = \text{constant}$$

$$\begin{aligned} \text{so from [5.2,5.6,5.7], } \sigma_R &= 0.0245 \times 10^{-7} \times 10.56 \times 10^{-7} \times (2.31808 \times 10^{-7})^{-1} \\ &= \pm 0.111 \times 10^{-7} \text{ cm} \end{aligned}$$

so

$$R_H = 10.56 \pm 0.111 \text{ nm} \quad (5.8)$$

A second measurement of the same sample under the same conditions, gave a of  $R_H = 10.92 \text{ nm}$ . The mean value of radius is 10.74, and the standard deviation for this two measurements is,  $\sigma_{RM}=0.18 \text{ nm}$ . The cumulative standard deviation is [34]:

$$\sigma_R = (\sigma_{IM}^2 + \sigma_{RM}^2)^{1/2} = (0.0245^2 + 0.18^2)^{1/2} \quad (5.9)$$

$$\sigma_R = 0.182 \text{ nm} \quad (5.10)$$

where  $\sigma_{IM}$  is the standard deviation for the individual measurement, and  $\sigma_{RM}$  is the repeated measurements's standard deviation. The above example clearly illustrates that the individual measurement deviation is negligible compared to the repeated measurements standard deviation, so it will not be taken into account in the rest of our work.

The different repeatabilities are given in the Appendix 1 and their magnitude varies from less than 3% to 30 % in the aggregated regime where irreproducibilities are due to the nonequilibrium structures.

To simplify the analysis of PEC formation, it was decided to do all the experiments in or near the dilute polymer concentration regime, defined by  $C_p < C_p^*$ , where  $C_p^* = \frac{DP}{4/3\pi R_g^3}$  (2.18).

Figure 5.1.2 is the determination of the dilute regime concentration. Four different NaPSS concentrations were used,  $C_1=10^{-5}\text{g/ml}$ ,  $C_2=5 \times 10^{-5}\text{g/ml}$ ,  $C_3=10^{-4}\text{g/ml}$ ,  $5 \times 10^{-4}\text{g/ml}$  at ionic strength of  $I=0.01\text{M}$ . This test was done at the lowest ionic strength studied in this work,  $I=0.01\text{M}$  where the magnitude of intermolecular electrostatic interactions are greatest.

In the dilute regime, electrostatic and hydrodynamic interactions between the polymer molecules are negligible, and the only forces present are the thermal

Brownian forces. Generally the diffusion coefficient of a polymer molecule in

solution is given by [53] :  $D=D_0\{1+(\frac{K_{eff}^2}{2C_s} + A_2)C_P\}$ , where D stands for the

diffusion coefficient at polymer concentration  $C_P$ ,  $D_0$  is the infinite dilution diffusion coefficient,  $K_{eff}$  is the effective charge of the macromolecule,  $C_s$  is the salt concentration and  $A_2$  is the second virial coefficient, characteristic of the excluded volume. The dilute regime occurs when the second term inside the brackets is negligible because either due to low concentration or when the second virial coefficient is very small. In the dilute regime, the diffusion coefficient is only a function of structural features, temperature, and solvent viscosity. In this region the plot of the diffusion coefficient vs concentration is constant [53].

In the semidilute regime, defined by  $C_P > C_P^*$  or  $C_P$  where the second term of above equation is significant, the chains start to overlap considerably so that diffusion is a cooperative process with characteristic length given by the distance between the the entanglements. In this regime, the diffusion coefficient increases with increasing concentration. At even higher concentrations, the concentrated regime, the motion gets slower, because of the increasing bulkiness of the structure and the diffusion coefficient starts to decrease. In this regime the diffusion coefficient decreases with increasing concentration [11,12,13].

Figure 5.1.2 shows that the dilute region is for  $C < 10^{-4}$  g/ml, because hydrodynamic radius is constant (results are within expected experimental error), which means that diffusion coefficient is also constant. In this work the final NaPSS concentration was  $10^{-4}$  or  $5 \times 10^{-5}$  g/ml.

Figure 5.1.3 was the same test performed this time for two different NaPSS concentration in PEC, at ionic strength of  $I=0.01M$ . The hydrodynamic radius is almost constant again, ( $5 \times 10^{-5}$  g/ml, 41nm) and ( $5 \times 10^{-4}$  g/ml, 38.75nm), thus the diffusion coefficient is constant which means that  $C=[5 \times 10^{-5}, 5 \times 10^{-4}]$  is indeed in the dilute regime.

Table 5.1.1 is a test of filtration technique. This test was performed in

order to verify that no aggregates were filtered, from a solution of  $Z=0.612$  and  $I=0.1M$ , using the  $0.2\mu m$  filter. In this solution  $Z > Z_{crit}$ , so PEC aggregates have already formed. UV absorbance measurements before and after the filtration agreed with each other. This proves that the concentration of the NaPSS remains the same after the filtration and that the particles sizes are not bigger than 200 nm.

**Table 5.1.2 Test of filtration technique**

**NaPSS MW:1,200,000**

**PLL MW:10,200**

**I=0.1M, T=25°C, pH=7**

**Z=0.612**

PEC solution's UV O.D. absorbance at 261.5nm	
Nonfiltered	0.510
Filtered	0.480

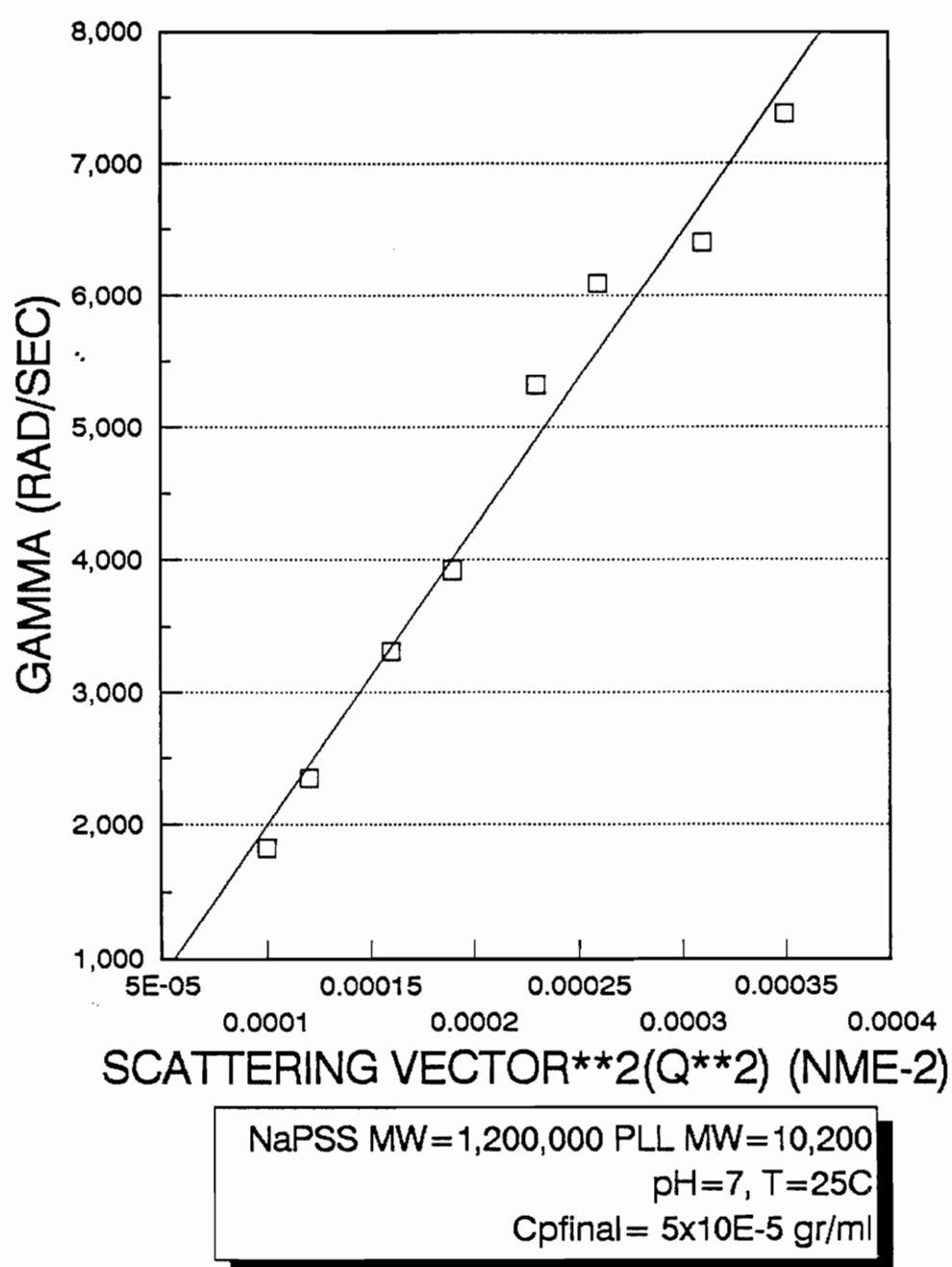
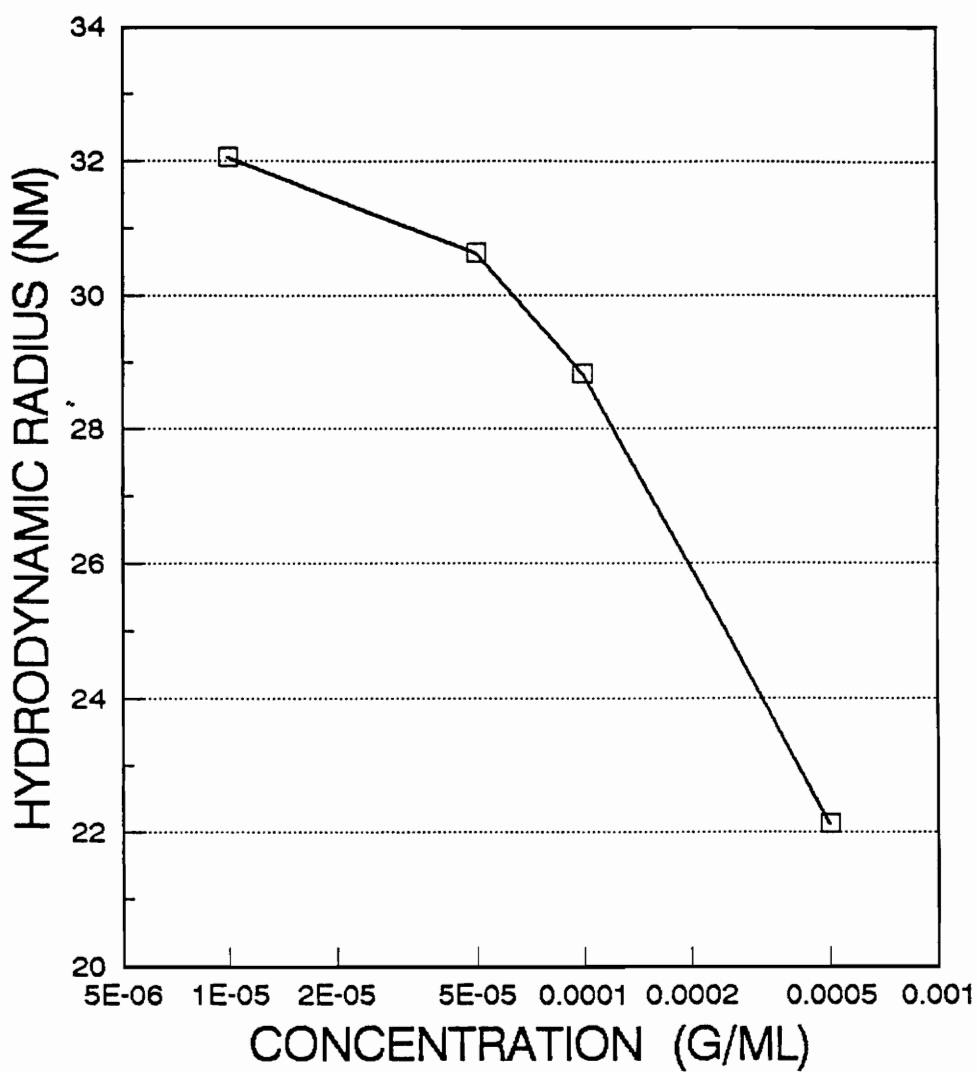
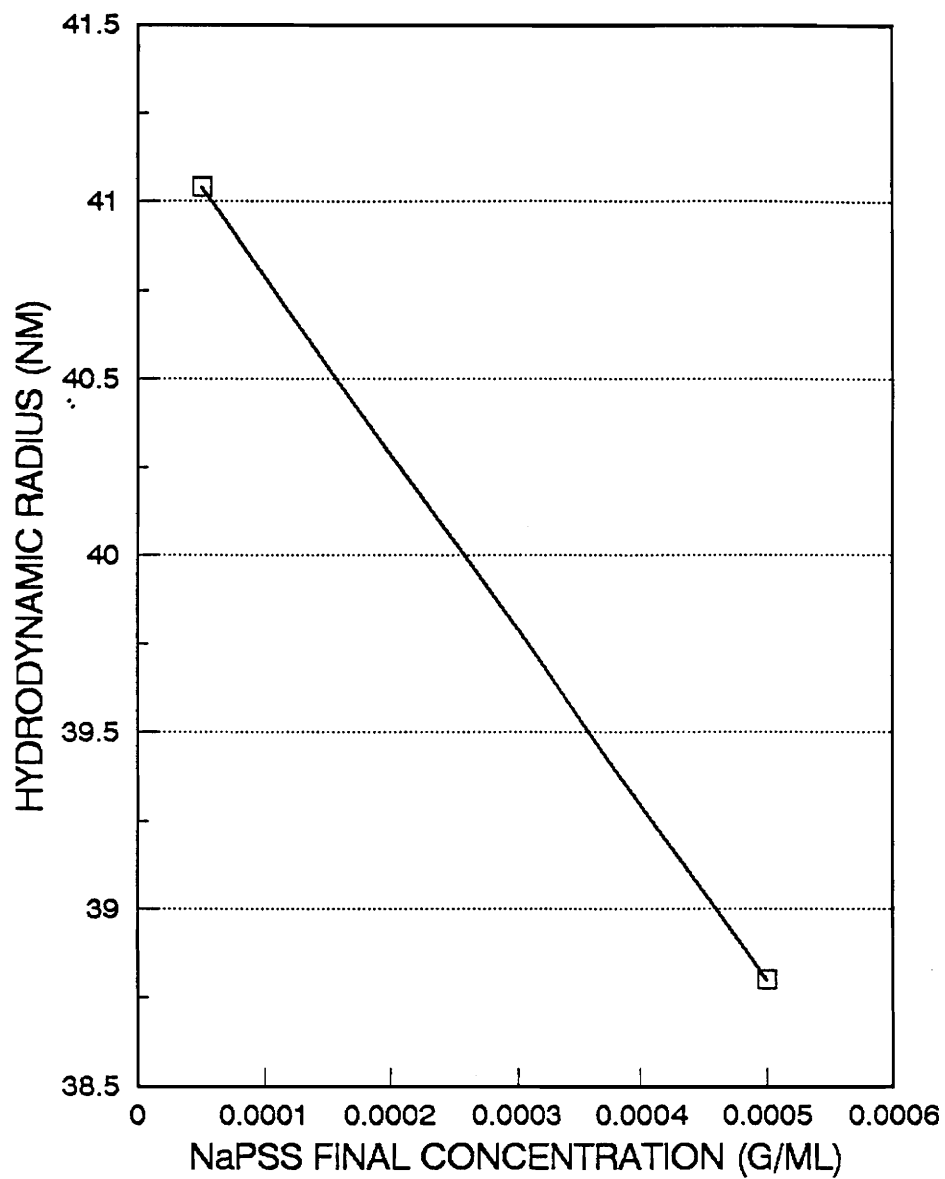


FIGURE 5.1.1 DETERMINATION OF HYDRODYNAMIC RADIUS,  $R_h$ .



NaPSS IN  $I=0.01\text{M}$  NaCL SOLUTION  
NaPSS MW: 1,200,000  
pH =7 T=25C

FIGURE 5.1.2 DETERMINATION OF THE DILUTE REGIME



NaPSS : 1,200,000 PLL: 10,200  
I=0.1M Z=0.51 pH=7 T=25C

FIGURE 5.1.3 DETERMINATION OF PEC DILUTE REGIME

## 5.2. Pure Polymer data

### 5.2.1. Sodium Polystyrene sulfonate

The two NaPSS samples studied in this work had weight average molecular weight of  $1.2 \times 10^6$  and 200,000, with  $M_w/M_n$  values of 2.2 and 1.56 respectively. The hydrodynamic radii reported in this work were z-average sizes. A measure of the polydispersity of the sample is given by the polydispersity option of the software defined as  $P = \frac{\mu}{I}$  (4.14), which actually is the reduced second cumulant (details in Chapter 4).

Figure 5.2.1.1. shows the effect of the ionic strength on the hydrodynamic radius of pure NaPSS. The Hydrodynamic radius decreases as the salt concentration increases due to salt ion screening [53]. The three  $(R_H, I)$  pairs represented on the figure are: (34nm, 0.01M), (25nm, 0.1M), (23nm, 1M) each point being the average of at least three measurements.

The NaPSS chain is rather flexible compared to other polymers like DNA or Xanthan. At low ionic strengths it has an extended end-to-end distance, due to strong excluded volume and chain stiffening effects, discussed in details in Chapter 2. A large value of the total chain expansion factor  $\alpha_T$ , is expected, where  $\alpha_T$  is defined as :

$$\alpha_T = \alpha_z \frac{R_g^0(L_\kappa)}{(R_g^0)_\theta} \quad (2.13)$$

where  $\alpha$  is the expansion factor due to excluded volume effects, and  $R_g^0(L_\kappa)$  is the radius of gyration due to chain stiffening, and  $(R_g^0)_\theta$  are the unperturbed dimensions at theta conditions (see Chapter 2). This is due to electrostatic repulsions between the sulfonate charges on the chain (Chapter 2). As the ionic strength of the solution increases, charged groups on the NaPSS are screened more effectively from each other. Thus, electrostatic repulsions are reduced, and they are allowed to come closer, causing the expansion factor  $\alpha$  to decrease. The chain exhibits a more compact coil-like conformation. Shrinking of the chain

occurs upon the addition of salt if the polymer chain is largely hydrophobic, as is the case for NaPSS.

At  $I=4.1\text{Molar NaCl}$ , the NaPSS chain reaches its unperturbed dimensions (theta conditions) and  $\alpha_T=1$ . Further increases in ionic strength will induce further shrinking, due to hydrophobic interactions and finally the chain will collapse and precipitate. In the present research, ionic strength ranged from 0.01 to 1.0M NaCl, thus avoiding the theta conditions of NaPSS. Thus, these experiments were always conducted in a good solvent for NaPSS. Fig.5.2.1.2 shows that the hydrodynamic radius of NaPSS with molecular weight 1,200,000 varied from 33.5 nm at  $I=0.01\text{M}$  to 23 nm at  $I=1\text{M}$ .

### 5.2.2. Pure Poly-l-lysine data

Poly-l-lysine is a polypeptide, which exhibits a helix-coil transition common to many polypeptides [6-9,37-44,51,52]. There are at least four conformations known to exist in polypeptides [51,52]. The  $\alpha$ -helix, whose characteristic is the intramolecular hydrogen bond between the carbonyl oxygen of one amino acid residue and an amide hydrogen. The random coil, a structure devoid of order at all levels [43], which results when the helix melts due to destabilization of the H-bond, observed at high ionic strength [51]. The extended coil(left-handed helix), which exists at low ionic strength and low pH [51]. The  $\beta$ -pleated sheet structure, which results if extended chains are placed side by side so that efficient intermolecular hydrogen bonds are formed [44]. These conformations are complex functions of pH, temperature, concentration and ionic strength. There are different conformations adopted by the macromolecules under different thermodynamic and chemical conditions. "The stable spatial organization of a macromolecule for one given set of environmental conditions maybe unstable in other environments" [51]. Any large change in the equilibrium molecular properties resulting from small changes in the environmental conditions, considered to be cooperative phenomenon [51]. Transitions induced by heat or solvent polarity do not appear to be as highly cooperative as the ionization induced transition [51].

The polypeptide bond which stabilizes the  $\alpha$ -helix conformation is a hydrogen bond between the carbonyl oxygen of one amino acid residue and the amide hydrogen (Fig. 5.2.2.1)[37,39-44]. This structure can be disrupted either by heating, or with pH or solvent effects.

The  $\alpha$ -helix forms under conditions, where repulsive electrostatic forces between the protonated lysyl groups are reduced compared to attractive hydrogen bond forces, which stabilize the  $\alpha$ -helix. These conditions include: 1. high pH, which reduces the degree of protonation and hence the effective charge density, 2. Low temperatures, which maximizes the H-bond strength relative to

electrostatic repulsions [39] 3. Low ionic strength and high pH, where again the repulsive electrostatic forces are reduced due to the reduced degree of protonation of the PLL, so attractive intramolecular hydrogen bond forces are favored [51].

The  $\alpha$ -helix has an effective cylindrical diameter 2.5 nm and for a MW=62,000, behaves as a rigid rod [51]. Thus salt-free PLL, with lower molecular weight, such as 10,200 and 50,000 used in this research, is expected to form rigid, rodlike  $\alpha$ -helix structures at pH>10. The extended coil conformation forms under conditions where the electrostatic forces between the fixed, protonated  $\text{RNH}_3^+$  groups introduced some local structure in the coil form. Jamieson [51] writes: "at low ionic strength, the charge on the pendant amine groups of the polymer introduces some local structure in the "coil" form (pH<9.5) giving it a characteristic CD spectrum which has been correlated with an extended "kinked" lefthanded helical conformation".

The random coil is characteristic of linear chain polyelectrolytes when no intra-or intermolecular association occurs. It is favored by higher temperatures [44] and high ionic strength [51].

The  $\beta$ -structure, which is the less well-characterized structure [38], forms under conditions where the individual chains are allowed to approach each other and form hydrogen bonds. These include high PLL concentration, high pH, and high temperature which favor the formation of hydrophobic interactions and high ionic strength [38].

Our main concern here was to identify the possible conformation, under different conditions, with DLS measurements. Since the conformation of the PLL was expected to affect PEC formation and structure, it is important to study the effects of ionic strength I, pH, and temperature on the pure PLL. These effects are discussed next.

**Temperature effects:** The temperature induced melting of the  $\alpha$ -helix to the random coil conformation is less cooperative than the helix to coil transition

caused by lowering the pH from 10.8 to 7 [42]. In [43] it is reported that a plot of viscosity  $\eta$  vs temperature for a polypeptide undergoing helix-coil transition indicates a broad range in temperatures over which the transition occurs. The reason for this is that PLL chain is tightly packed in the  $\alpha$ -helix conformation. However when the temperature rises, the mean vibrational displacement of each atom becomes larger which is equivalent to enlarging the VanderWaals radii. Thus, the helix is forced to come apart. This doesn't occur simultaneously for all the residues, but rather gradually as a residue converts from the helical state. This gives rise to the random coil conformation which is quite long lived. At even higher temperatures, the hydrogen bond is disrupted totally, the PLL chain assumes a totally random conformation with higher conformational entropy, where the hydrophobic interactions increase in magnitude. For PLL complexed with chondroitin sulfate (C6S), at  $\text{pH} \simeq 7$ , Blackwell reports [9], this melting temperature to be  $47^\circ\text{C}$ . However, in this particular study the PLL transition occurred while complexed with C6S, which will most likely affect the transition. At a certain higher temperature,  $T_\beta$ , nonpolar interactions bring the chains together, and intermolecular hydrogen bonding starts to occur [38]. For PLL, at 0.2M NaCL, and  $\text{pH} \simeq 11$ , this temperature is reported [38] to be  $32^\circ\text{C}$ . It is also reported [38], that this transition is irreversible on cooling, whereas below  $T_\beta$  all the transitions are reversible on cooling, and the PLL assumes again the  $\alpha$ -helical state.

Table 5.2.2.2 shows the diffusion coefficient of PLL as a function of its thermal history. The first data point is the diffusion coefficient measured at  $25^\circ\text{C}$  with no prior heating of the PLL. The second data point is the diffusion coefficient of PLL at  $25^\circ\text{C}$  again, but the PLL being heated in  $47^\circ\text{C}$  for about 35 min. The final data point was obtained after heating at  $47^\circ\text{C}$  for 1 day and measuring again at  $25^\circ\text{C}$ . The diffusion coefficients vary by 11%, which is within the precision of the DLS experiment. Thus, they are effectively the same, thus, proving that any conformation transition that does occur due to temperature changes at 0.1Molar are reversible. A more accurate measurement of the helix content requires circular dichroism experiments.

***Ionic strength effect:*** Figure 5.2.2.2. display the effects of temperature and ionic strength on, pure PLL of 50,000 molecular weight, for  $\text{pH} \simeq 6.8$ . At  $I=0.01\text{M}$ , and at  $\text{pH}<10.8$ , PLL is at its extended coil conformation [51]. At neutral pH and ionic strength  $I=0.1\text{M}$ , poly-l-lysine is an extended coil again [52]. The diffusion coefficient increases with ionic strength which is expected since an extended coil polyelectrolyte will contract as ionic strength increases. At  $I=1\text{M}$  the chain is in a random coil conformation, and the size is more compact. This is in agreement with Jamieson [51]. At low ionic strength of  $I=0.01\text{M}$ , the diffusion coefficient is lower, thus meaning that the particle is larger, and it gets higher as the ionic strength increases. A possible explanation is that at low ionic strength the electrostatic interactions are so large, that repulsive forces between the bulky substituents, carrying the charges, are strong. This can cause, the chain to bend, "exposing" the charges to the aqueous media, surrounding the chain, and at the same time bringing thus the amide and the carbonyl closer (due to higher hydrophobicity in this part of the chain), thus forming the intramolecular hydrogen bonding. This conformation is also, entropically favored, because the chain assumes a cylindrical rigid-rodlike shape, with the charges on the surface [52] and the hydrophobic part "protected" in the interior of the cylinder. A reasonable explanation for this "melting" of the helix conformation is that the increased screening of the charges allows the big bulky group of the side chain which carries the charges, to approach each other. This is likely to induce vibrational modes in the chain which destroy the helix conformation. This also suppress the electrostatic field around the molecule, enhancing thus the hydrophobicity. The chain then has to assume a conformation which expose the minimum surface, minimizing thus the free energy. This conformation is of the random coil, with a high conformational entropy.

At temperature  $T=47^\circ\text{C}$ , however, the picture is very different. The sharp drop in diffusion coefficient as the ionic strength increases from  $I=0.01\text{M}$  to  $I=1\text{M}$ , suggests that the PLL undergoes a conformation transition, with the possible formation of a  $\beta$ -sheet structures [38,52], which according to Davidson

[38], their rate of formation is higher the higher the concentration of the random coil. At  $I=0.01M$ , though, the behavior is totally different, thus, the diffusion coefficient increases upon heating, which indicates a more compact structure. Assuming that at this low ionic strength the coil has an extended "kinked" lefthanded helical conformation [51], upon heating the intramolecular hydrogen bond is disrupted forming thus a random coil with a higher diffusion coefficient.

**pH effects** :Figure 5.2.2.3 presents the effects of pH on the hydrodynamic radius of  $I=0.1M$  solution of pure PLL. At  $pH = 7$  the chain has a higher diffusion coefficient, than in  $pH=9.8$  and  $pH=11.2$ . We believe that under the conditions of  $pH=7$ , the chain is still a random coil. At  $pH \simeq 9.8$  the chain is in the helix conformation, or a mixture of  $\alpha$ -helix and  $\beta$  structure, due to the large sizes determined by light scattering. At  $pH \simeq 9.8$  PLL and at  $I=0.1M$  only 50% of its side groups are protonated [52]. This reduces the electrostatic forces, hydrophobicity increases and an intermolecular "hydrogen-bond" structure is favored. Especially at the pH of 11.2, where the hydrophobicity is very high, because of the small percentage of the charged side chains (almost 0%), the chains are allowed to come closer due to nonpolar interactions and an intermolecular hydrogen bond is favored, leading to  $\beta$ -structures, and an increase to size, due to aggregate formation [52].

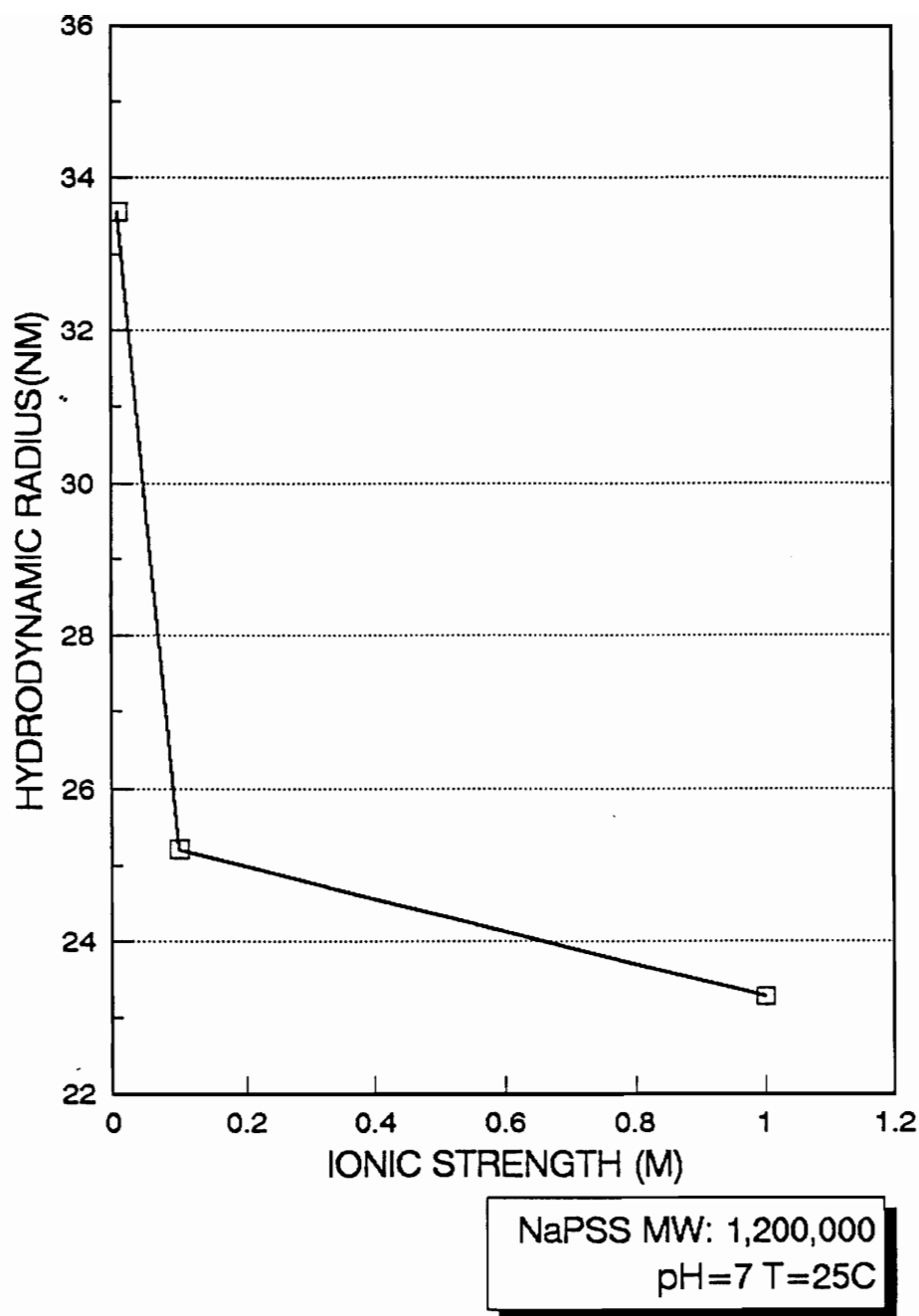


FIGURE 5.2.1.1 THE EFFECT OF IONIC STRENGTH ON HYDRODYNAMIC RADIUS OF NaPSS.

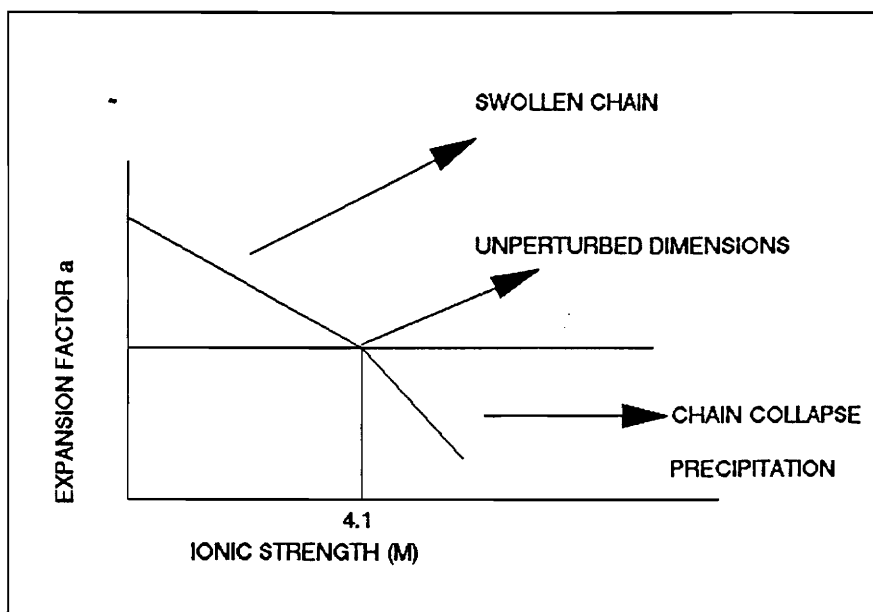


FIGURE 5.2.1.2 EXPANSION FACTOR VS IONIC STRENGTH

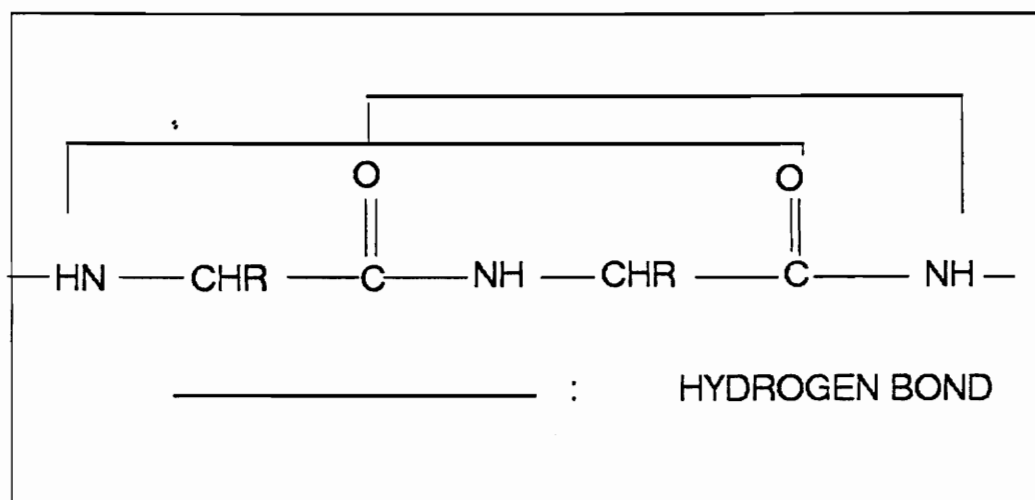


FIGURE 5.2.2.1 THE POLYPEPTIDE  $\alpha$ -HELIX BOND

**Table 5.2.2.2. PLL 's thermal history dependence**

**MW=50,000g/mole**

**I=0.1M,  $C_{PLL}=7.64 \times 10^{-4}$ g/ml**

	<b>Diffusion coefficient (<math>\text{cm}^2/\text{sec}</math>)</b>
<b>A</b>	$2.72 \times 10^{-7}$
<b>B</b>	$2.59 \times 10^{-7}$
<b>C</b>	$2.45 \times 10^{-7}$

where A= no thermal treatment

B = 30 min at  $47^\circ\text{C}$ , and back to  $25^\circ\text{C}$ .

C = 24 h. at  $47^\circ\text{C}$ , and back to  $25^\circ\text{C}$ .

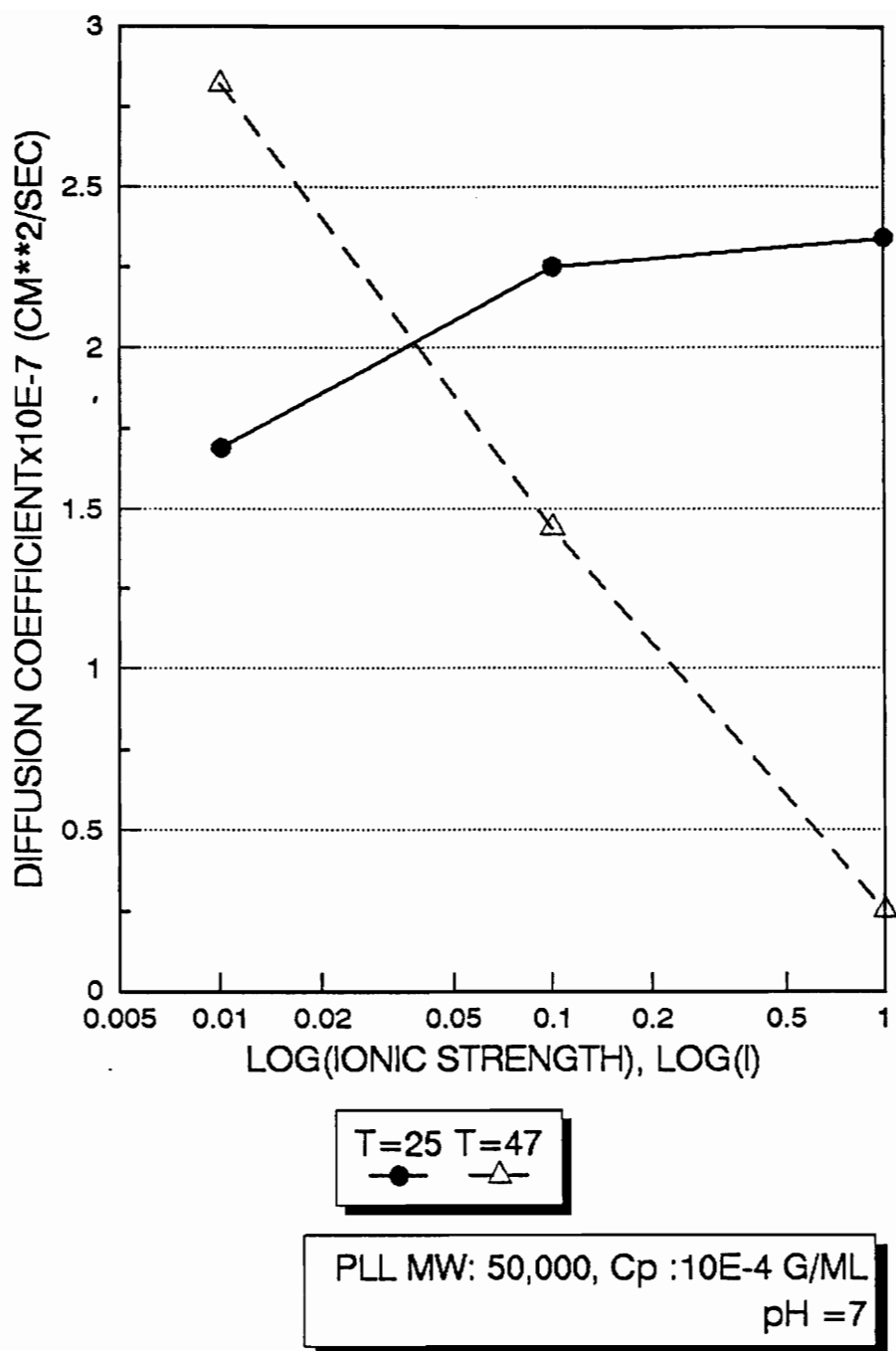
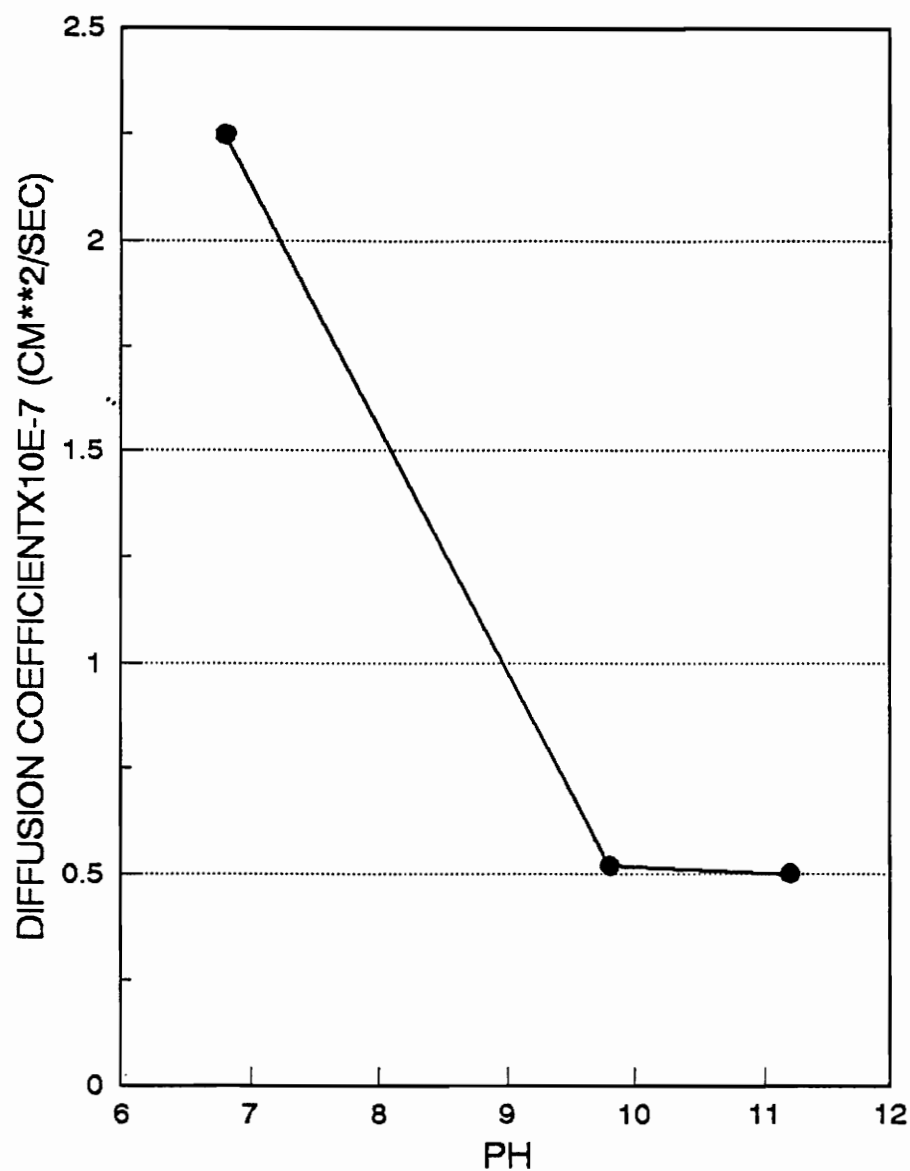


FIGURE 5.2.2.2 TEMPERATURE EFFECTS ON PURE PLL



PLL MW : 50,000  
Cp : 10 E-4 G/ML , I=0.1M  
T=25 C NO THERMAL PRETREATMENT

FIGURE 5.2.2.3 pH EFFECTS ON PURE PLL

### 5.3 Polyelectrolyte Complex data

In this final section of the results presentation, the study of a PEC system is going to be described. PLL/NaPSS complex behavior was studied as a function of the ionic strength, the temperature, the pH of the solution, as well as the molecular weights of the host and guest molecules. Some possible mechanisms for PEC formation and the onset of aggregation will be described in terms of the above factors, as well as the PLL conformational transition.

#### 5.3.1 Ionic strength effects

Figure 5.3.1.1 presents the effect of ionic strength on the onset of aggregation for the PLL/NaPSS system. Multihost aggregation results from binding of two or more NaPSS host molecules due to complexation with PLL. Intramolecular complexation of PLL and NaPSS, however, should lead to coil shrinkage and collapse of the NaPSS host. Each point is an average of at least three measurements. Raw data and reproducibility tests are shown in Appendix#1.

The principal observations are: i) The onset of multihost NaPSS aggregation, defined as  $Z_{crit}$  on the x-axis, shifts to lower values of  $Z$  as the ionic strength decreases.

ii) For  $Z < Z_{crit}$ , the hydrodynamic radii are effectively constant, i.e.,  $R_H$  is not a function of  $Z$  for  $Z < Z_{crit}$ . This suggests little or no intramolecular complexation is occurring. This contradicts Kabanov's observations for the PDMAEMA · HCl/PP polyelectrolyte system [19].

iii) At  $I=1M$ , slight host NaPSS coil shrinkage occurs at  $Z < 0.65$ , followed by a sharp collapse of the NaPSS molecule between  $0.65 < Z < 0.880$ . This is very likely due to intra-host complexation of the PLL with NaPSS, which neutralizes

the NaPSS charges, causing coil shrinkage. This agrees qualitatively with Kabanov's general findings [19].

At  $I=0.01M$  the aggregation begins almost right away,  $0.070 < Z_{crit} < 0.123$ . At  $I=0.1M$  begins in the vicinity of  $Z=0.44$ ,  $0.44 < Z_{crit} < 0.530$ . At  $I=1M$  we didn't reach the aggregation regime at least up to  $Z_{max} \simeq 0.880$ .

Presumably at low ionic strengths and  $pH=7$  PLL has an extended coil conformation [51,52]. Also NaPSS is at its extended conformation due to low ionic strength (especially at  $I=0.01M$ ). Electrostatic attraction between the PLL and NaPSS should be quite strong. The free energy of carrying PLL charges into the ion atmosphere of NaPSS is negative and is counterbalanced by the decreased entropy. Thus, the PLL stops at a distance from the NaPSS ion where  $\Delta G_{el}$  is minimum [37]. At low ionic strengths this distance is much closer to the NaPSS ions, due to the strong electrostatic field. NaPSS sites are more accessible at this extended conformation. So PLL approach is favored not only from an electrostatic free energy point of view but also from an entropic one, since the bulky side groups of NaPSS repel each other, so they allow PLL approach. Kabanov explains the aggregation of those structures, as a result of increased hydrophobic interactions between the structures (Fig.5.3.1.3.) [19]. Another possible mechanism can be this of intermolecular  $\beta$ -structure. Fruitfull collisions between these structures, can possibly lead to intermolecular hydrogen-bonds between the PLL chains (Fig.5.3.1.2). The increased hydrophobicity of this structure may cause phase separation and probably after some time precipitation [38]. In this work we didn't check the time dependence of this structure. A third possible mechanism is that of the PLL serving as a "bridge" between two host molecules (Fig.5.3.1.4.)

As the ionic strength increases, the flexible NaPSS chain contracts due to reduced electrostatic repulsion. As the ionic strength increases, the electrostatic binding energy for PLL and NaPSS to form interhost complexes decreases to the extent that the binding energy becomes than  $kT$  energy at room temperature. Thus, interhost complex formation is suppressed at high ionic

strength. However, the I=1M data clearly show the formation of an intrahost complex for  $Z > 0.69$  due to charge neutralization of the NaPSS backbone.

### 5.3.2 Temperature effects

The temperature effect was studied as three different but interrelated cases as shown below. "Thermal history" refers to the temperature history that either the pure PLL had before mixing with NaPSS or the PEC had after mixing.

CASE # 1	CASE#2	CASE#3
No thermal history	PLL heated as: 5°→47°→25°C	PEC heated:5→47→25°C
I=0.1M	I=0.1M	I=0.1M

The temperature of the decalin bath is going to be symbolized as A: T=25°C, and B: T=47°C. Thus, case #1A means neither the PLL or the complex had undergone a thermal treatment, and the measurement was conducted at T=25°C.

CASE#1: Tables 5.3.2.1(#1A), 5.3.2.2(#1A), 5.3.2.3(#1A), 5.3.2.6(#1A, #1B) present the hydrodynamic radius vs Z, at I=0.1M, and the polymer concentration shown in the tables.

In the first three tables both PLL and PEC have not undergone any kind of thermal treatments. We clearly notice that  $Z_{crit}$  lies between [0.44-0.530]. Actually,  $Z=0.51$  must be right on the "borderline", since there have been some cases where aggregation already begun (5.3.2.6A). PEC's generally are very sensitive to their environment and large nonequilibrium structures are formed abruptly. Only slight differences in mixing procedure, stock solutions concentrations for example, can cause the aggregation to begin sooner. In this case  $Z_c=0.51$  is only slightly higher.

Within the aggregation region,  $Z > Z_{crit}$ , the lack of reproducibility of PEC size is due to the highly nonequilibrium structures.

CASE#2: (Tables 5.3.2.4, 5.3.2.5) Thermal cycling of the PLL, before

complexing didn't seem to affect the  $Z_{crit}$ . It is reported in the literature [38], that PLL heating under  $T_\beta$ , where  $T_\beta$  is the temperature where  $\beta$ -structures are formed, is completely reversible after cooling, and the PLL assumes again the conformation that has in the original state. For the table 5.3.2.5. the PLL was heated at 59°C, for 30 min. In [38], it is reported that for I=0.2M and after 1 hour,  $\beta$  structures formed. Our condition were different and certainly the time of heating was much less than the time required for the transition (1h.). In any case, as it was stated above, the PEC doesn't behave any differently after having received the above treatment. In the case of 5.3.2.5B (Case#2B), we see again the temperature effect on PEC, which is clearly breaking up the complex.

CASE#3: (Tables 5.3.2.7, 5.3.2.8) In this case PEC was originally not thermally treated. Aggregation occurred at  $Z_{crit}=0.44$  with  $R_H=90.49$  nm in Table 5.3.2.6.A (Case#1A). Then the same sample was heated for 30 minutes to 47°C. It seems that this kT energy was enough in some cases to break those structures and convert them to smaller ones (Table 5.3.2.7, CASE#3A). In fact at  $Z_{crit}= 0.44$  after the above treatment(Case#3A), the size dropped from 90.49nm to 24.5, which is the size of the single NaPSS chain. The same phenomenon was observed for  $Z=0.530$ , although this time the final size is a somewhat larger than this of the NaPSS chain, indicating that the new structures may also be nonequilibria structures but they are much less nonequilibria structures compared to the original ones (see also 5.3.2.8A). Raising the temperature in the decalin bath at 47°C, CasesB, we measured the kinetics of this nonequilibria structures size reduction (Fig. 5.3.2.1, 5.3.2.2). As a matter of fact at  $T=47^\circ\text{C}$  (5.3.2.6.B, case#1B) both sizes of the 0.44 and 0.530 dropped to the NaPSS single chain size. The same observation was made for the less nonequilibria structures (5.3.2.7.B, Case#3B) when they were heated up to 47°C.

The reason for this breaking-up of the complex may be:

- i) A conformation change from an extended coil to random coil, or
- ii) Temperature just melt down the complex, because kT energy is much

higher than the electrostatic forces which keep the complex together. This may occur, regardless of the conformation.

### 5.3.3 The effect of pH on PEC's binding

Figure 5.3.3.1 shows the effect of pH on PEC's binding. Two experiments were performed. The first was at  $\text{pH} \simeq 7$  and the second was at  $\text{pH} \simeq 10.8$ . The ionic strength was  $I=0.1\text{M}$  in both cases and no thermal treatment was performed in PLL or PEC. Again here we observe, that in case of  $\text{pH}=7$ , the aggregation begins at 0.44, and no significant change in size occurs before the onset of aggregation. Upon increasing the pH, however, the aggregation ceases to occur and the  $R_H$  drops again at those of the single NaPSS host, i.e., at ( $\text{pH}=7$ ,  $Z=0.44$ ,  $R_H=82$ ) whereas at ( $\text{pH}=10.8$ ,  $Z=0.530$   $R_H=30\text{nm}$ ). As pH increases, the PLL chain becomes less protonated and thus loses its ability to bind to NaPSS. The reason that the size drops to the single NaPSS chain by partly neutralizing PLL, may indeed suggest the picture of PLL bridges that we introduced above (5.3.1.). The picture here can possibly be as follows: PLL binds with NaPSS at  $I=0.1\text{M}$  and  $\text{pH}=7$ , as an extended coil. At  $\text{pH}=10.8$ , one can notice a decrease in size with increasing  $Z$ , for  $Z < Z_{crit}$ . This trend is quite significant, experimentally (32.5 to 25nm). This can be explained by the fact that, since PLL is partly uncharged, binding with NaPSS charges, cause the hydrophobicity of the PEC chain to decrease to a greater extend than  $\text{pH}=7$ , where PLL is highly charged. This is in agreement with Kabanov's results [19]. In the case of  $\text{pH}=10.8$ , if a  $Z_{crit}$  exists, it is shifted to higher values, again because of the lesser ability of the PLL to bind, since its charge density is lower. In this work, the  $Z_{crit}$  for  $\text{pH}=10.8$  wasnot reached. Even though pure PLL, seems to form  $\beta$ -structures at such a high pH, it seems that mixing with NaPSS, either disrupts this structure or shifts its onset to even higher pH.

### 5.3.4 The effect of Molecular Weight in PEC's binding

The effect of the molecular weight of both NaPSS and PLL on PEC formation are described in this section.

Kabanov, in [19] reports that degree of polymerization of the host molecules must be greater than the degree of polymerization of the guest, in

order for the NPEC to form. The smaller the  $\frac{DP_{host}}{DP_{guest}}$  ratio is the smaller the value of the  $Z_{crit}$ .

In this set of experiments we change both NaPSS and PLL molecular weight and see how molecular weight affects the onset of aggregation. In all cases the degree of polymerization (and thus the molecular weight), of the host remained smaller than that of the guest (PLL).

The following polyelectrolyte complex systems were studied:

PEC#	Molecular Weight(NaPSS)	Molecular weight(PLL)
1	1,200,000	10,200
2	200,000	10,200
2	200,000	50,000

**I=0.01M** Figure 5.3.4.1. presents the behavior of the above polyelectrolyte systems at I=0.01M. In this case, the aggregation begins in a lower  $Z_{crit}$  for PEC1 and PEC2. It is probable that electrostatic effects dominates the onset of interhost aggregation. The elctrostatic potential around the NaPSS is so high, that complexes forming at extremely low values of Z.

**I=0.1M** Figure 5.3.4.2. shows that NaPSS molecular weight change don't affect  $Z_{crit}$ , which in both cases is around 0.44. Obviously the sizes are much smaller this time, due to the lower MW of the host PE. The behavior is exactly the same and this is more obvious at I=0.1M(Fig.5.3.4.2.). The onset of

aggregation at a lower value of  $Z$  when the molecular weight of PLL increases. This again indicates that the intensity of aggregation is a function of guest molecule degree of Polymerization or it would be better to say of the relative degrees of polymerization of the host and guest molecule. This also support again the idea of "PLL bridges". This supports the view that, the hydrophobic interactions becomes more important than the electrostatic ones.

**I=1M:** At  $I=1M$  again we did not see any aggregates up to  $Z=1$  (5.3.4.3.). Again here the electrostatic field around the NaPSS, is suppressed by the high ionic strength screening effects that  $kT$  energy is enough to break the complex.

**I=0.01M** Figure 5.3.4.1. presents the same experiment at  $I=0.01M$ . In this case, the aggregation begins in a lower  $Z_{crit}$  for PEC1 and PEC2. Here we are forced to believe that electrostatic effects dominates the phenomenon. The electrostatic potential around the NaPSS is so high, that complexes forming right away (5.3.2).

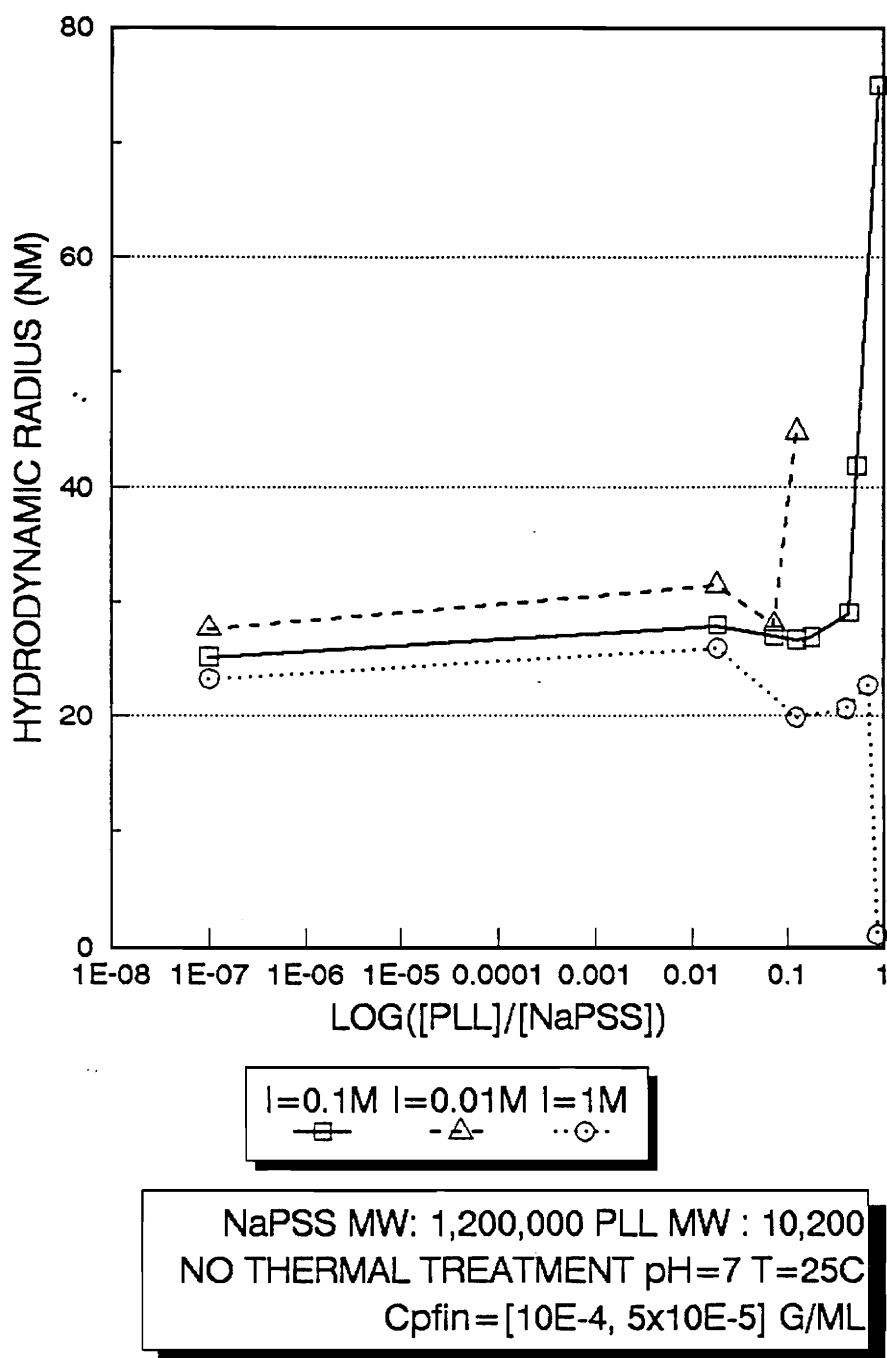


FIGURE 5.3.1.1 IONIC STRENGTH EFFECTS ON PEC'S FORMATION

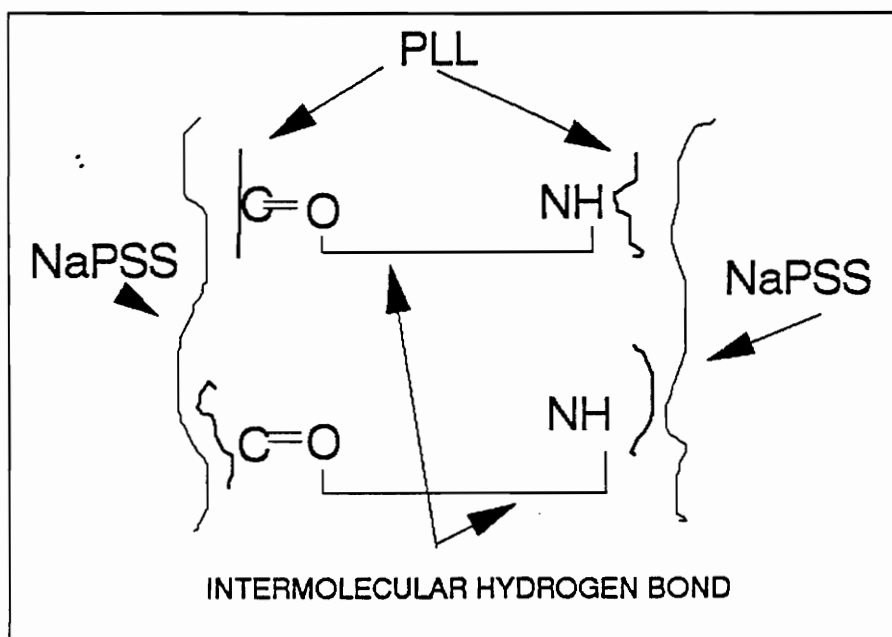


FIGURE 5.3.1.2 PLL BRIDGES THROUGH  $\beta$ -STRUCTURES.

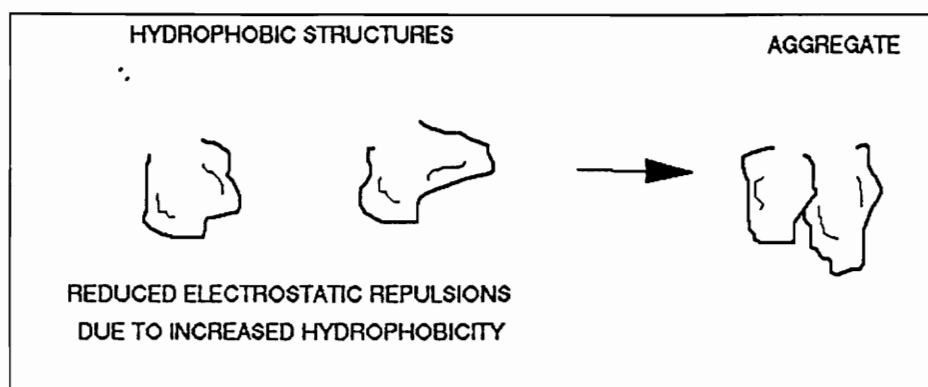


FIGURE 5.3.1.3 KABANOV'S MODEL FOR PEC'S AGGREGATION.

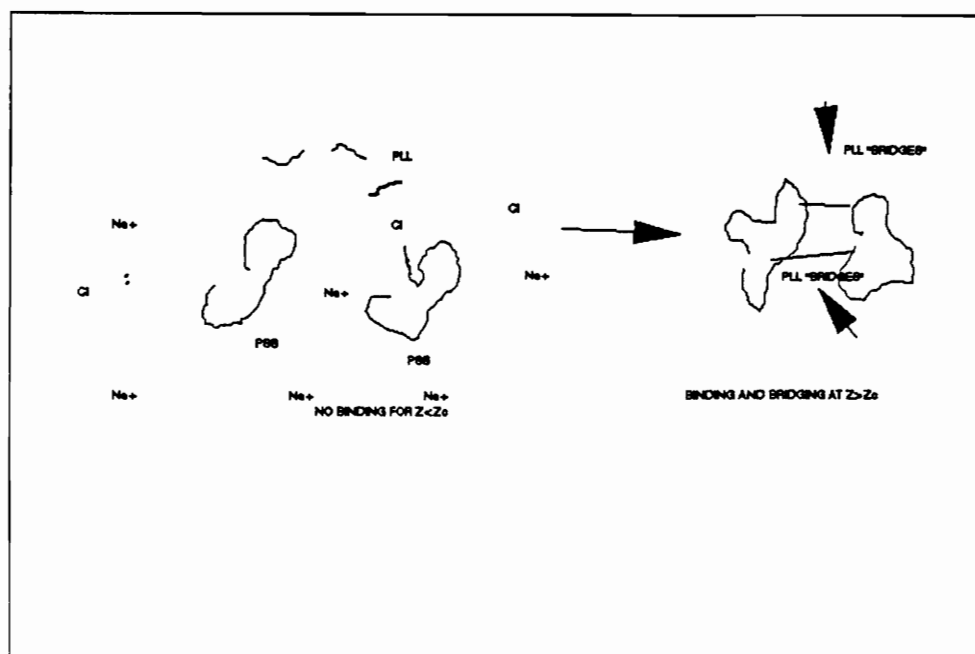


FIGURE 5.3.1.4 PLL "BRIDGES" MODEL.

Table 5.3.2.1. Polymer ratio vs Hydrodynamic Radius.

Conditions:  $C_{NaPSSin}$ :  $2.33 \times 10^{-3}$  g/ml

$C_{NaPSSfin}$ :  $10^{-4}$  g/ml

$C_{PLLin}$ :  $8.64 \times 10^{-4}$  g/ml

I=0.1M

Thermal History: None

Z	$R_H$ (nm)
0.000	28.74
0.018	27.95
0.071	31.48
0.124	27.43
0.176	28.70
0.441	29.24
0.529	72.04

**Table 5.3.2.2 Polymer ratio vs Hydrodynamic Radius.**

Conditions:  $C_{NaPSSin}$ :  $2.342 \times 10^{-3}$  g/ml  
 $C_{NaPSSfin}$ :  $4.9 \times 10^{-5}$  g/ml  
 $C_{PLLin}$  :  $5.204 \times 10^{-4}$  g/ml  
 $I = 0.1$  M  
Thermal History : None

Z	$R_H$ (nm)
0.071	27.05
0.124	24.73
0.176	28.96
0.441	23.94
0.529	40.67
0.882	87.02

**Table 5.3.2.3. Polymer ratio vs Hydrodynamic Radius.**

Conditions:  $C_{NaPSSin}$ :  $1.33 \times 10^{-3}$  g/ml  
 $C_{NaPSSfin}$ :  $10^{-4}$  g/ml  
 $C_{PLLin}$  :  $3.23 \times 10^{-4}$  g/ml  
 I=0.1 M  
 Thermal History: None

Z	R <sub>H</sub> (nm)
0.000	21.70
0.071	24.33
0.441	21.72
0.882	63.00

Table 5.3.2.4. Polymer vs Hydrodynamic Radius.

Conditions:  $C_{NaPSSin}: 2.33 \times 10^{-3} \text{ g/ml}$   
 $C_{NaPSSfin}: 10^{-4} \text{ g/ml}$   
 $C_{PLLin}: 10^{-3} \text{ g/ml}$   
 $I=0.1 \text{ M}$   
Thermal History: PLL heated as:  
 $5^{\circ}\text{C} \rightarrow 47^{\circ}\text{C} \rightarrow 25^{\circ}\text{C}$

Z	$R_H \text{ (nm)}$
0.000	26.56
0.018	27.73
0.071	27.86
0.124	27.16
0.176	27.04
0.441	93.40

**Table 5.3.2.5. Polymer vs Hydrodynamic Radius.**

**Conditions:**  $C_{NaPSSin}$ :  $2.33 \times 10^{-3}$  g/ml

$C_{NaPSSfin}$ :  $10^{-4}$  g/ml

I=0.1M

**Thermal History:** PLL heated to 59°C  
for 30 min. and let go back to 25°C

**A** Left side Decalene bath's T =25°C

**B** Right side Decalene bath's T = 47°C

Z	R <sub>H</sub> (nm)	Z	R <sub>H</sub> (nm)
0.071	25.18	0.071	—
0.124	26.61	0.124	26.22
0.176	24.850	0.176	27.80
0.441	71.03	0.441	29.12

**Table 5.3.2.6. Polymer vs Hydrodynamic Radius.**

Conditions:  $C_{NaPSSin}$ :  $2.33 \times 10^{-3}$  g/ml  
                   $C_{NaPSSfin}$ :  $10^{-4}$  g/ml  
                  I=0.1M  
                  Thermal History: None  
                  Left side Decalene bath's T =25°C  
                  Right side Decalene bath's T = 47°C

Z	R <sub>H</sub> (nm)	Z	R <sub>H</sub> (nm)
0.441	90.49	0.441	24.43
0.529	98.29	0.529	25.57
0.690	117.22	0.690	—

**Table 5.3.2.7 Polymer vs Hydrodynamic**

**Radius.**

Conditions:  $C_{NaPSSin}$ :  $2.33 \times 10^{-3}$  g/ml

$C_{NaPSSfin}$ :  $10^{-4}$  g/ml

I=0.1M

Thermal History: PEC heated to  $47^{\circ}\text{C}$

for 30 min. and let go back to  $25^{\circ}\text{C}$

A Left side Decalene bath's  $T = 25^{\circ}\text{C}$

B Right side Decalene bath's  $T = 47^{\circ}\text{C}$

Z	$R_H$ (nm)	Z	$R_H$ (nm)
0.441	24.50	0.441	24.16
0.529	38.33	0.529	29.81
0.690	92.380	0.690	87.42

**Table 5.3.2.8. Polymer ratio vs Hydrodynamic**

**Radius.**

Conditions:  $C_{NaPSSin}: 2.33 \times 10^{-3} \text{g/ml}$

$C_{NaPSSfin}: 10^{-4} \text{g/ml}$

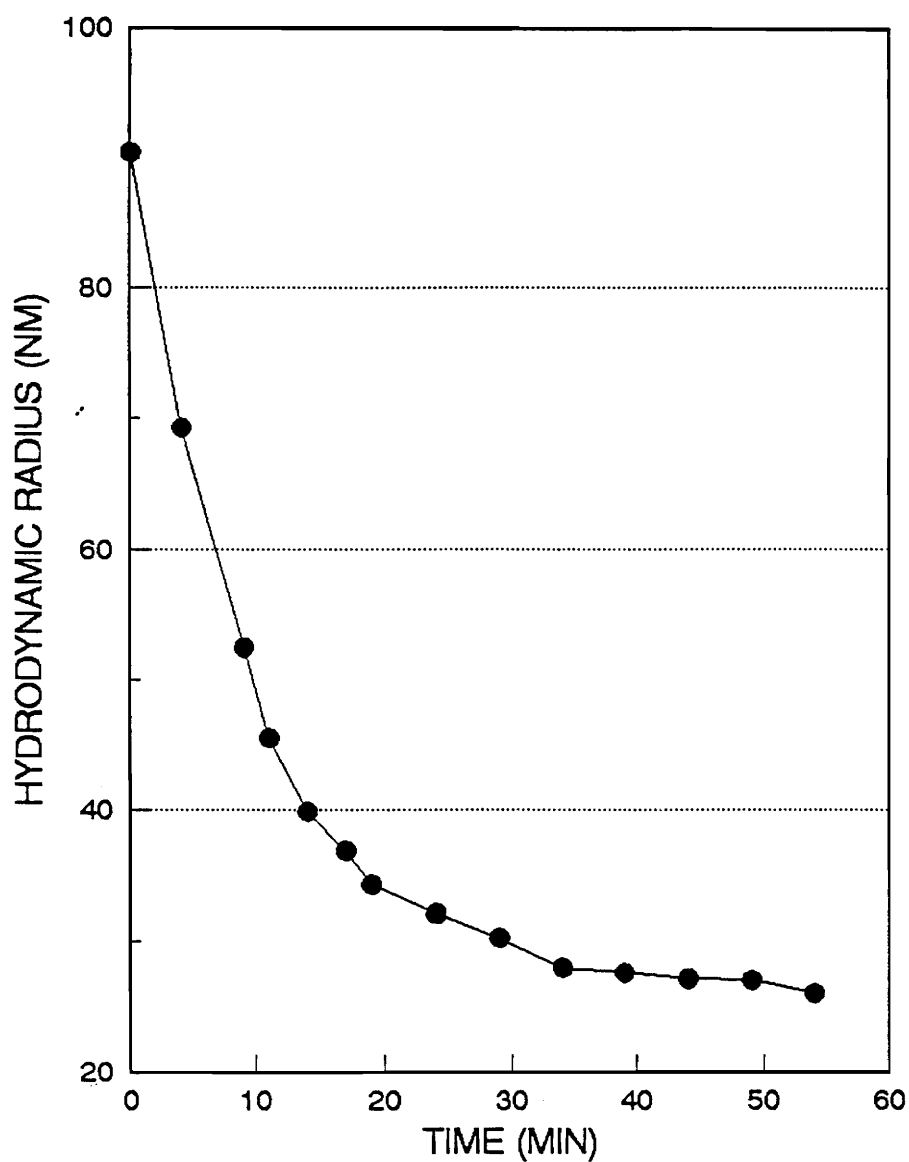
$C_{PLLin}: 10^{-3} \text{g/ml}$

$I=0.1\text{M}$

Thermal History : PEC heated at  $50^{\circ}\text{C}$

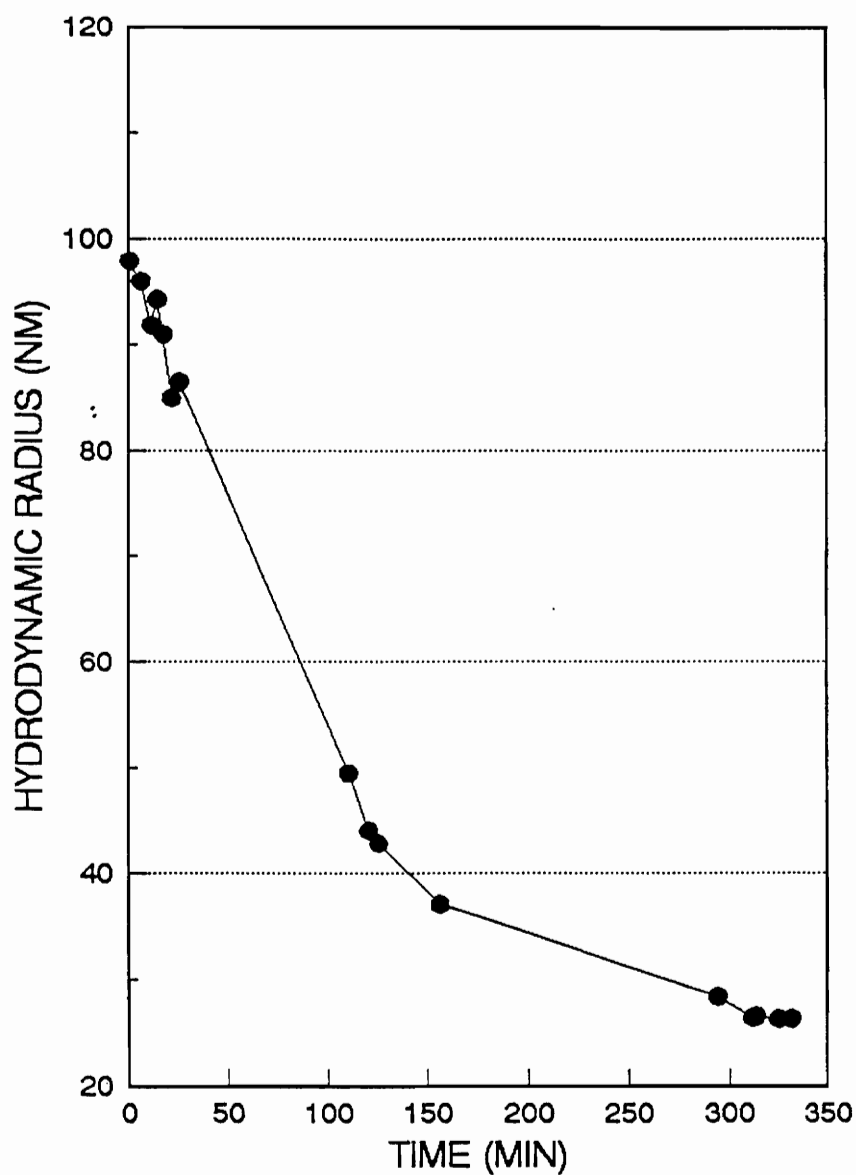
for 25min and then let it go back to  $25^{\circ}\text{C}$ .

Z	$R_H$ (nm)
0.018	27.73
0.071	31.12
0.124	27.93
0.176	27.54
0.441	24.95
0.529	28.31



NaPSS MW=1,200,000 PLL MW=10,200  
Z=0.441 pH=7 T=47C I=0.1  
FIGURE CORRESPONDS TO TABLE 5.3.2.6

FIGURE 5.3.2.1 KINETICS OF PEC'S SIZE REDUCTION WITH TEMPERATURE.



NaPSS MW=1,200,000 PLL MW=10,200  
 $Z=0.53$  pH=7 T=47C I=0.1M  
 FIGURE CORRESPONDS TO TABLE 5.3.2.6.

FIGURE 5.3.2.2 KINETICS OF PEC'S SIZE REDUCTION WITH TEMPERATURE.

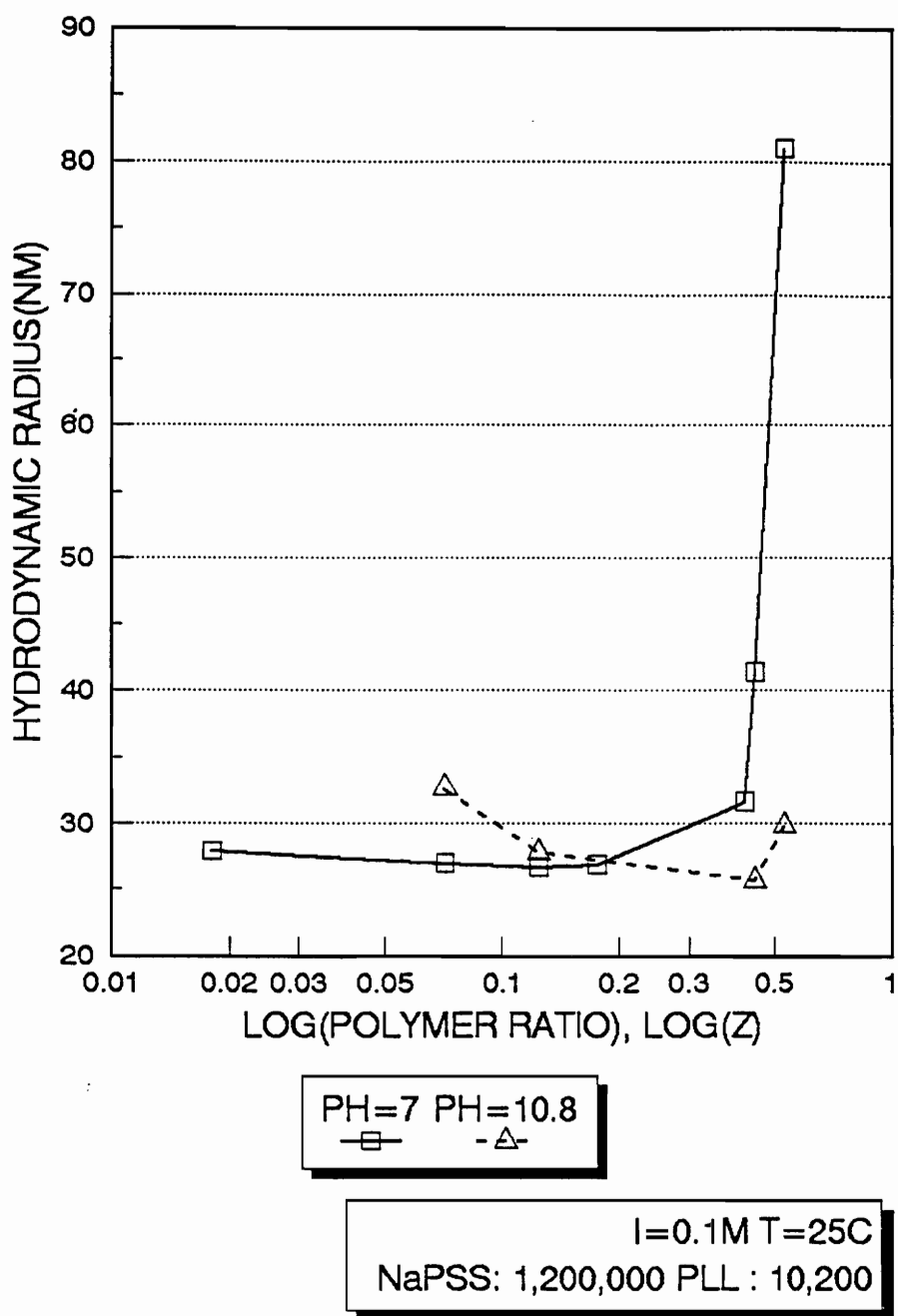


FIGURE 5.3.3.1 pH EFFECTS ON PEC BINDING

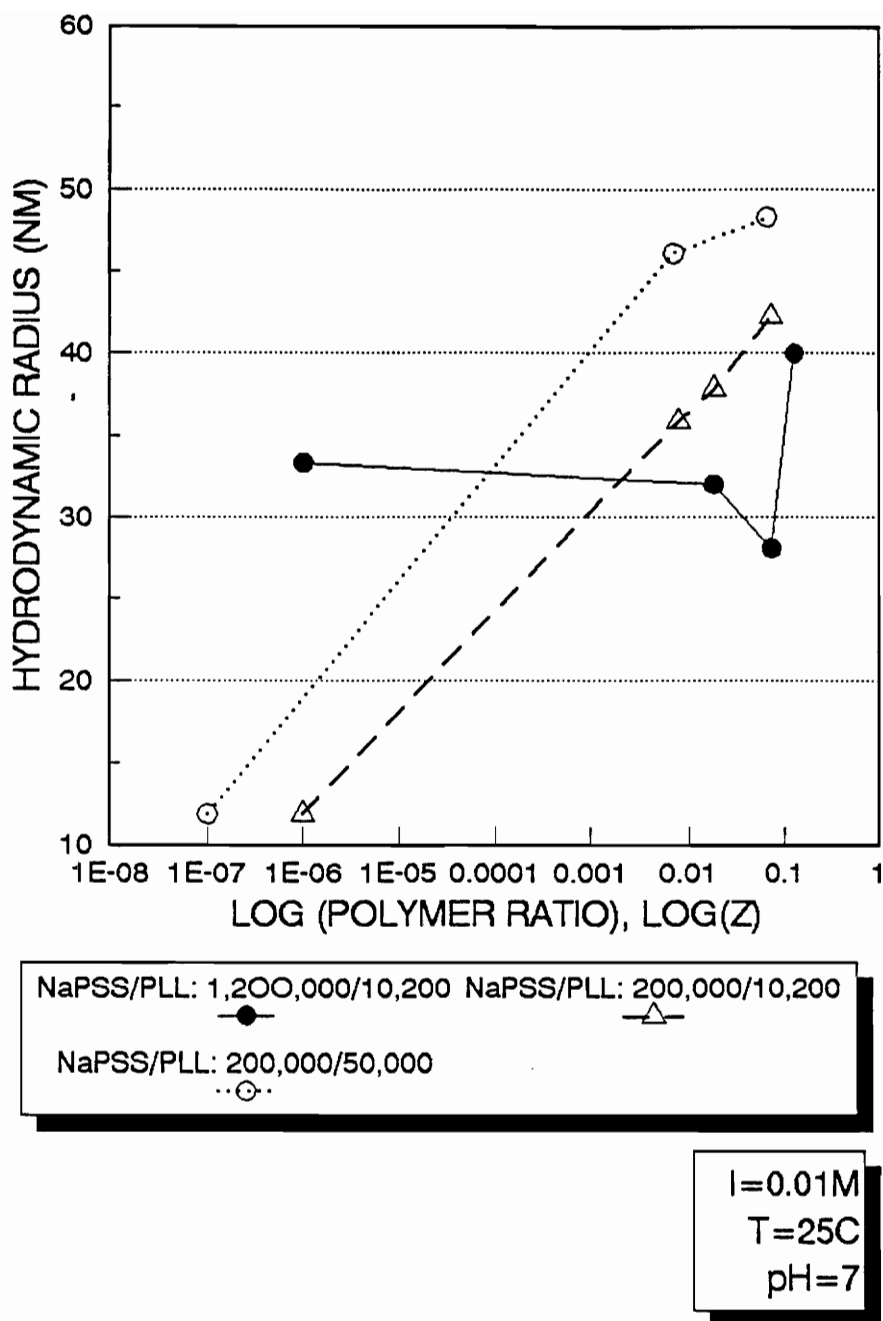


FIGURE 5.3.4.1 EFFECT OF MOLECULAR WEIGHT ON PEC'S BINDING  
 I=0.01M

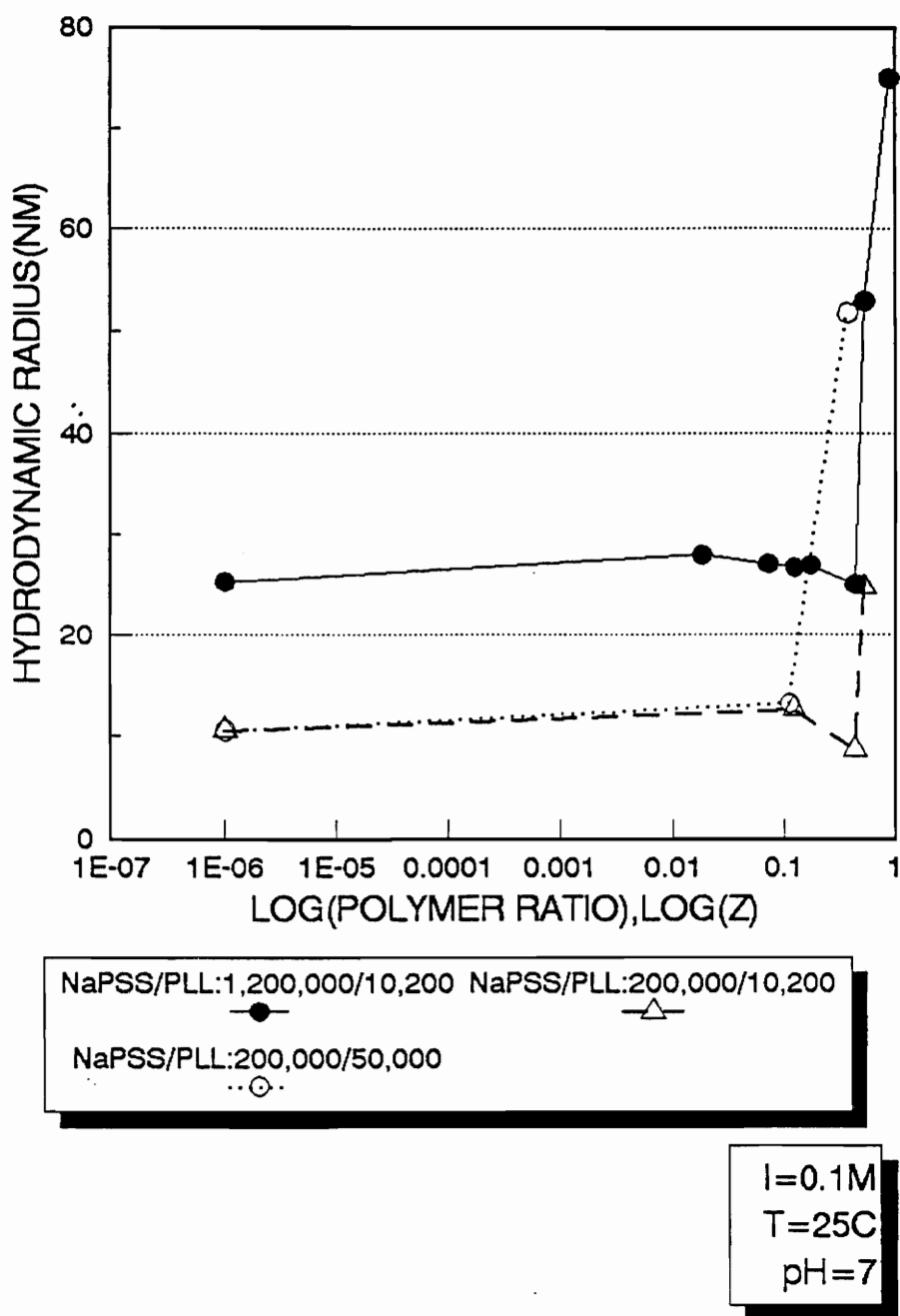


FIGURE 5.3.4.2 EFFECT OF MOLECULAR WEIGHT ON PEC'S FORMATION  
 I=0.1M

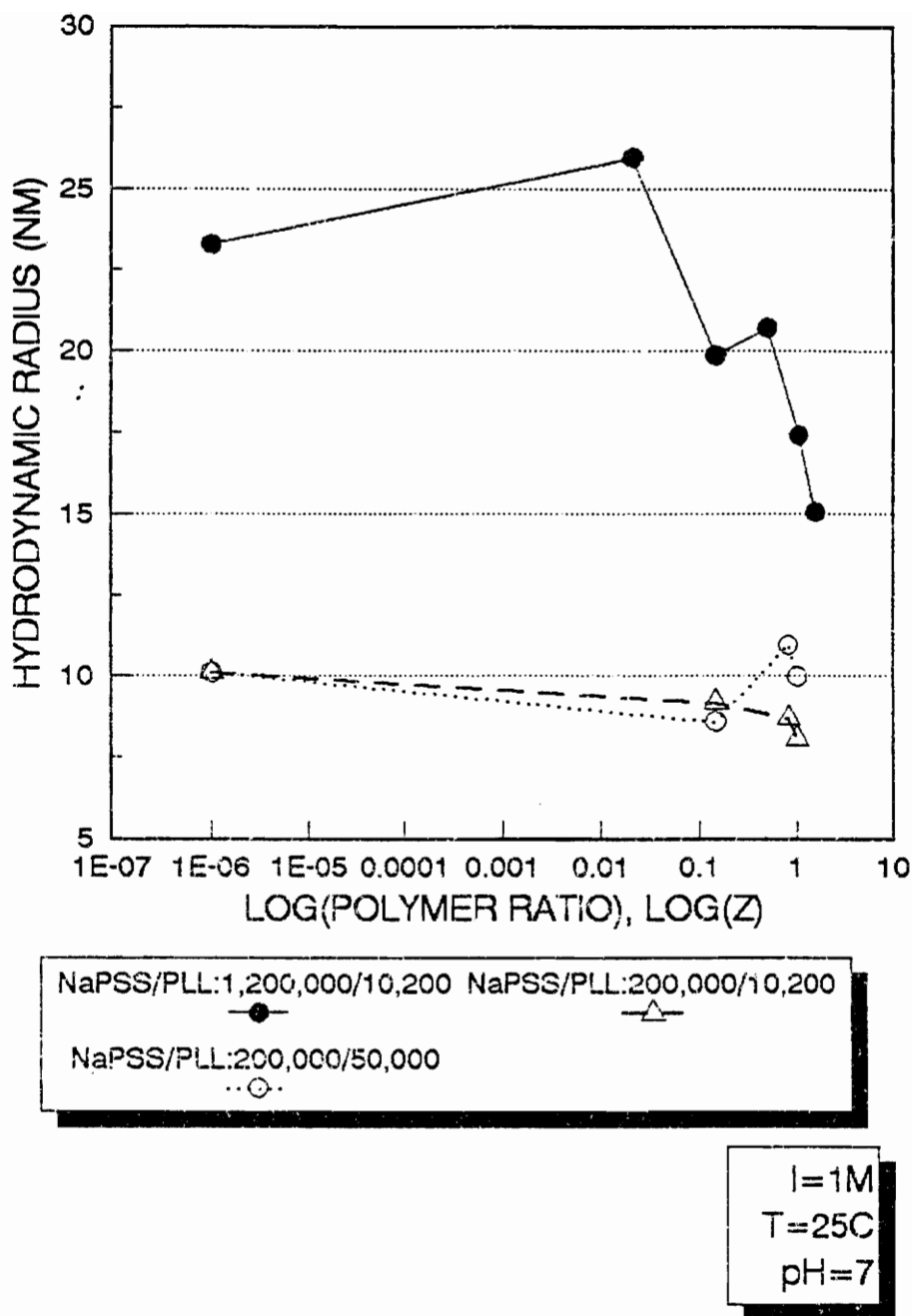


FIGURE 5.3.4.3 EFFECT OF MOLECULAR WEIGHT ON PEC FORMATION

I=1M

## 6.0 CONCLUSIONS & FUTURE WORK

### 6.1 Conclusions

In this work the PEC system, NaPSS/PLL was studied. Dynamic light scattering was used to characterize the dynamic properties of the system. The translational diffusion coefficient was measured from which the hydrodynamic radius,  $R_H$ , of the complexes was evaluated.

A single chain regime below a  $Z_{crit}$  was observed.  $Z_{crit}$  is a function of polymer concentration, charge densities of both chains, ionic strength and ability of PE's to bind (degree of dissociation and conformation). For  $Z > Z_{crit}$ , large nonequilibrium structures formed, whose size was difficult to reproduce.

PLL helix-coil transition may play an important role in controlling PEC's behavior. This is a function of pH, temperature, ionic strength.

Our principal observations were:

(1) The onset of multihost NaPSS aggregation,  $Z_{crit}$ , shifts to lower values of  $Z$  as the ionic strength decreases. For  $Z < Z_{crit}$ , the hydrodynamic radii are effectively constant. This suggests little or no intermolecular complexation is occurring. This contradicts Kabanov's observations [19]. At high ionic strength,  $I=1M$ , slight host NaPSS coil shrinkage occurs followed by a sharp collapse of the NaPSS molecule. This agrees qualitatively with Kabanov's general findings [9]. No inter-host aggregates were formed in this regime, at least up to  $Z=1$ .

(2) Temperature plays an important role which may be coupled with the conformational properties of PLL. Unfortunately, it wasn't clear from DLS experiments only, what the precise conformation of PLL was at different temperatures. Definitely, it is not a highly cooperative transition, which means

that is possible to find both helix and coil form in a broad range of temperatures around the "melting temperature" (47°C). At  $T \geq 47^\circ\text{C}$ ,  $kT$  energy breaks up the large nonequilibrium structures, to smaller ones or even to the original single molecule chain size. Upon cooling, the resulting structure is smaller, and this new state may be a quite stable meta-stable state. These different "degrees of PEC's break-up" , may be coupled with PLL conformation.

(3) Increasing pH ( $\simeq 10.8$ ), also has an effect on PEC's formation and size. The latter takes the single NaPSS chain size at pH=10.8, which seems to be coupled again with PLL's decreasing binding capacity, due to decreasing charge density.

(4) Molecular weight experiments raised some more questions, like in what extend PE's relative size seems to be important in  $Z_{crit}$  values. We observed

$$\text{that for } \frac{M_{NaPSS}}{M_{PLL}} = \frac{1.2 \times 10^6}{10,200} \simeq 117 \text{ and } \frac{M_{NaPSS}}{M_{PLL}} = \frac{200,000}{10,200} = 19 \text{ the } Z_{crit} \text{ was}$$

exactly the same, but when increasing even further the PLL molecular weight

$$\left( \frac{M_{NaPSS}}{M_{PLL}} = \frac{200,000}{50,000} = 4 \right), Z_{crit} \text{ occurs in lower values. This may correlate}$$

with the geometrical constraints of the system and may be consistent with our idea of "PLL bridging". Some possible pictures of the system, is (i) PLL binding to NaPSS depends on both NaPSS and PLL conformational state and possible reasons for the onset of aggregation, may be  $\beta$ -structures between PLL molecules (ii) Complexes aggregate because of their increased hydrophobicity which reduce the electrostatic repulsions between them [19] (iii) Simply PLL acts as a "bridge" connecting two host molecules.

## 6.2. Future work

A number of questions have been raised by this work. There still a lot of work to be done in order to better predict and model this difficult system's behavior. Some suggestions are:

- (1) Circular dichroism for helicity or conformation of PLL before and after complexation.
- (2) Small angle X-ray scattering for internal structure.
- (3) Binding mechanism, Host-guest-host, or Guest-guest needs to be elucidated.
- (4) Further probe of host/guest molecular weight effects.
- (5) p-D-lysine experiments could be useful in comparing with PLL.
- (6) Other polyamino acids with different helix-coil transitions and hydrogen bonding capacity.
- (7) DNA/polycations experiments and correlation with in-vivo experiments.

APPENDIX 1. REPRODUCIBILITY TESTS

Table App 1. Reproducibility tests for NaPSS:1,2×10<sup>6</sup> and PLL:10,200  
PEC's. Ionic strength I=0.1M, pH ≈ 7, T=25°C.

Z	R <sub>H</sub> (nm)#1	R <sub>H</sub> (nm)#2	R <sub>H</sub> (nm)#3	R <sub>H</sub> (nm)#4
0		21.70	28.74	
0.018			27.95	
0.071		24.33	31.48	25.18
0.124	24.73		28.7	26.61
0.176	28.96			24.85
0.415				31.64
0.441	23.94	21.72	29.25	41.38
0.529	40.67		72.04	42.97
0.882	87.02	63		

**Table App 2. Reproducibility tests for NaPSS:1,2 × 10<sup>6</sup> and PLL:10,200 PEC's. Ionic strength I=1M, pH ≈ 7, T=25°C**

Z	R <sub>H</sub> (nm)#1	R <sub>H</sub> (nm)#2	R <sub>H</sub> (nm)#3
0	25.07	20.88	23.89
0.018	25.96		
0.124		19.86	
0.176			32.28
0.415			20.68
0.529			28.9
0.882	20.78	16	
1.320	15.03		

**Table App 3. Reproducibility tests for NaPSS:1,2 × 10<sup>6</sup> and PLL:10,200 PEC's. Ionic strength I=0.01M, pH ≈ 7, T=25°C.**

Z	R <sub>H</sub> (nm)#1	R <sub>H</sub> (nm)#2
0	31.26	24.1
0.018	33.95	28.98
0.071	27.86	28.17
0.124	42.13	37.38

**Table App.4 Reproducibility tests**

NaPSS : 200,000 g/mole

PLL : 10,200 g/mole

pH=7

$C_{NaPSSin} : 3.8245 \times 10^{-3}$  g/ml

$C_{NaPSSfin} : 5 \times 10^{-5}$  g/ml

$C_{PLLin} : 6.72 \times 10^{-4}$  g/ml

T : 25 °C

I (M)	Z	$R_H(\text{nm})(1)$	$R_H(\text{nm}) (2)$
0.1	0	10.56	10.92
0.1	0.112	12.63	
0.1	0.441	9.12	8.32
0.1	0.529	24.66	28.92

**Table App.5 Reproducibility tests**

NaPSS : 200,000 g/mole

PLL : 50,000 g/mole

pH=7

$C_{NaPSSin} : 3.8245 \times 10^{-3}$  g/ml

$C_{NaPSSfin} : 5 \times 10^{-5}$  g/ml

$C_{PLLin} : 2.19 \times 10^{-4}$  g/ml

T : 25 °C

I (M)	Z	$R_H(\text{nm})(1)$	$R_H(\text{nm}) (2)$
0.1	0	10.56	10.92
0.1	0.112	13.20	
0.1	0.38	56.62	46.95

Table App.6 Reproducibility tests

NaPSS : 200,000 g/mole

PLL : 10,200 g/mole

pH=7

$C_{NaPSSin} : 3.8245 \times 10^{-3}$  g/ml

$C_{NaPSSfin} : 5 \times 10^{-5}$  g/ml

$C_{PLLin} : 6.72 \times 10^{-4}$  g/ml

T : 25 °C

I (M)	Z	$R_H(\text{nm})(1)$	$R_H(\text{nm}) (2)$
1.0	0	10.13	10.01
1.0	0.124	9.200	
1.0	0.69	8.700	8.30
1.0	0.864	8.100	7.800

Table App.7 Reproducibility tests

NaPSS : 200,000 g/mole

PLL : 50,000 g/mole

pH=7

$C_{NaPSSin} : 3.8245 \times 10^{-3}$  g/ml

$C_{NaPSSfin} : 5 \times 10^{-5}$  g/ml

$C_{PLLin} : 2.12 \times 10^{-4}$  g/ml

T : 25 °C

I (M)	Z	$R_H(\text{nm})(1)$	$R_H(\text{nm}) (2)$
1.0	0	10.13	10.01
1.0	0.112	8.600	
1.0	0.629	10.46	7.950

Table App.8 Reproducibility tests

NaPSS : 200,000 g/mole

PLL : 10,200 g/mole

pH=7

$C_{NaPSSin}$ :  $3.8245 \times 10^{-3}$  g/ml

$C_{NaPSSfin}$  :  $5 \times 10^{-5}$  g/ml

$C_{PLLin}$  :  $6.72 \times 10^{-4}$  g/ml

T : 25 °C

I (M)	Z	$R_H$ (nm)(1)	$R_H$ (nm) (2)
0.01	0	11.87	12.15
0.01	0.018	37.83	14.29
0.01	0.071	43.24	49.12

Table App.9 Reproducibility tests

NaPSS : 200,000 g/mole

PLL : 50,000 g/mole

pH=7

$C_{NaPSSin}$ :  $3.8245 \times 10^{-3}$  g/ml

$C_{NaPSSfin}$  :  $5 \times 10^{-5}$  g/ml

T : 25 °C

I (M)	Z	$R_H$ (nm)(1)	$R_H$ (nm) (2)
0.01	0	11.87	12.15
0.01	0.017	33.42	42.34
0.01	0.064	48.27	54.93

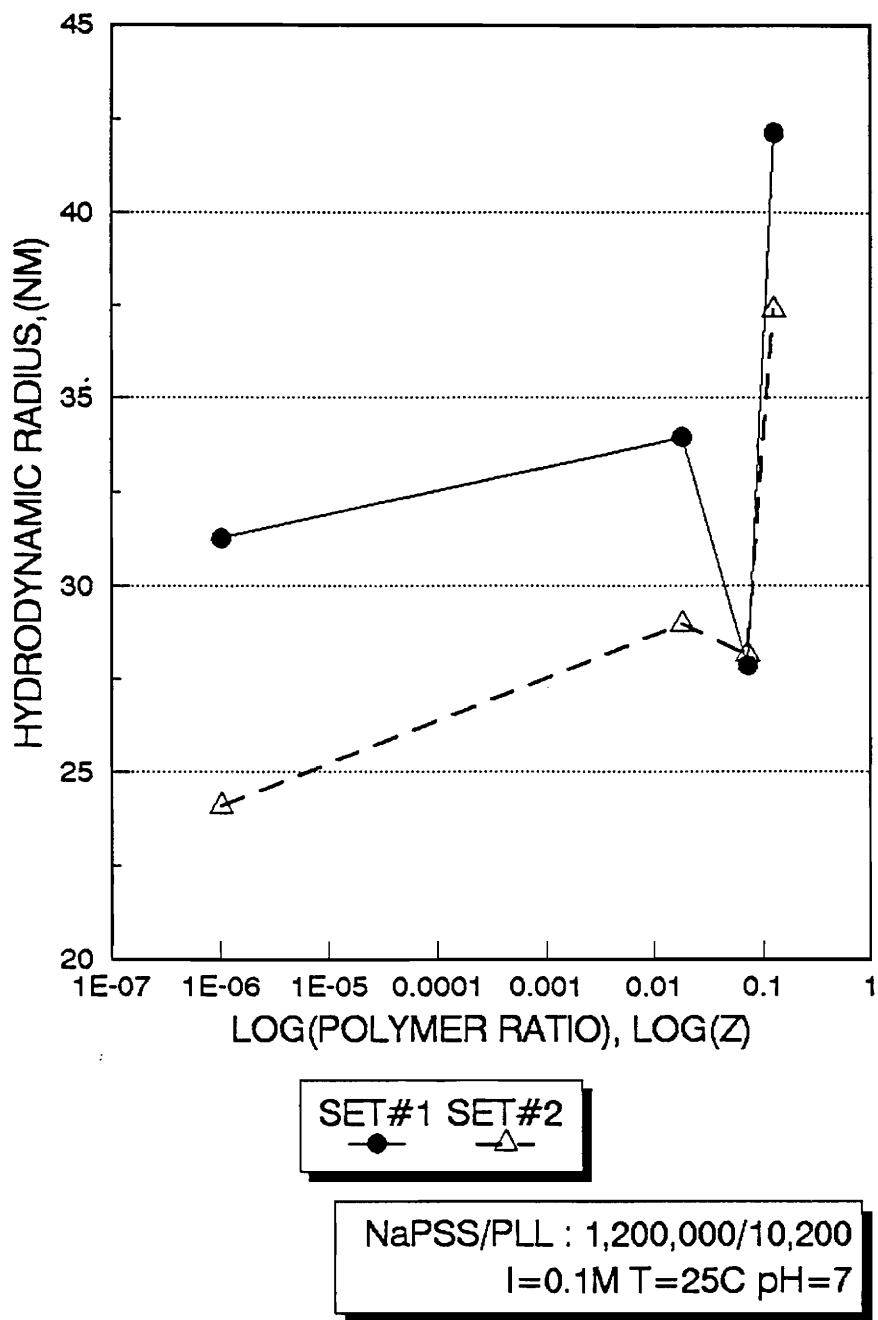


FIGURE APP 1.1 REPRODUCIBILITY TEST

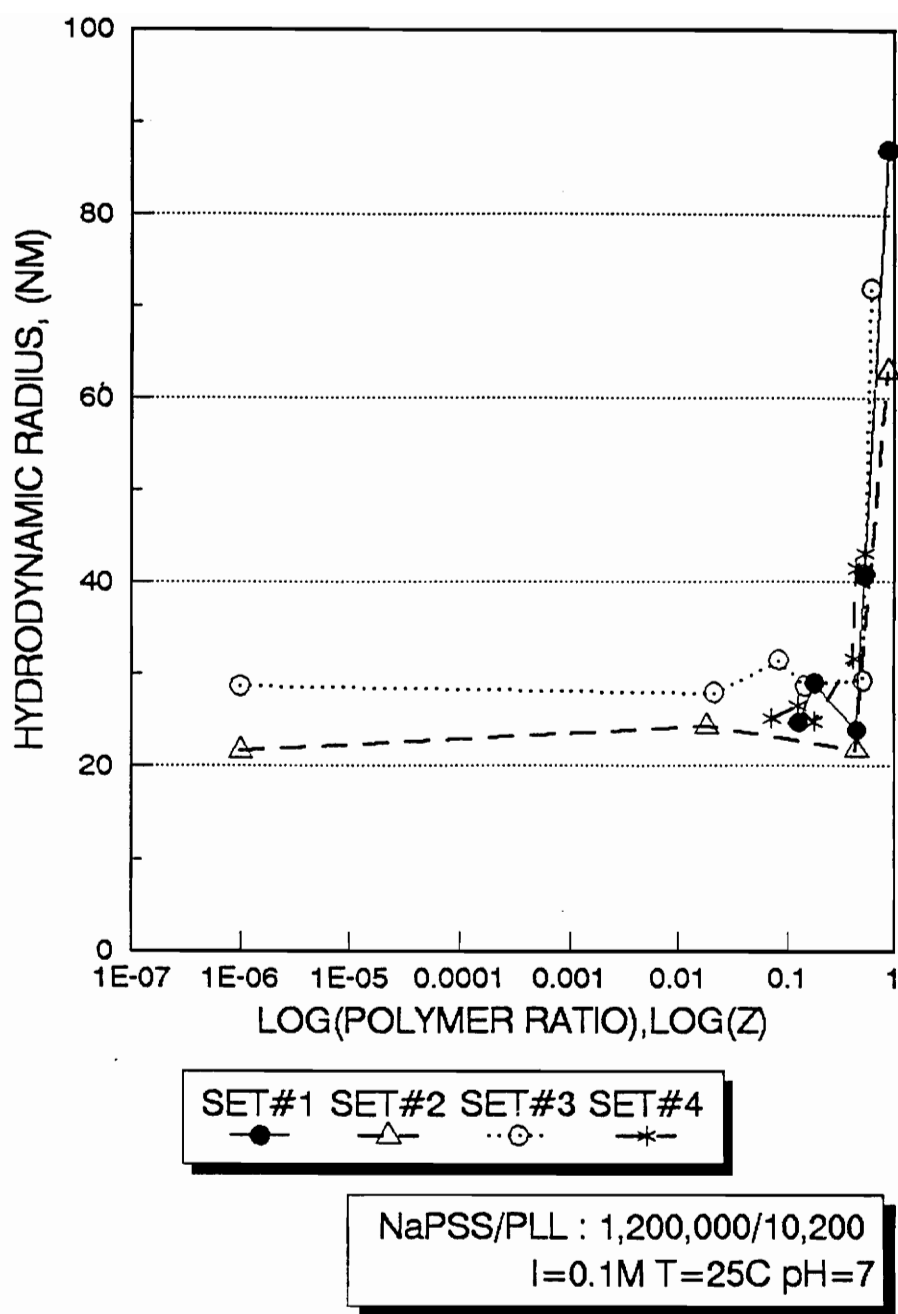


FIGURE 1.2 REPRODUCIBILITY TEST

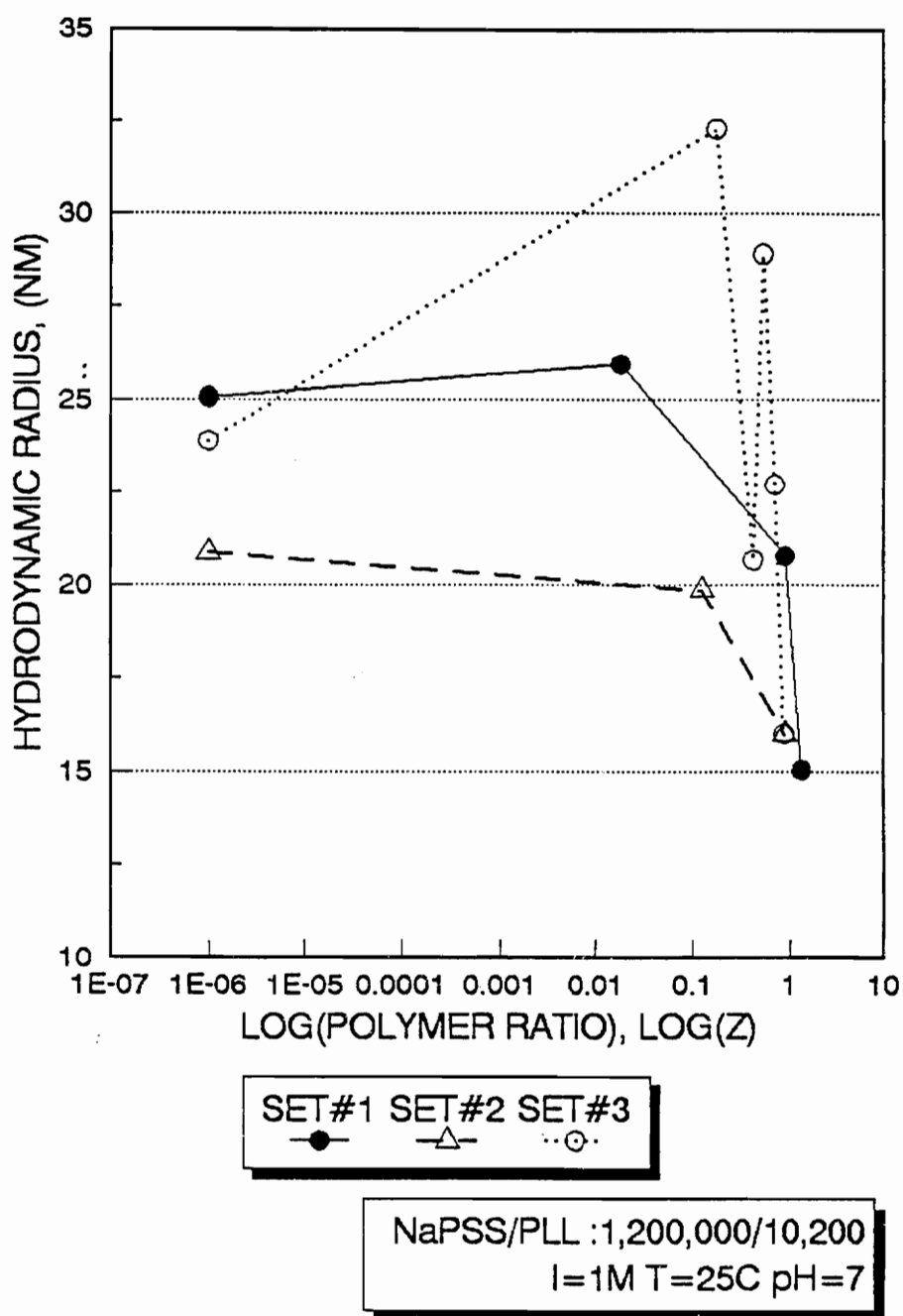


FIGURE APP 1.3 REPRODUCIBILITY TEST

## APPENDIX 2. SOFTWARE

The following program performs a least square first order analysis to calculate the diffusion coefficient, the standard deviation of it as well as the hydrodynamic radius,  $R_H$  from Stokes law. It was performed by SigmaPlot version 4.1.

```
COL(1) = Yi; GAMMA
COL(2) = Xi; Q2
COL(3) = RSD/100
COL(4) = COL(3)*COL(1);σi
COL(5) = COL(4)2; σi2
COL(6) = COL(2)/COL(5); Xi/σi2
COL(7) = COL(1)/COL(5) ; Yi2/σi2
COL(8) = [COL(1)*COL(2)]/COL(5); Xi*Yi/σi2
COL(9) = COL(2)2/COL(5) ; Xi2/σi2
COL(10) = 1/COL(5) ; 1/σi2
K = TOTAL(COL(6))2; (∑Xi2/σi2)2
L = TOTAL(COL(9)); ∑Xi2/σi2
M = TOTAL (COL(6)); ∑Xi/σi2
N = TOTAL (COL(8)); ∑XiYi/σi2
O = TOTAL(COL(7)); ∑Yi/σi2
COL(11) =TOTAL(COL(10))*L -M2;Δ
COL(12) = 1/COL(11)*(TOTAL(COL(10))*L -M*O);BETA
COL(13) = 1/COL(11)*(L*O-M*N);ALPHA
COL(14) = 1/COL(11)*L; σA
COL(15) = 1/COL(11)*TOTAL(COL(10));σB
COL(16) = kT/6π $\eta$ 
COL(17) = COL(16)/COL(12); RH
```

## BIBLIOGRAPHY

1. Philip Molineux, "Water Soluble Synthetic Polymers:properties and behavior", Vol. II, (1984).
2. Polymer Letters edition, Journal of Polymer Science, vol.18, 695, (1980).
3. Johannes Smid, Daryle Fish, Encycl. of Polym. Sc. and Engin., Vol. 11, (1988).
4. R.M.Davis, Proposal submitted to Jefress Memorial Trust, (1990).
5. Fumio Oosawa, "Polyelectrolytes", pg 1-12, (1971).
6. R.A.Gelman, W.B.Rippon, J.Blackwell, Biopolymers, Vol. 12, 511,(1986).
7. R.A.Gelman, J.Blackwell, Biopolymers, Vol. 15, 139,(1974).
8. K.P.Schodt, J.Blackwell, Biopolymers, Vol. 15, 469,(1976).
9. K.P.Schodt, M.F.McDonell, A.M.Jamieson, J.Blackwell, Biopolymers, Vol.10, No 3, 701,(1977).
10. W.B.Russel, Jour. of Pol. Sc., Vol. 20, 1233, (1982).
11. R.S.Koene, M.Mandel, Macromolecules, Vol. 16, No 2, 220,(1983).
12. R.S.Koene, T.Nicolai, M.Mandel, Macromolecules, Vol. 16, 227, (1983).
13. R.S.Koene, T.Nicolai, M.Mandel, Macromolecules, Vol. 16, 231, (1983).
14. T.Odijk, A.C. Howaart, Jour. of Pol. Science, PP, Vol.16, 627, (1978).
15. R.M.Davis, ACS Proposal, Submitted on 2/11/1991.
16. E.Tsuchuda, Y.Osada, K.Sanada, Jour. of Pol. Sc., Vol. 10, 3397, (1972).
17. T.Okubo, N.Mohri, Macromolecules, Vol. 21, 2744, (1988).
18. A.S.Veis, "Biological Polyelectrolytes", ed. Marcel Dekker Inc., N.Y., (1970).
19. V.A.Kabanov, A.B.Zezin, Pure and Applied Chemistry, 343,(1984).
20. S.K.Chatterjee, Yadav, S.Chosh, Khan, Jour. of Pol. Sc., Vol. 27, 3855, (1989).
21. Die Makromolekulare Chemie, 175, 603, (1974).
22. W.Foster, Pol. Science and Technology, vol 2, 3, (1974).

23. H.Flock, E.Rausch, Pol. Science and Technology, vol 2, 21, (1973).
24. D.L.Sussman, E.Chun-Chin Wang, Pol. Science and Technology,vol 2, 75, (1973).
25. D.C.MacWilliams, J.H.Rogers, T.J.West, Pol. Science and Technology, vol 2, 105,(1973).
26. W.Regelson, Pol. Science and Technology, vol. 2, 161, (1973).
27. V.A.Kabanov,Macromol. Chem, Macromol. Symp., vol 1, 101, (1986).
28. V.A.Kabanov, A.V.Kabanov, I.N.Astalyeva, Preprint ACS meeting, Atlanta, April 1991.
29. V.A.Kabanov, V.Izumudov, T.Bronick, O.Saburova, A.B.Zezin, Makromol. Chem, Rapid Communications, 9, (1988).
30. W.Carroll, H.Eisenberg, Journal of Pol. Science, part A-2, vol. 1, 599, (1966).
31. I.E.Nagasawa, J. of Phys. Chem, 71, 885, (1967).
32. W.Burchard, Macromolecules Chem, Macromol. Symp., 18, 1, (1988).
33. R.Pecora, Dynamic Light Scattering, (1985).
34. P.Bevington, Data Reduction and Error Analysis for the Phys. Sciences, (1969).
35. Paul C.Hiemenz, Polymer Chemistry. The basic Concepts,Marcel Dekker, Inc., (1984).
36. Digital Correlator Operator's Manual, Brookhaven Instr. Corp., (Sept. 1986).
37. E.G.Richards, An introduction to physical properties of large molecules in solution, (1980).
38. B.Davidson, G.Fasman, Biochemistry, vol.6(6), 1616, (1967).
39. J.Schellman, Theory of helix-Coil transition in Biopolymers, pg.357, (1955).
40. J.Schellman, Theory of helix-Coil transition in Biopolymers, pg.387, (1958).
41. D.Poland, H.Sceraga, Theory of helix-Coil transition in Biopolymers, pg.406, (1965).
42. L.Peller, Theory of helix-Coil transition in Biopolymers, pg.443, (1959).
43. A.J.Hopfinger, Conformational properties of Macromolecules, pg.169, (1973).
44. A.Walton, J.Blackwell, Biopolymers, pg.376, (1973).
45. R.Davis, Macromolecules, vol.24(5), 1149, (1991).

46. R.Davis, W.B.Russel, Journal of Polymer Science, Part B:Polymer Phys., vol.24, 511, (1986).
47. E.Tsuchida, Die Makromolekulare Chemie, vol.175, 603, (1974).
48. V.A.Kabanov, A.B.Zezin, V.A.Izumrudov, T.K.Bronitch, N.M.Kabanov, O.V.Listova, Makromol.Chem., Macromol.Symp., vol.39, 155, (1990).
49. V.A.Kabanov, A.B.Zezin, V.A.Izumrudov, T.K.Bronitch, K.N.Bakeev, Makromol.Chem., Suppl.13, 133, (1985).
50. A.B.Zezin, V.A.Izumrudov, V.A.Kabanov, Makromol.Chem., Macromol.Symp. 26 249, (1989).
51. A.M.Jamieson, L.Mack, A.G.Walton, Biopolymers, vol.11, 2267,(1972).
52. P.Y.Chou, H.A.Scheraga, Biopolymers, vol.10, 657, (1971).
53. M.Drifford, J.P.Dalbiez, Biopolymers, vol.24, 1501, (1985).
54. Nagasawa, J. of Phys.Chem., vol.71, 885, (1967).
55. C.Tanford, Physical Chemistry of Macromolecules, John Wiley&Sons, Inc., New York, (1961).

## VITA

The author was born on June 18, 1965 in Athens, Greece. After graduating from High school in Athens in 1983, she joined the "National Technical University of Athens" in Athens, Greece. She earned a Bachelor's Degree in Chemical Engineering in 1988. In Fall 1989, she joined the Chemical Engineering department at Virginia Tech, in the Master's program. She completed the requirements for a Masters Degree on June 21st, 1991.